UNITED STATES
DEPARTMENT OF THE INTERIOR
GEOLOGICAL SURVEY

GEOLOGIC, GEOPHYSICAL, AND IN SITU STRESS INVESTIGATIONS
IN THE VICINITY OF THE DINING CAR CHIMNEY,
DINING CAR/HYBLA GOLD DRIFTS,
NEVADA TEST SITE

By
U.S. GEOLOGICAL SURVEY

With a section on GEOLOGIC INVESTIGATIONS
By D. R. Townsend[1] and M. J. Baldwin[1] and

a section on GEOPHYSICAL INVESTIGATIONS
By R. D. Carroll[2] and

a section on IN SITU STRESS INVESTIGATIONS
By W. L. Ellis[2] and J. E. Magner[2]

[1]Fenix & Scisson, Inc., Mercury, Nev.
[2]U.S. Geological Survey, Denver, Colo.

FOREWORD

The Hybla Gold experiment was a low-yield nuclear event located in the U12e.20 drift of the E-tunnel complex in Rainier Mesa, Nevada Test Site. The event was detonated on November 1, 1977. The location of the Hybla Gold event was unique in that it was situated near the expended Dining Car event, a low-yield nuclear event detonated in the U12e.18 drift on May 4, 1975. The main drift of the Hybla Gold complex passed within 3 m (10 ft) of the chimney formed by the collapse of the Dining Car cavity. Thus, the Hybla Gold drift mining enabled the most extensive examination of postshot effects near a collapsed cavity since the Rainier event was detonated in 1957. Although the Rainier event remains the most extensively visually documented postshot tunnel reentry in the chimney region, measurements in the Hybla Gold drift complex have added extensively to that experience.

This report comprises three chapters detailing the geologic, geophysical, and in situ stress data gathered in the period January through June 1977, in the course of mining and drilling in the Hybla Gold/Dining Car region. These investigations confirm several observations reported previously for the Rainier event, i.e., a zone of microfailure observable in thin-section and in physical properties exists adjacent to the chimney. In addition, however, a number of investigations add new information to our understanding of effects near the detonation point. Shear waves were found to be highly diagnostic in the microcracked zone near the chimney as well as of zones of failure at greater range not discernible by other techniques. Extensive in situ stress measurements made by the hydrofracture and overcore techniques indicate changes in the orientation and magnitude of the pre-Dining Car stress field. The hydrofracture technique further suggests pronounced gradients in minimum stress magnitudes over short distances at some locations in the postshot stress regime.

Finally, acknowledgment is made to the aid and encouragement of J. W. LaComb of the Defense Nuclear Agency who provided the impetus, direction, and much of the conceptual planning for these investigations.

R. D. Carroll

CONTENTS

CONTENTS--Continued

ILLUSTRATIONS

ILLUSTRATIONS--Continued

GEOLOGIC INVESTIGATIONS

By

D. R. Townsend and M. J. Baldwin

ABSTRACT

The Hybla Gold experiment was conducted in the U12e.20 drifts of the E-tunnel complex beneath the surface of Rainier Mesa at the Nevada Test Site. Though the proximity of the Hybla Gold working point to the chimney of the Dining Car event was important to the experiment, the observable geologic effects from Dining Car on the Hybla Gold site were minor. Overburden above the working point is approximately 385 m (1,263 ft). The pre-Tertiary surface, probably quartzite, lies approximately 254 m (833 ft) below the working point.

The drifts are mined in zeolitized ash-fall tuffs of tunnel bed 4, subunits K and J, all of Miocene age. The working point is in subunit 4J. Geologic structure in the region around the working point is not complex. The U12e.20 main drift follows the axis of a shallow depositional syncline. A northeast-dipping fault with displacement of approximately 3 m (10 ft) passes within 15.2 m (50 ft) of the Hybla Gold working point. Three faults of smaller displacement pass within 183-290 m (600-950 ft) of the working point, and are antithetic to the 3-m (10-ft) fault.

Three exploratory holes were drilled to investigate the chimney of the nearby Dining Car event. Four horizontal holes were drilled during the construction of the U12e.20 drifts to investigate the geology of the Hybla Gold working point.

INTRODUCTION

The Hybla Gold experiment was located in the U12e.20 drifts of the E-tunnel complex, Rainier Mesa, Area 12, NTS (Nevada Test Site) (figs. 1, 2, 3; pl. 1). The geometry of the Hybla Gold experiment and its proximity to the Dining Car chimney were of major importance. For a summary of the geology of the Dining Car (U12e.18) drifts, see Steele and others, 1978. The Hybla Gold WP (working point) is approximately 83 m[1] (272 ft) east of the Dining Car WP.

The Hybla Gold WP is located at CS 4+45[2] in the main drift, at Nevada State coordinates N. 270,554 m, E. 192,683 m, and at an elevation of 1,882 m (6,175 ft). The water table in this area is at an elevation of approximately 1,524 m (5,000 ft), which corresponds to a depth below the WP of about 358 m (1,17𝑗 ft). The U12e.20 main and auxiliary drifts begin in subunit K of tunnel bed 4 of Tertiary age, and penetrate stratigraphically downsection to subunit J of tunnel bed 4. The WP is located in subunit 4J. Seven exploratory holes were drilled prior to and during the construction of the U12e.20 drifts to evaluate the stratigraphy and structural geology of the site. The drill holes also helped define the chimney of the nearby Dining Car (U12e.18) experiment.

Acknowledgments

D. L. Hoover of the USGS (U.S. Geological Survey) directed the geologic mapping. J. N. Morrison of F&S (Fenix & Scisson, Inc.), and S. G. Steele, F. Maldonado, and E. C. Jenkins of the USGS assisted in mapping and compiling the tunnel geology. F. M. Byers, Jr., and R. P. Snyder of the USGS mapped the surface geology of Rainier Mesa. D. L. Healey, C. H. Miller, and F. E. Currey

---

[1]To convert meters to feet, multiply meter by 3.2808.
[2]CS 4+45 refers to construction stations in the tunnel complex in accordance with surveying practice, and is measured in English units. To convert to meters, multiply foot by 0.3048.
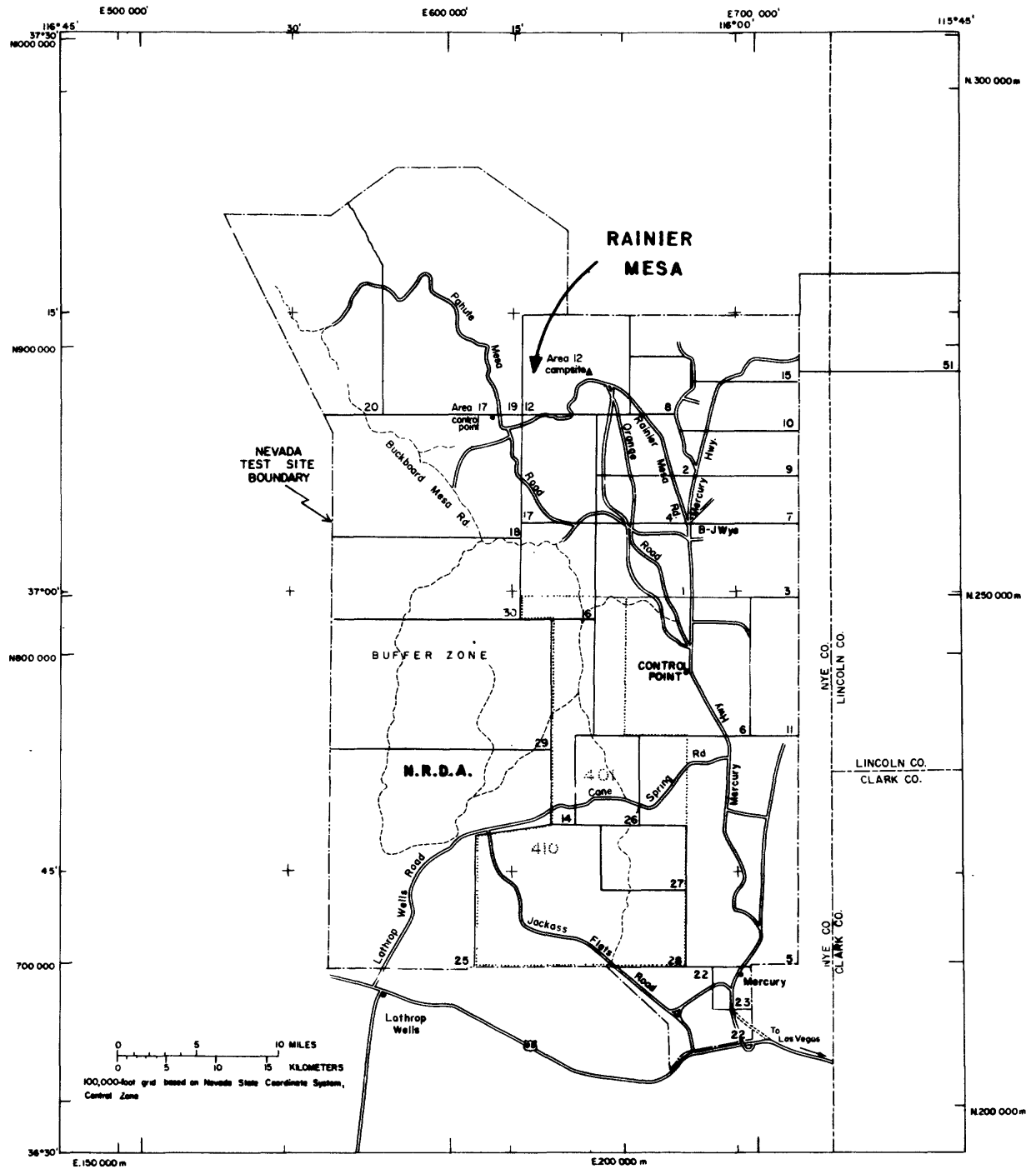
Figure 1.--Index map of the Nevada Test Site.
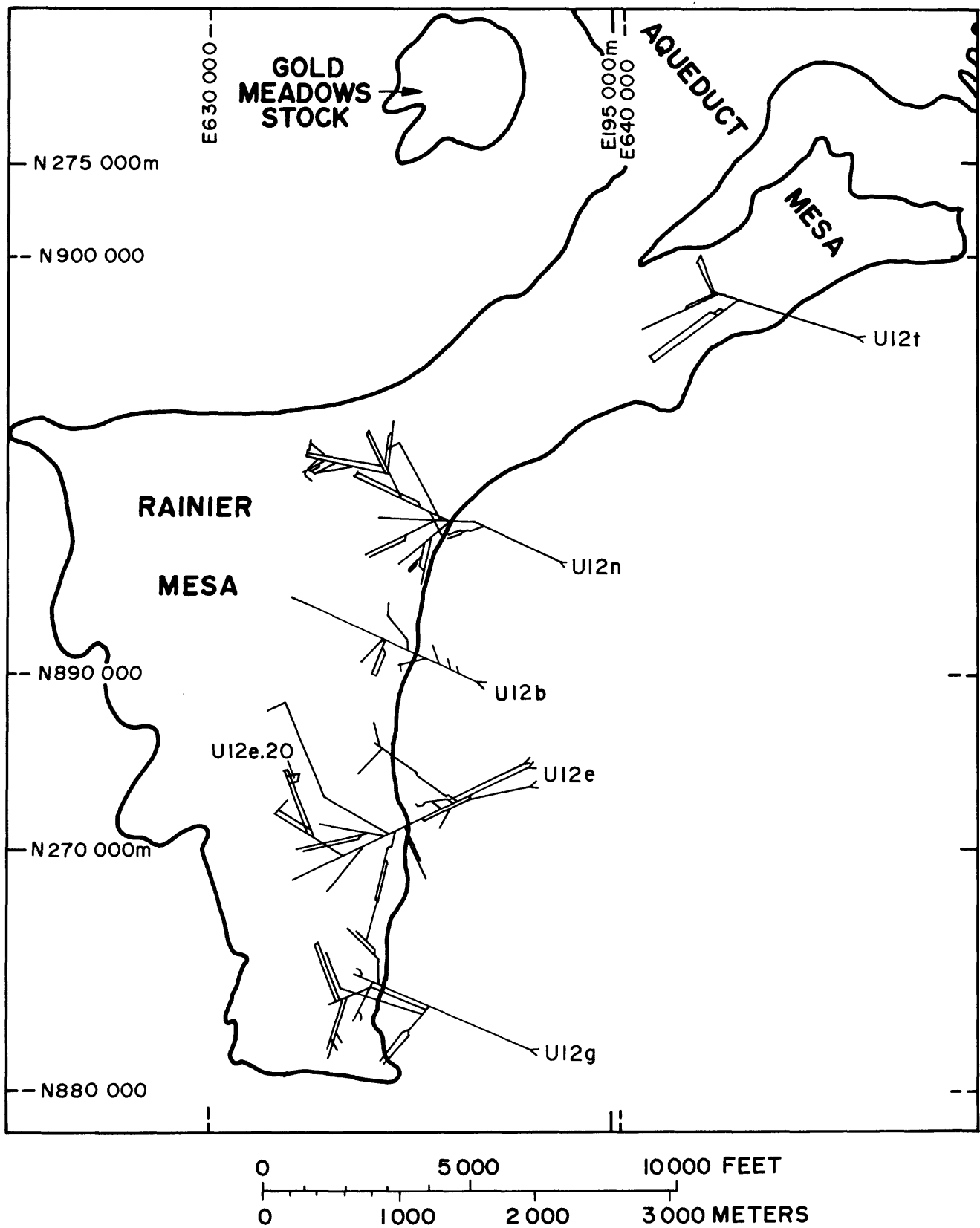
Figure 2.--Index map of Rainier Mesa showing location of U12e tunnel complex.
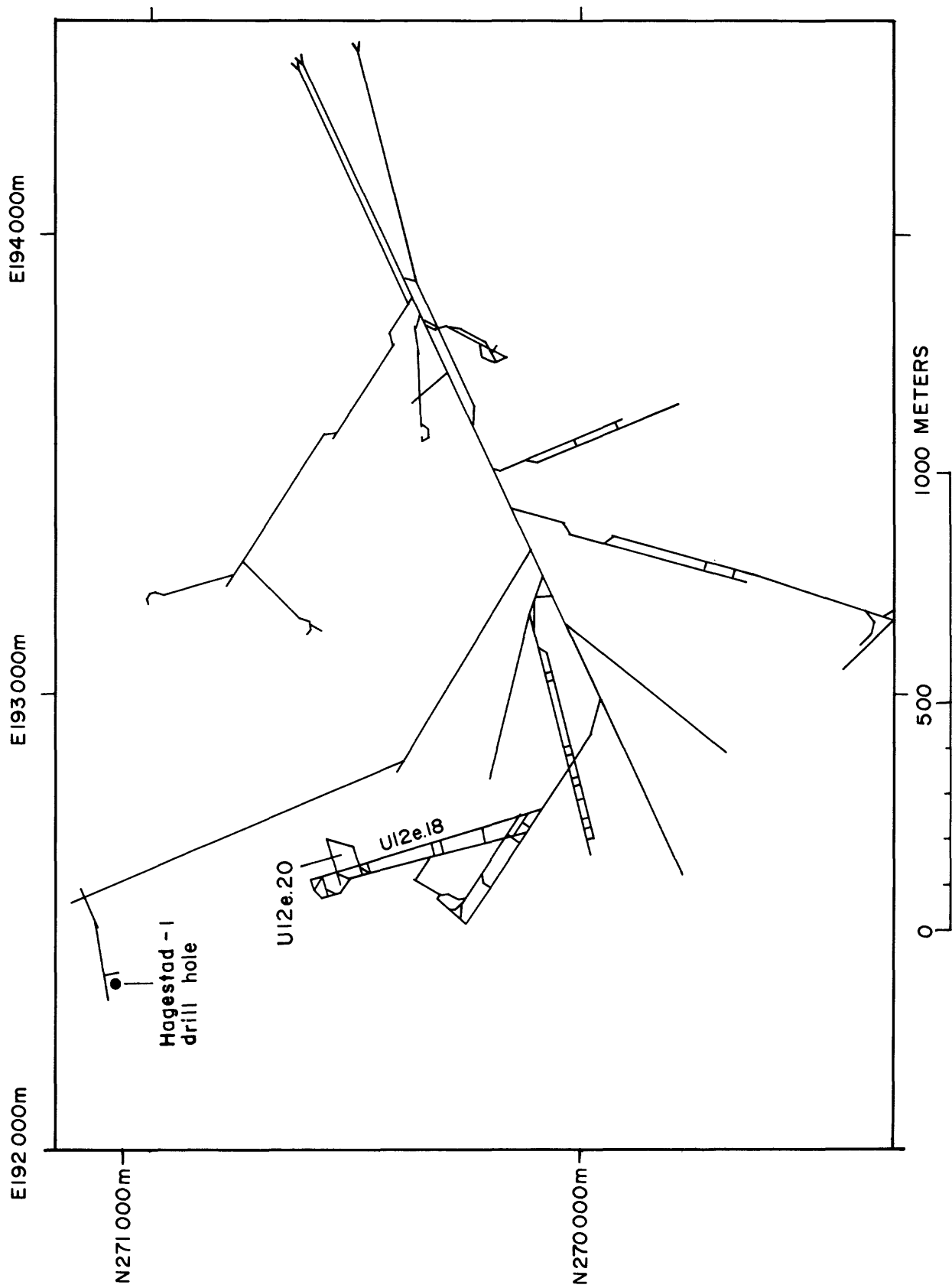
Figure 3.--Index map of U12e tunnel complex, showing location of the U12e.20 (Hybla Gold) drifts.

E194 000m

E193 000m

E192 000m

N271 000m

N270 000m

U12e.20

U12e.18

Hagestad -1
drill hole

0   500   1000 METERS

5

of the USGS provided the gravity data used to construct the structural contour map of the pre-Tertiary surface. The DNA (Defense Nuclear Agency) provided support for all geological investigations.

STRATIGRAPHY

Rainier Mesa is an erosional feature consisting of approximately 625 m (2,050 ft) (in the region of E-tunnel) of Tertiary volcanic ash-fall and ash-flow tuffs deposited on an irregular pre-Tertiary surface. The pre-Tertiary rocks under the E-tunnel complex consist generally of quartzite on the west and dolomite on the east. The general stratigraphy of Rainier Mesa is presented on figure 4 and tunnel-level geology on figure 5.

The overburden above the U12e.20 WP is approximately 385 m (1,263 ft) (figs. 6, 7). The stratigraphic units and their thicknesses, as estimated from the UE12e#1 vertical drill hole and cross-section reconstructions, are as follows: the Rainier Mesa Member of the Timber Mountain Tuff, 103.6 m (340 ft); the Paintbrush Tuff, 213.4 m (700 ft); the Grouse Canyon Member of the Belted Range Tuff, 6.1 m (20 ft); tunnel bed 5, 21.3 m (70 ft); tunnel bed 4, subunit K, 35.1 m (115 ft); and part of tunnel bed 4, subunit J, 6.1 m (20 ft).

The Hybla Gold WP is in tunnel bed 4, subunit J, and the cavity region extends into subunit 4K. Subunit 4J is composed of massive calc-alkaline ash-fall tuff with a few thin beds of peralkaline ash-fall tuff. Subunit 4K consists of thick-bedded, zeolitized, peralkaline ash-fall tuff with beds of calc-alkaline ash-fall tuff. See table 1 for mineralogical analyses of samples from subunit 4J.

The pre-Tertiary surface lies approximately 254 m (833 ft) below the U12e.20 WP (figs. 6, 7). The presence of Paleozoic quartzite in the Hagestad-1 drill hole (fig. 3), about 564 m (1,850 ft) northwest of the WP,

Table 1.--X-ray mineralogical analyses of two samples from the region of the Hybla Gold experiment

[Analyses by P. D. Blackmon, U.S. Geological Survey]

Sample No. and location	Description	Minerals present	Estimated amounts (parts in ten) tr=trace=<5%;<1=5-9%
U12e.20 UG-3 at 37.3 m (122.5 ft), Hybla Gold working point	Subunit 4J Zeolitized ash-fall tuff	Montmorillonite	1
		Illite-mica	tr
		Mordenite and Clinoptilolite	4
		Quartz	1
		Feldspar	2+
		Cristobalite-opaline silica	tr
		Amorphous (Ash?)	1
U12e.20 main drift, left rib, at CS 2+77	Subunit 4J Zeolitized ash-fall tuff	Montmorillonite	1
		Illite-mica	tr
		Clinoptilolite and Mordenite	5
		Quartz	<1
		Feldspar	1+
		Cristobalite-opaline silica	<1
		Amorphous (Ash?)	<1

Eon/Era	System	Series	Formation	Member or unit and symbol
Cenozoic Era	Tertiary	Miocene	Timber Mountain Tuff	Rainier Mesa Member Tmr
			Paintbrush Tuff	Tiva Canyon Member Tpc Tp
			Stockade Wash Tuff	Tsw
			Bedded and ash-flow tuffs of Area 20	Trab
			Bedded tuff of Dead Horse Flat Tdhb	
			Belted Range Tuff	Grouse Canyon Member Tbg
			Tunnel beds	Unit 5 Tt5
				Unit 4 Tt4 Subunits AB, CD, E, F, G, H, J, K[1]
				Unit 3 Tt3 Subunits A, BC, D[2]
			Belted Range Tuff	Tub Spring Member Tbt
			Tunnel beds	Unit 2 Tt2
			Crater Flat Tuff	Tcf
			Tunnel beds	Unit 1 Tt1
			Redrock Valley Tuff	Trv
			Older tuffs	Tot
			Paleocolluvium	Tc
Mesozoic Era	Cretaceous		Quartz monzonite of Gold Meadows stock	Kqm
Paleozoic Era	Devonian Silurian Ordovician Cambrian		Paleozoic rocks, undivided	Pz [3]
			Wood Canyon Formation	€Єw
Proterozoic Eon			Stirling Quartzite	Ɔ Ɔ[3]

[1]K is the youngest.
[2]D is the youngest.
[3]In some drill holes, paleocolluvium of Tertiary age (Tc) rests on Paleozoic or Precambrian rocks.

Figure 4.--General stratigraphy of Rainier Mesa area, Nevada Test Site.
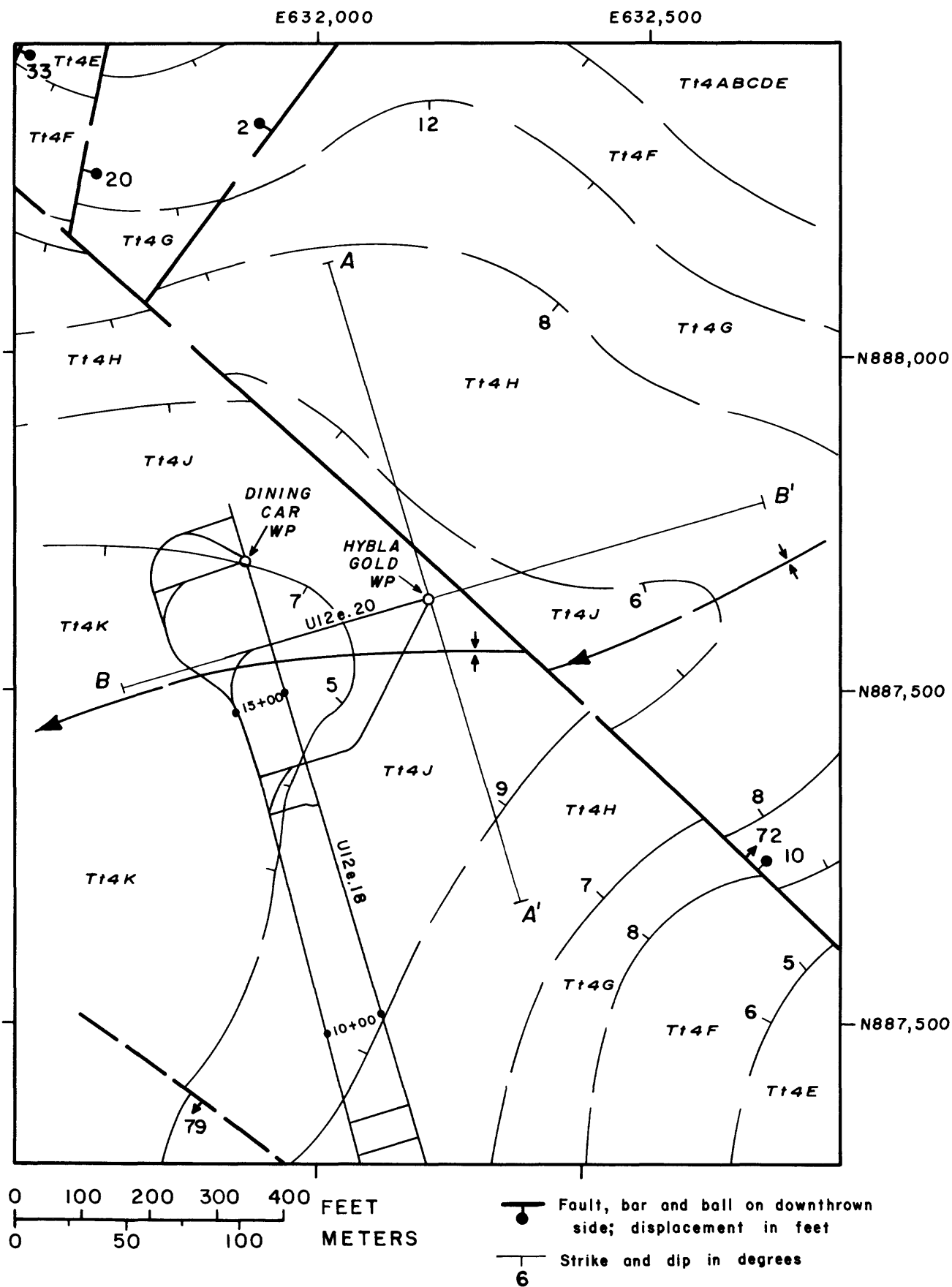
Figure 5.--Tunnel-level geology of the Hybla Gold area.
(See fig. 4 for explanation of geologic unit symbols.)
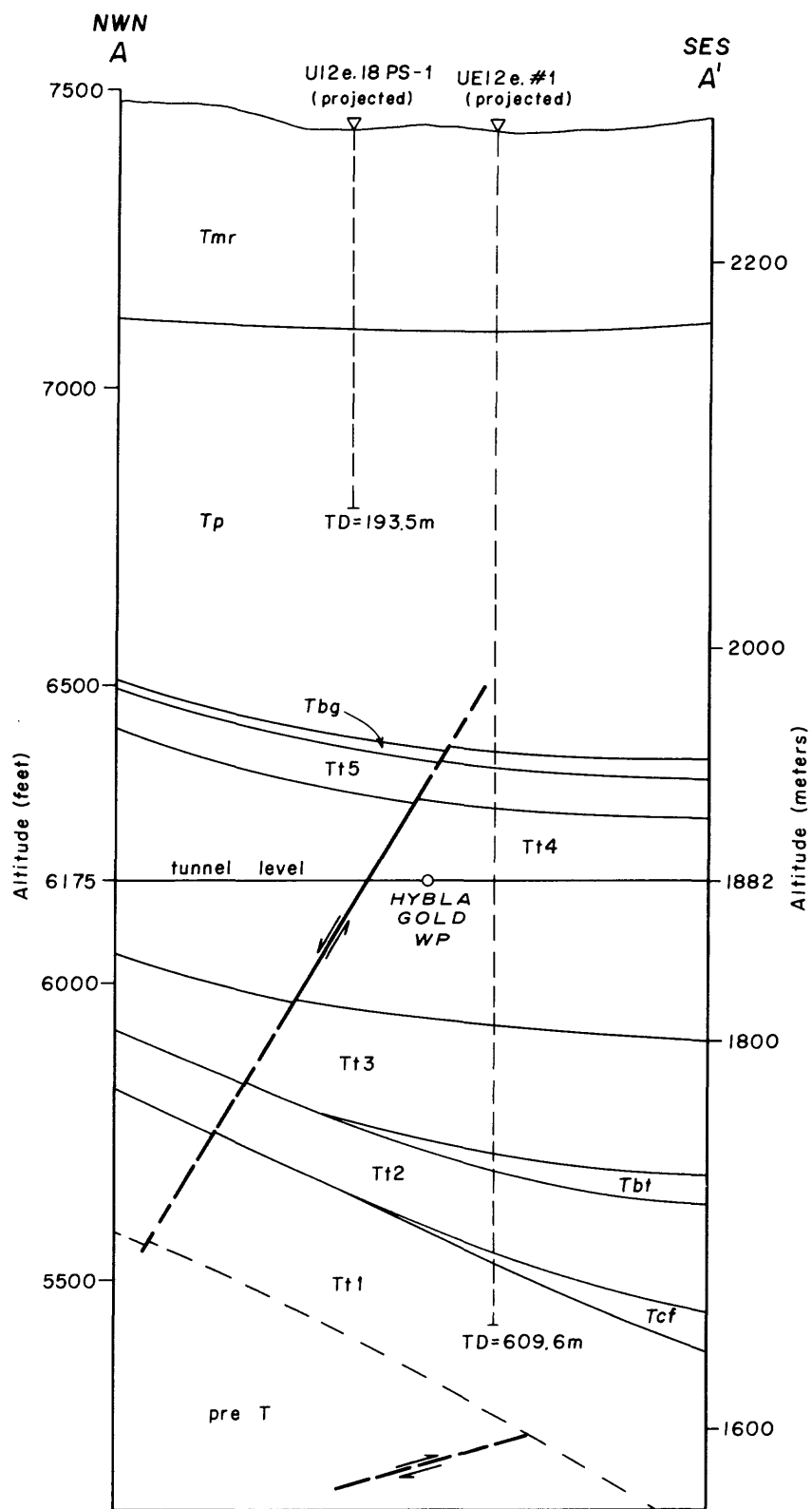
Figure 6.--Cross section A-A' through Hybla Gold working point,
normal to the Hybla Gold main drift. (See fig. 4 for
explanation of geologic unit symbols.)
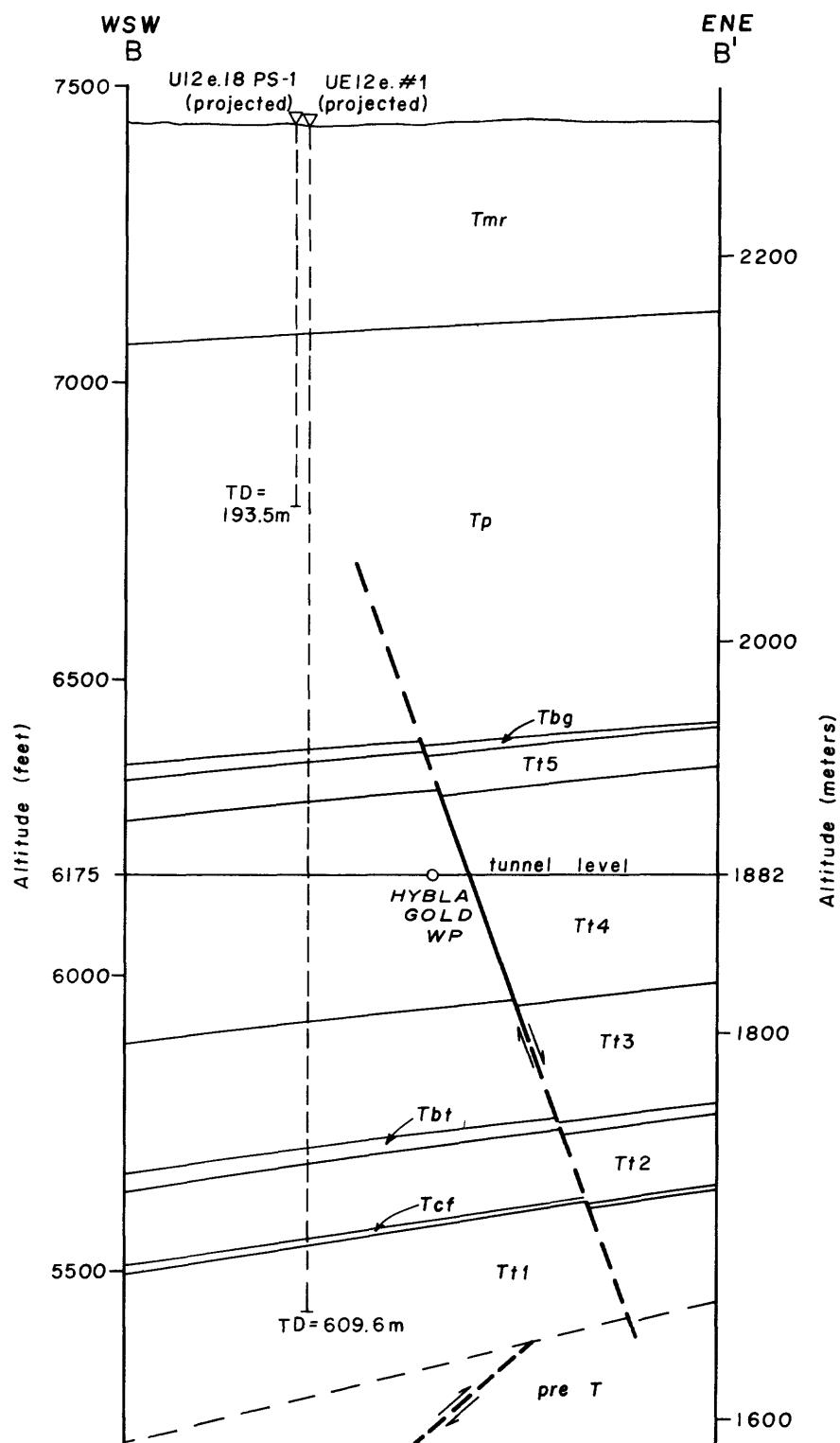
Figure 7.--Cross section B-B' through Hybla Gold working point,
along the Hybla Gold main drift. (See fig. 4 for explana-
tion of geologic unit symbols.)

suggests that the pre-Tertiary surface below the WP is also quartzite (fig. 8).

STRUCTURE

No significant structural features have been mapped in the vicinity of the Hybla Gold SGZ (surface ground zero). A photo lineation trending north-northwest is visible about 488 m (1,600 ft) west of SGZ, but field examination revealed no evidence of a fault of other structure (fig. 9). An east-west-trending monocline has been mapped approximately 114 m (375 ft) north of SGZ. This feature is represented by a steepening of the dip of the Rainier Mesa ash-flow tuff, and has been traced to a length of about 670 m (2,200 ft). Two possible origins are suggested for this feature: (1) the monocline is the surface expression of deposition over an erosional feature; or (2) the monocline is the expression of the end of an individual flow of the Rainier Mesa ash-flow unit.

At tunnel level, the U12e.20 drifts penetrate a small northeast-trending depositional syncline, the limbs of which dip 6°-7° (fig. 5). The Hybla Gold main drift parallels the axis of the fold. Detailed mapping of the Hybla Gold main drift showed a few small discontinuous fractures and faults (pl. 2). Many of the fractures are of low angle and show horizontal movement. These fractures are probably shock-induced as a result of the nearby Dining Car event. Few fractures were mapped in the auxiliary drift, possibly due to its greater distance from the Dining Car WP.

A classification system developed to quantify fault characteristics, as they relate to containment, is presented in table 2. No Class A faults cut the U12e.20 drifts, but four faults have been mapped in nearby drifts and exploratory drill holes. All four faults show normal displacements of less than 3 m (10 ft) (fig. 5). The northwest-striking fault, which passes about
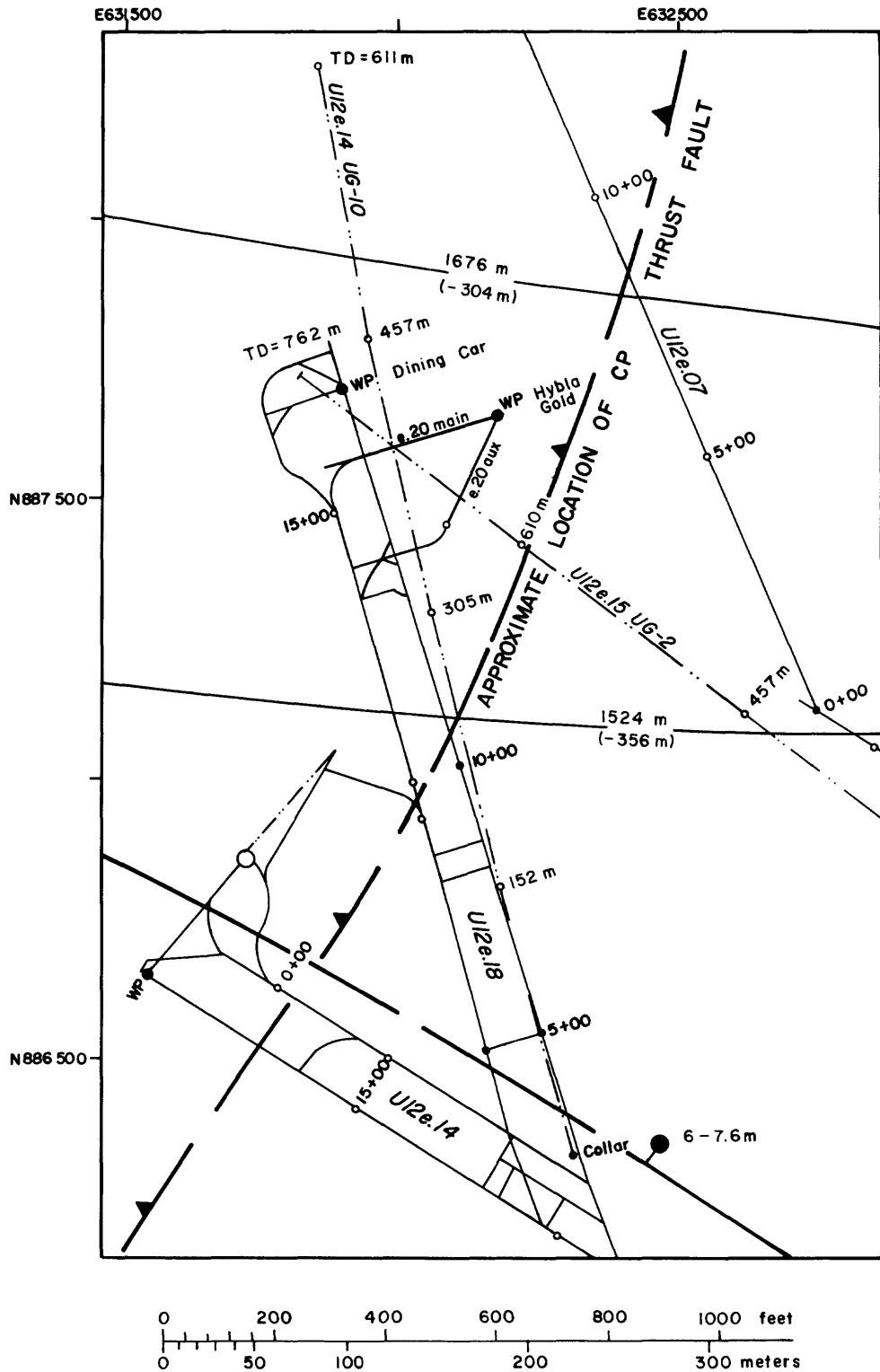
Figure 8.--Topographic map of pre-Tertiary surface below the U12e.20 (Hybla Gold) drifts.

13
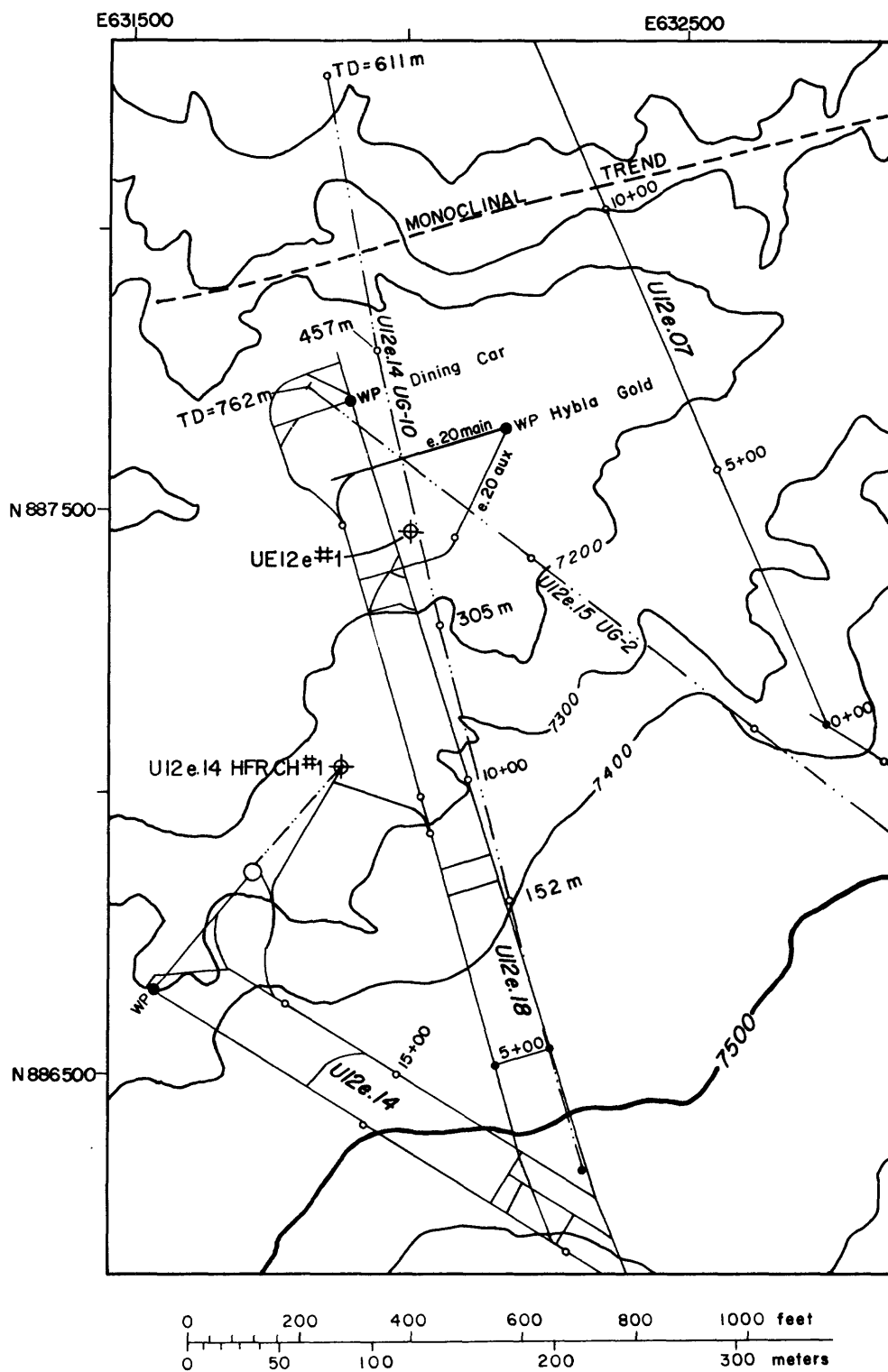
Figure 9.--Surface structural geology over the U12e.20 (Hybla Gold) drifts.

Table 2.--<u>Fault classification for tunnel sites</u>

Class	Description
A	May have any or all of following characteristics:
	1. Extends to surface.
	2. Connects two tunnels (bypass tunnels are not included as a second tunnel).
	3. Displacement is more than 3 m (10 ft).
	4. Fracture zone is 0.6 m (2 ft) wide or more at fault.
B	May be changed to Class A with more information or mining. May have one or more following characteristics:
	1. Displacement is less than 3 m (10 ft).
	2. Probable or known fault length is 61 m (200 ft) or more.
	3. Fracture zone is 0.6 m (2 ft) wide or less and is not healed or tightly filled.
C	May be changed to Class A or B with more information. Must have all of following characteristics:
	1. Less than 1.5 m (5 ft) of displacement.
	2. Probable or known fault length is 61 m (200 ft) or less.
	3. No associated fracturing.
	4. Fault is healed or tightly filled.

15.2 m (50 ft) northeast of the U12e.20 WP has been mapped in the U12e and

U12e.07 drifts, and identified in drill holes U12e.14 UG-10, U12e.20 HF-5, and

U12e.20 UG-2. The report on Dining Car geology (Steele and others, 1978)

reported this fault to be a reverse fault. Further investigation and

reinterpretation, however, showed that this fault is a normal fault. This

fault is classified as a Class A fault because it connects two tunnels. The

other three faults strike northeast and pass 183-290 m (600-950 ft) from the

Hybla Gold WP. These faults have been mapped in the U12e.07 drift, and the

fault nearest the Hybla Gold WP was seen in the U12e.14 UG-10 drill hole. All

three of these faults can be classified as Class C faults.

The pre-Tertiary surface below the Hybla Gold drifts is believed to be

cut by the CP thrust fault. The WP is west of the probable trace of the

thrust fault on the pre-Tertiary surface (fig. 8). Data on this fault are

scanty, but it is believed to trend north-northeast and is known not to extend

into the overlying tuffs (figs. 6, 7). The approximate shape of the pre-

Tertiary surface under the U12e.20 drifts slopes toward the south (figs. 6, 7,

8).

ENGINEERING GEOLOGY

The Hybla Gold main and auxiliary drifts penetrate zeolitized and

competent tuffs of tunnel bed 4, subunits K and J. The mappable effects of

the nearby Dining Car experiment on the Hybla Gold rocks were limited to

discontinuous fractures and faults (pl. 2). No continuous fractures were

observed which could be related to the Dining Car explosion. The tuff in the

U12e.20 drifts tended to disaggregate at the closest approach to the Dining

Car WP. Slabbing occurred in the main drift near CS 3+50. This slabbing may

have been the result of explosion-induced shock-loading from the Dining Car

event. Standard ground support techniques, which included rock-bolting, wire

mesh, and shotcrete, controlled these problems (Fenix & Scisson, Inc., written commun., 1978). A study by Terra Tek, Inc., for the DNA (Butters and LaComb, 1980) was undertaken to examine material properties of rocks in the Hybla Gold area both before and after the Dining Car event. Certain changes in physical properties did occur, and the development of microfractures in conjunction with the Dining Car explosion is postulated to be the cause of these changes. Water encountered during the mining of the main and auxiliary drifts was probably the result of down-dip flow of perched water toward the axis of the syncline.

DRILL HOLES

No lengthy zones of incompetent rock were found in the nearby vertical exploratory drill hole UE12e#1. Exploratory holes U12e.14 UG-10 and U12e.15 UG-2 were drilled before either Dining Car or Hybla Gold drifts were mined. Drill hole U12e.14 UG-10 intersected two of the faults in the area of the Hybla Gold WP. Drill hole U12e.15 UG-2 did not penetrate any of the faults near the Hybla Gold WP, but did pass through the region of the U12e.20 main and auxiliary drifts.

Drill holes U12e.18 DNRE-1 and U12e.18 DNRE-2 were drilled from tunnel level into the Dining Car chimney, and the vertical hole U12e.18 PS-1 was drilled from the surface (pl. 1; figs. 6, 7). Drill hole U12e.18 DNRE-1 was drilled horizontally from the U12e.18 main drift reentry into the Dining Car chimney. The boundaries of the chimney were mapped in the hole at 57.6-60.7 m (189-199 ft), and 130.8-136.9 m (429-449 ft). Drill hole U12e.18 DNRE-2 was drilled at a 30° angle up into the Dining Car chimney, and penetrated the chimney at 65.5-67.1 m (215-220 ft). Drill hole U12e.18 PS-1 was drilled from the surface of Rainier Mesa over the Dining Car WP into the chimney, which was mapped at 171.6 m (563 ft) in the drill hole (S. G. Steele, written commun., 1977).

17

Four horizontal holes were drilled in the vicinity of the Hybla Gold site. Exploratory holes U12e.20 UG-1, U12e.20 UG-2, and U12e.20 UG-3 were drilled to aid geologic investigations, and drill hole U12e.20 HF-5 was drilled for a hydrofracturing experiment. No faults were penetrated in drill hole U12e.20 UG-1, which was drilled from the U12e.18 main drift reentry and directed south of the Dining Car chimney area to a TD (total depth) of 157 m (515 ft). Drill hole U12e.20 UG-2 was drilled from the U12e.18 main drift and directed north of the Dining Car chimney to a TD of 124.4 m (408 ft). The fault northwest of the Hybla Gold WP was penetrated in this hole. Drill hole U12e.20 UG-3 was drilled along the alinement of the U12e.20 main drift to the WP before the drift was mined. The U12e.20 HF-5 hole was drilled from the WP northe st to TD of 27.7 m (91 ft), and also intersected the fault seen in the U12e.20 UG-2 drill hole (fig. 5, pl. 2).

SUMMARY

The Hybla Gold (U12e.20) drifts parallel the axis of a small depositional syncline, and penetrate ash-fall tuffs of tunnel bed 4, subunits K and J. No faults cross the experiment drifts. Four small-displacement normal faults were mapped in drill holes.

The design of the Hybla Gold experiment required its siting near the chimney of the Dining Car event. Detailed observations in the Hybla Gold drifts showed that the mappable geologic effects of the Dining Car explosion were limited to discontinuous faults and fractures; however, laboratory tests revealed fracturing on a microscopic scale.

REFERENCES CITED

Butters, S. W., and LaComb, J. W., 1980, Effect of shock loading on rock properties and in situ states: Terra Tek Report DNA-5380T, 34 p.

Steele, S. G., Fairer, G. M., Carroll, R. D., and Cunningham, M. J., 1978, U.S. Geological Survey investigations in connection with the Dining Car event, U12e.18 tunnel, Rainier Mesa, Nevada Test Site: U.S. Geological Survey Report USGS-474-246, 66 p.; available only from U.S. Department of Commerce, National Technical Information Service, Springfield, VA 22161.

GEOPHYSICAL INVESTIGATIONS

By

R. D. Carroll

ABSTRACT

The Hybla Gold tunnel complex passed within 3 m (10 ft) of the chimney formed by the collapse of the Dining Car event. Geophysical surveys in the chimney rubble and adjacent rock consisted of density, gamma-ray, caliper, resistivity, seismic, and temperature surveys in horizontal and vertical drill holes. Resistivity, magnetic, and shear- and compressional-wave seismic surveys were obtained in the tunnels. No density contrast was noted between chimney material and the tuff outside the chimney. The major changes in the properties measured in situ occurred expectedly in the velocity, temperature, and radioactivity of the chimney material. Outside the chimney the major measured effect was on the in situ shear-wave velocity, which was reduced as much as 50 percent of preshot values. This is about 2 1/2 times the percent reduction in the associated compressional-wave velocity. In addition, the postshot in situ shear velocities measured within the entire Hybla Gold complex were lowered to the extent that they are less than any observed for preshot experience in 15 other tunnels. The in situ shear-velocity data also indicate a demarcation, reflected by a strong velocity discontinuity, between tuff within about one chimney radius of the chimney boundary and the material at greater ranges. This zone is also defined in comparisons of preshot and postshot core velocities. Changes in the core velocity at greater ranges are not generally observed. The core velocities are consistently higher than in situ data throughout the entire complex.

The in situ shear-velocity data are believed to reflect two zones outside the chimney. An inner zone of microfailure, or pervasive failure of the tuff matrix due to shock loading, and a zone of macrofailure due to failure along joints, bedding planes, and occasional new fractures. The difference in the ability of the laboratory and in situ techniques to sample these mechanisms is the main reason for the observed differences in velocity.

The in situ shear velocity data also suggest that the zone of macrofailure includes the entire Hybla Gold drift complex and extends to a range of greater than three chimney radii from the WP which was the limit of the postshot seismic surveys. Thus, the shear velocity appears to be a highly diagnostic measurement in terms of defining the range of effects of nuclear explosions.

INTRODUCTION

Geophysical logging and seismic surveys were made in connection with the Hybla Gold event (U12e.20 drift) in order to characterize the rock properties in the vicinity. Geophysical investigations in vertical and horizontal drill holes and tunnel seismic studies made in the vicinity of and prior to Dining Car (U12e.18 drift) have been previously reported (Carroll and Cunningham, 1978). Data pertinent to comparisons with Hybla Gold are included in this report. Geophysical studies were made in both horizontal and vertical holes drilled into the Dining Car chimney prior to the mining of the Hybla Gold tunnel complex. The purpose of the studies was to investigate the properties of the rock in and near the cavity and chimney formed by the Dining Car event. After mining of the Hybla Gold complex, seismic, resistivity, and magnetic surveys were made in the tunnel and in boreholes to further define the bulk properties of the rock surrounding the chimney. A summary of the geophysical investigations is listed in table 3. With the exception of

21

Table 3.--Summary of geophysical data obtained in connection with the
Hybla Gold event

Drill holes

Hole designation	Geophysical logs	Logging organization
U12e.18 PS-1	Density, gamma-ray/neutron, caliper, geophone survey	Birdwell
U12e.20 UG-1	Gamma-ray (2), caliper, temperature (2)	Birdwell
	Geophone survey	USGS
U12e.20 UG-2	Gamma-ray, caliper, temperature	Birdwell
	Geophone survey	USGS
U12e.18 DNRE-1	Gamma-ray, caliper, temperature	Birdwell
	Gamma-ray, density, geophone survey	USGS
U12e.18 DNRE-2	None	---
U12e.20 HF-5	Resistivity, geophone survey	USGS

Tunnel

Tunnel station	Geophysical survey
CS 1+84 - 4+26 (main drift)	Shear- and compressional-wave velocity survey
CS 1+64 - 4+28 (main drift)	Magnetic field intensity and inclination
CS 0+76T[1] - 4+05 (main drift)	Resistivity
CS 2+00 - 4+20 (auxiliary drift)	Shear- and compressional-wave survey

[1]"T" refers to station in tail drift (pl. 1).

U12e.18 PS-1, which was drilled into the chimney from the surface of Rainier Mesa, all of the holes listed in table 3 were drilled from tunnel level. Locations where geophysical surveys were made in the tunnel are shown on plate 1.

Acknowledgments

INVESTIGATIONS IN HOLES IN THE DINING CAR CHIMNEY AREA

The locations of the five holes (one vertical and four horizontal) drilled in the vicinity of the Dining Car chimney prior to the mining of the Hybla Gold drift complex are shown on plate 1. Three of these holes (PS-1, DNRE-1, DNRE-2) directly penetrated the chimney region and the other two (UG-1, UG-2) sampled the rock immediately adjacent. No geophysical measurements were made in the U12e.18 DNRE-2 drill hole.

U12e.18 PS-1 Vertical Drill Hole

The U12e.18 PS-1 drill hole was drilled from the top of Rainier Mesa directly above the postshot Dining Car WP to a depth of 196.6 m (635 ft), penetrating the ash flow of the Rainier Mesa Member and bottoming in the vitric Paintbrush Tuff. The geophysical logs obtained in the hole are shown on figure 10 and the reduced density data are listed in table 4. The data on figure 10 are digital reproductions, the digitization performed on 1.5-m (5-ft) intervals. A velocity survey was obtained using an inhole geophone and a
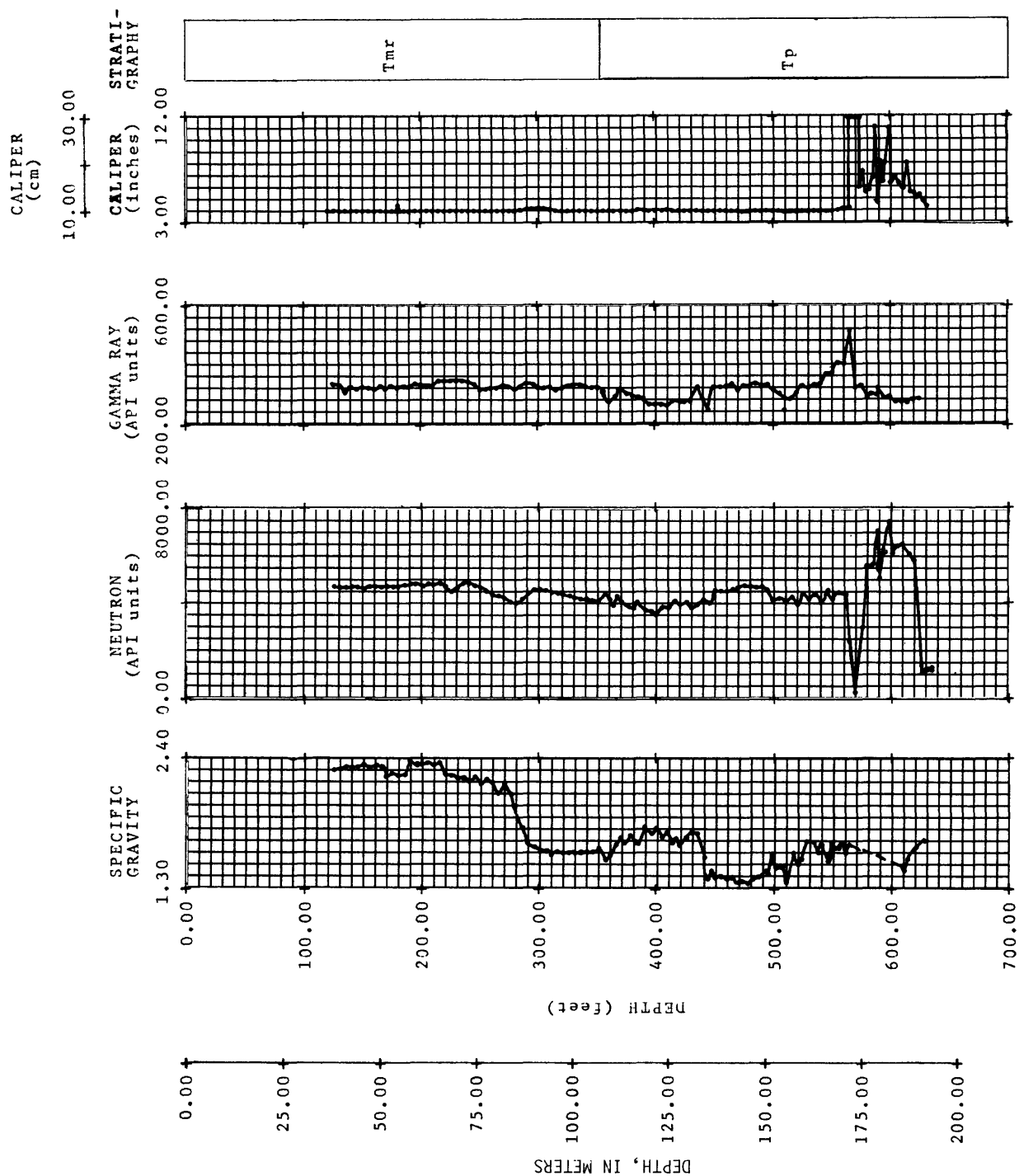
Figure 10.--Results of geophysical logging in U12e.18 PS-1 hole.

24

Table 4.--Values of specific gravity from density log--U12e.18 PS-1

Depth (feet)		Depth (meters)		Specific Gravity	
.1250e	3	.3810e	2	.2300e	1
.1300e	3	.3962e	2	.2310e	1
.1350e	3	.4114e	2	.2330e	1
.1400e	3	.4267e	2	.2320e	1
.1450e	3	.4419e	2	.2330e	1
.1500e	3	.4572e	2	.2350e	1
.1550e	3	.4724e	2	.2320e	1
.1600e	3	.4876e	2	.2330e	1
.1650e	3	.5029e	2	.2330e	1
.1700e	3	.5181e	2	.2240e	1
.1750e	3	.5334e	2	.2270e	1
.1800e	3	.5486e	2	.2250e	1
.1860e	3	.5669e	2	.2260e	1
.1900e	3	.5791e	2	.2380e	1
.1960e	3	.5974e	2	.2350e	1
.2000e	3	.6096e	2	.2350e	1
.2050e	3	.6248e	2	.2360e	1
.2100e	3	.6400e	2	.2340e	1
.2150e	3	.6553e	2	.2360e	1
.2200e	3	.6705e	2	.2260e	1
.2250e	3	.6858e	2	.2250e	1
.2300e	3	.7010e	2	.2230e	1
.2350e	3	.7162e	2	.2230e	1
.2400e	3	.7315e	2	.2200e	1
.2450e	3	.7467e	2	.2240e	1
.2500e	3	.7620e	2	.2180e	1
.2550e	3	.7772e	2	.2220e	1
.2600e	3	.7924e	2	.2190e	1
.2650e	3	.8077e	2	.2100e	1
.2700e	3	.8229e	2	.2180e	1
.2760e	3	.8412e	2	.2090e	1
.2800e	3	.8534e	2	.1990e	1
.2860e	3	.8717e	2	.1810e	1
.2900e	3	.8839e	2	.1680e	1
.2960e	3	.9022e	2	.1650e	1
.3010e	3	.9174e	2	.1620e	1
.3060e	3	.9326e	2	.1610e	1
.3100e	3	.9448e	2	.1580e	1
.3150e	3	.9601e	2	.1610e	1
.3200e	3	.9753e	2	.1600e	1
.3250e	3	.9906e	2	.1600e	1
.3300e	3	.1005e	3	.1600e	1
.3350e	3	.1021e	3	.1610e	1
.3400e	3	.1036e	3	.1610e	1
.3450e	3	.1051e	3	.1610e	1
.3500e	3	.1066e	3	.1640e	1
.3560e	3	.1085e	3	.1540e	1
.3600e	3	.1097e	3	.1580e	1
.3650e	3	.1112e	3	.1670e	1
.3690e	3	.1124e	3	.1730e	1

Table 4.--Values of specific gravity from density log--U12e.18 PS-1--Continued

Depth (feet)		Depth (meters)		Specific Gravity	
.3720e	3	.1133e	3	.1690e	1
.3770e	3	.1149e	3	.1750e	1
.3830e	3	.1167e	3	.1680e	1
.3900e	3	.1188e	3	.1820e	1
.3960e	3	.1207e	3	.1760e	1
.4000e	3	.1219e	3	.1810e	1
.4050e	3	.1234e	3	.1730e	1
.4090e	3	.1246e	3	.1770e	1
.4140e	3	.1261e	3	.1680e	1
.4170e	3	.1271e	3	.1720e	1
.4200e	3	.1280e	3	.1660e	1
.4260e	3	.1298e	3	.1730e	1
.4300e	3	.1310e	3	.1770e	1
.4350e	3	.1325e	3	.1760e	1
.4410e	3	.1344e	3	.1560e	1
.4440e	3	.1353e	3	.1380e	1
.4470e	3	.1362e	3	.1450e	1
.4500e	3	.1371e	3	.1390e	1
.4550e	3	.1386e	3	.1400e	1
.4600e	3	.1402e	3	.1380e	1
.4640e	3	.1414e	3	.1390e	1
.4700e	3	.1432e	3	.1350e	1
.4730e	3	.1441e	3	.1360e	1
.4780e	3	.1456e	3	.1340e	1
.4820e	3	.1469e	3	.1380e	1
.4870e	3	.1484e	3	.1400e	1
.4930e	3	.1502e	3	.1450e	1
.4950e	3	.1508e	3	.1420e	1
.4980e	3	.1517e	3	.1580e	1
.5020e	3	.1530e	3	.1480e	1
.5070e	3	.1545e	3	.1480e	1
.5110e	3	.1557e	3	.1350e	1
.5170e	3	.1575e	3	.1600e	1
.5210e	3	.1588e	3	.1500e	1
.5240e	3	.1597e	3	.1550e	1
.5280e	3	.1609e	3	.1700e	1
.5340e	3	.1627e	3	.1690e	1
.5380e	3	.1639e	3	.1600e	1
.5410e	3	.1648e	3	.1670e	1
.5460e	3	.1664e	3	.1530e	1
.5490e	3	.1673e	3	.1690e	1
.5550e	3	.1691e	3	.1640e	1
.5580e	3	.1700e	3	.1680e	1
.5610e	3	.1709e	3	.1600e	1
.5640e	3	.1719e	3	.1670e	1
.6090e	3	.1856e	3	.1490e	1
.6110e	3	.1862e	3	.1450e	1
.6150e	3	.1874e	3	.1550e	1
.6220e	3	.1895e	3	.1650e	1
.6290e	3	.1917e	3	.1700e	1

Vibroseis[3] surface source. The Vibroseis results are shown on figure 11 and listed in table 5.

Core recovery was lost in the hole at 171.6 m (563 ft). This is coincident with excessive caving of the hole at 172.8 m (567 ft) indicated on the caliper log, thus, defining this depth as the top of the chimney. The tunnel-level elevation of Dining Car at 1,822.4 m (6,176 ft) places the top of the chimney at 210.0 m (689 ft) above the Dining Car WP.

Except for the erratic behavior of the geophysical logs caused by caving at the bottom of the hole, the log-derived properties are typical of the undisturbed geologic setting. The welded to nonwelded transition in the density of the Rainier Mesa Member at about 88.3 m (290 ft) is the only significant excursion on the logs above the top of the chimney.

The decrease in velocity with depth recorded on the inhole velocity survey reflects the effect of the high-velocity welded tuff of the Rainier Mesa Member overlying the low-velocity friable Paintbrush Tuff.

U12e.18 DNRE-1, U12e.20 UG-1 and UG-2 Horizontal Drill Holes

Of the horizontal holes, only U12e.18 DNRE-1 was drilled directly into the chimney from tunnel level (pl. 1). Both U12e.18 DNRE-1 and U12e.20 UG-2 produced water during logging. These holes were logged in February and March 1977, which was 22 months after the Dining Car event. The amplitudes of some of the logs have been suppressed on the figures to allow comparisons of all logs on the same scale.

Gamma-ray Logs

The gamma-ray logs obtained by Birdwell in U12e.18 DNRE-1 and U12e.20 UG-2 holes are shown on figure 12. The log run in the chimney in hole DNRE-1

---

[3]Use of brand name is for descriptive purposes only and does not necessarily constitute endorsement by the Geological Survey.
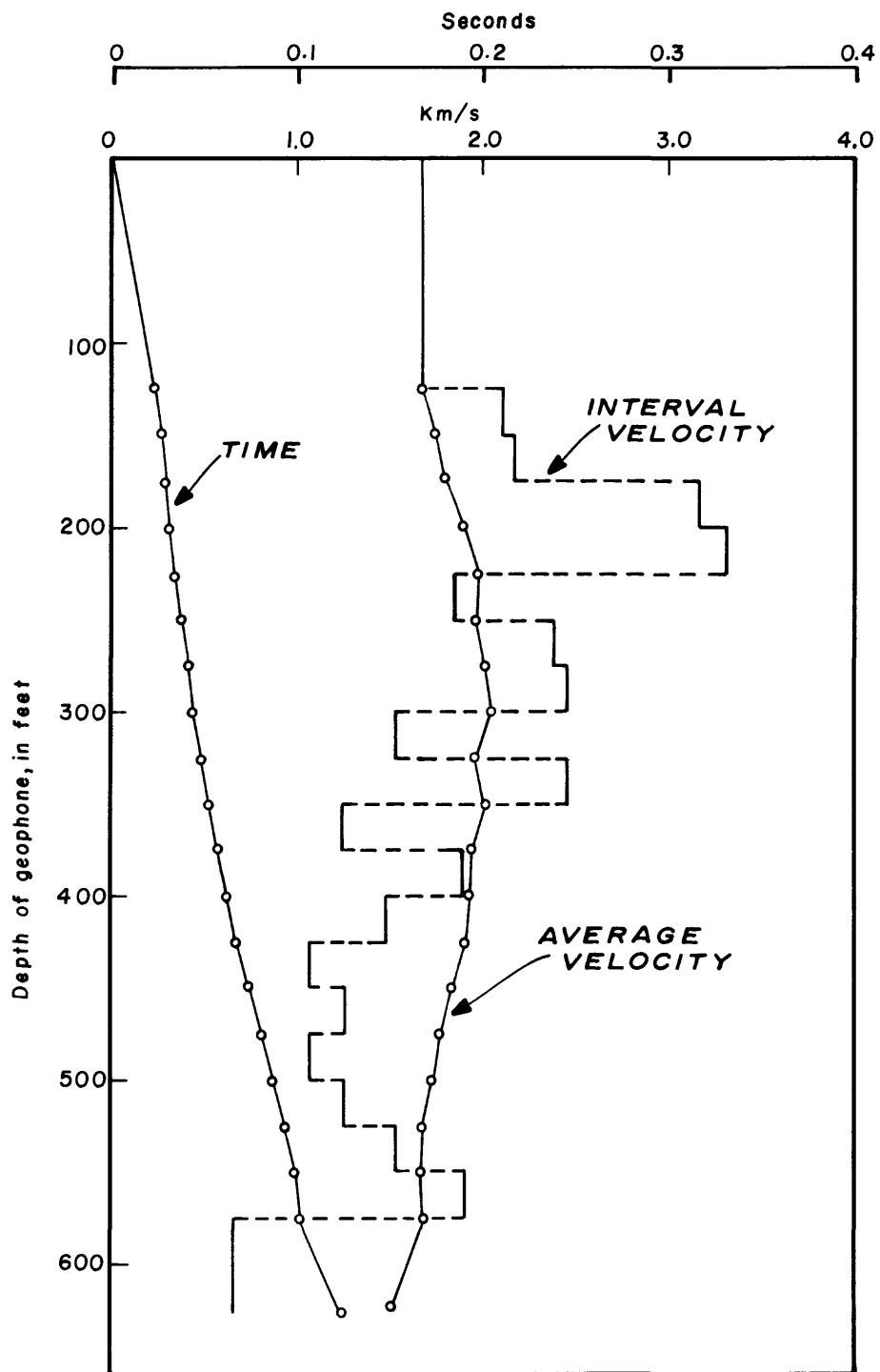
Figure 11.--Results of Vibroseis survey in U12e.18 PS-1 hole.
(Data from Birdwell, Inc.)

Table 5.--Birdwell interpretation of results of Vibroseis survey obtained in U12e.18 PS-1

[To convert from feet to meters, multiply by 0.3048]

SEISMIC VELOCITY SURVEY				
Depth (ft)	Grade of arrival[1]	Time (s)	Va^2 (m/s)	Vi^3 (m/s)
125	P	0.0226	1,686	1,686
150	F	.0262	1,745	2,117
175	F	.0297	1,796	2,177
200	P	.0321	1,899	3,175
225	P	.0344	1,994	3,313
250	G	.0385	1,979	1,859
275	G	.0417	2,010	2,381
300	G	.0448	2,041	2,458
325	G	.0498	1,989	1,524
350	F	.0529	2,017	2,458
375	G	.0590	1,937	1,249
400	G	.0630	1,935	1,905
425	G	.0681	1,902	1,494
450	F	.0751	1,826	1,088
475	F	.0811	1,785	1,270
500	G	.0881	1,730	1,088
525	G	.0942	1,699	1,249
550	G	.0992	1,690	1,524
575	P	.1032	1,698	1,905
600	?	---	---	---
625	P	.1262	1,509	663

[1]G=good, F=fair, P=poor.
[2]Va=average velocity.
[3]Vi=interval velocity.

GAMMA-RAY

(kilocounts/   (kilocounts/
  minute)   minute)

0.00   400.00   0.00   400.00

DEPTH, IN METERS

U12e.20, UG-1   U12e.18, DNRE-1   U12e.20, UG-2

Figure 12.--Gamma-ray logs obtained in three horizontal holes in
the Dining Car chimney area.

30
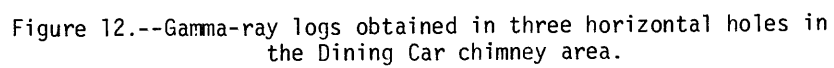
was a high-intensity log and is thus quite insensitive to low-level gamma
activity. No scale is available for that log. The far edge of the chimney
may be noted by the excursions on the log centered at 135 m (443 ft). Because
of the insensitivity of the log the near edge of the chimney cannot be
defined. A gamma-ray log (fig. 13) was also run through the near boundary of
the chimney by the USGS in order to ascertain the background effects of
radiation prior to running a density log in this hole. The near boundary of
the chimney may be defined from this log by noting the change in radiation
level near 58 m (190 ft).

The log run in the UG-2 hole is difficult to evaluate because it was run
inside the drill string. Consequently, the shielding effects of the drill
steel on the count rate result in a lower value than would be found in an open
hole. Because the gamma-ray tool used in this hole is similar to the one used
in the UE12e#1 vertical hole (Carroll and Cunningham, 1978), some direct
comparisons with normal background can be made. The UE12e#1 log indicates a
5-6 kilocounts/min count rate in the tunnel beds of interest with about a
1 kilocount/min reduction in the count rate in the casing at the surface.
This suggests that the log run in the UG-2 drill hole recorded a radiation
level essentially at the background level for the tuff.

The gamma-ray log from the UG-1 drill hole indicates a count rate above
background, particularly in the vicinity of the drifts associated with the
side pipe experiment on the Dining Car event.

Temperature Logs

The temperature logs from the three drill holes in and near the chimney
are reproduced on figure 14. The maximum reading in the chimney was about
60°C (141°F). Normal rock temperature in the tunnel beds as determined by the
author by monitoring thermistors anchored 12.2 m (40 ft) in the wall in the

BACKGROUND RADIATION, IN COUNTS/SECx10
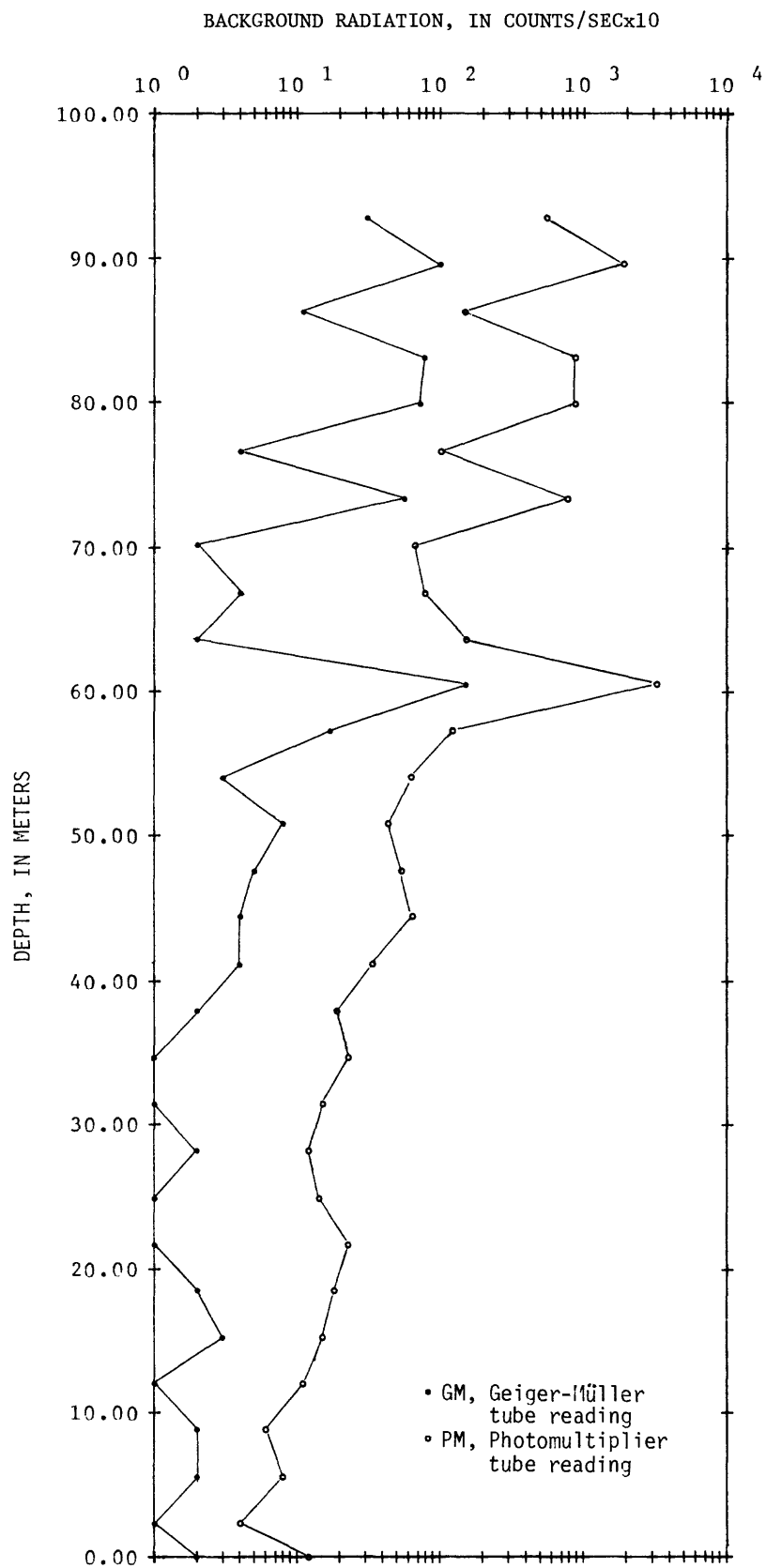
Figure 13.--Gamma-ray log obtained by USGS in portion of chimney in
U12e.18 DNRE-1 drill hole.
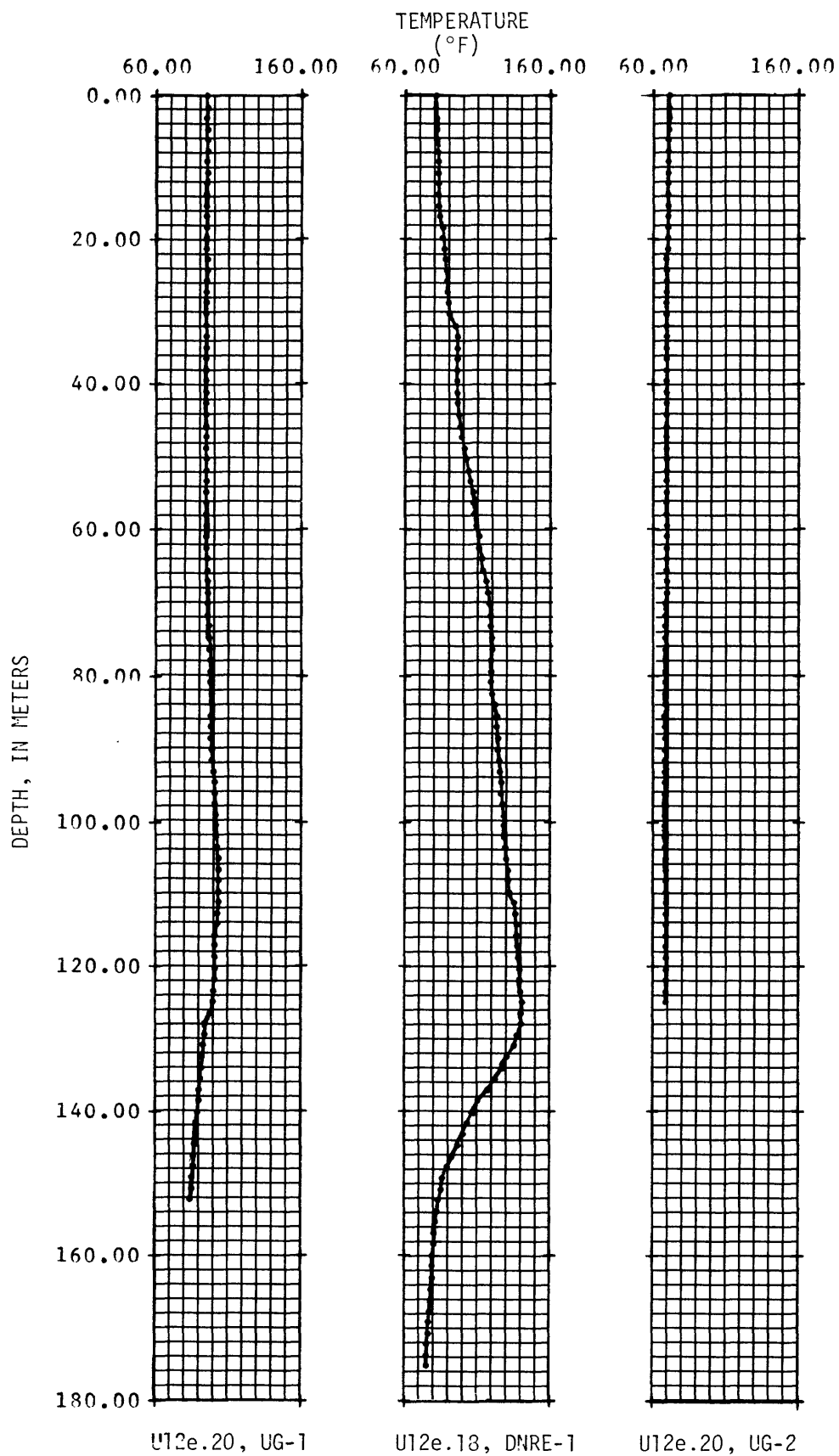
Figure 14.--Temperature logs obtained in three horizontal
holes in the Dining Car chimney area.

U12n.07 tunnel is 20°C (68°F). It is apparent that the rock in the UG-2 drill hole is essentially at normal temperature. The maximum temperature recorded in the UG-1 hole is about 39°C (103°F). The water flowing into the holes at the time of logging makes the significance of highs and lows difficult to assess. The maximum temperature in the UG-1 hole is located beyond the preshot location of the side pipe drift. The absence of anomalous temperatures in the UG-2 hole indicates asymmetry in the isotherms produced by the Dining Car event with respect to the WP, a condition which might be expected given the preshot geometry of the experimental drifts near the device.

Caliper Logs

The caliper logs obtained in the three holes in the chimney region are shown on figure 15. The logs all show deterioration of the holes. This does not appear to be a function of proximity to the chimney.

Density Log

A density log was run by the USGS in the DNRE-1 drill hole in an attempt to determine density contrasts in the chimney area. A dual detection density probe was run in the interval 14.9-95.7 m (49-314 ft). The data were obtained on discrete stations at 1.5-m (5-ft) intervals. The stations and values are listed in table 6.

To insure that radiation background did not affect the log, a log was run without the CS-137 gamma-ray source (fig. 13) and corrections were made where necessary to obtain the density.

The density log was obtained by pushing the tool inside NQ drill rod and out into the open hole using water pipe. A special sub was fabricated to replace the standard NQ drill bit in order to accommodate the tool diameter (5.4 cm). Density measurements were then made as the drill rod was pulled out
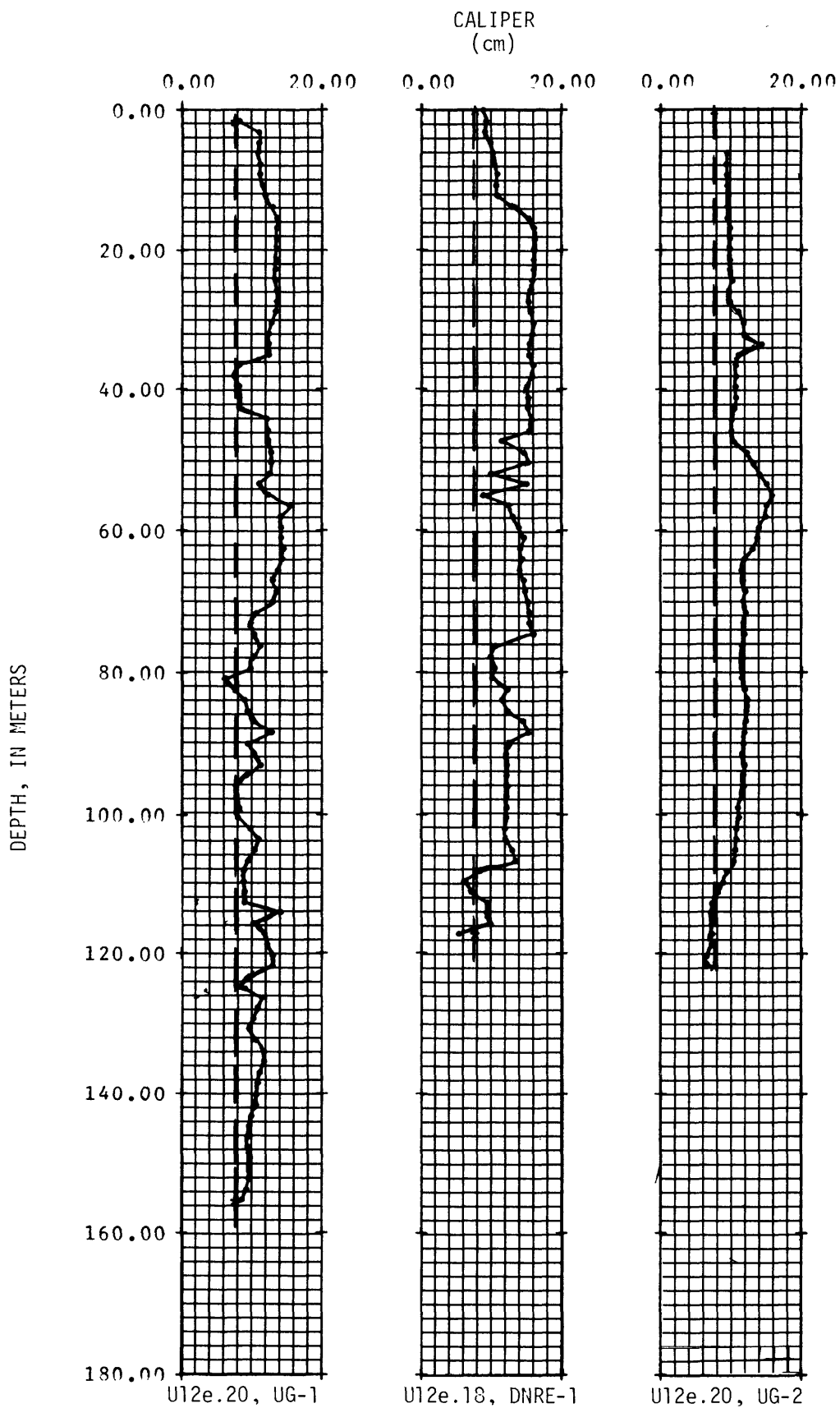
CALIPER
(cm)

Figure 15.--Caliper logs obtained in three horizontal
holes in the Dining Car chimney area.

35

Table 6.—Density values obtained in U12e.18,
DNRE-1 drill hole

[To convert from meters to feet, multiply by 3.2808]

Depth (meters)		Density (Mg/m^3)	
.1493e	2	.1910e	1
.1645e	2	.1930e	1
.1798e	2	.1820e	1
.1950e	2	.1840e	1
.2103e	2	.1900e	1
.2255e	2	.1850e	1
.2407e	2	.1750e	1
.2560e	2	.1825e	1
.2712e	2	.1780e	1
.2865e	2	.1800e	1
.3017e	2	.1805e	1
.3169e	2	.1930e	1
.3322e	2	.1880e	1
.3474e	2	.1860e	1
.3627e	2	.1885e	1
.3779e	2	.1900e	1
.3931e	2	.1815e	1
.4084e	2	.1845e	1
.4236e	2	.1865e	1
.4389e	2	.1835e	1
.4541e	2	.1880e	1
.4846e	2	.1825e	1
.5151e	2	.1870e	1
.5455e	2	.1800e	1
.5608e	2	.1840e	1
.5760e	2	.1785e	1
.5913e	2	.1930e	1
.6065e	2	.1860e	1
.6217e	2	.1800e	1
.6370e	2	.1890e	1
.6522e	2	.1800e	1
.6675e	2	.1910e	1
.6827e	2	.1620e	1
.6979e	2	.1770e	1
.7132e	2	.1700e	1
.7284e	2	.1870e	1
.7437e	2	.1830e	1
.7589e	2	.1830e	1
.7741e	2	---	
.7894e	2	---	
.8046e	2	.1940e	1
.8199e	2	.1820e	1
.8351e	2	.1860e	1
.8503e	2	.1850e	1
.8656e	2	.1920e	1
.8808e	2	.1950e	1
.8961e	2	.1850e	1
.9113e	2	.1790e	1
.9265e	2	.1700e	1
.9418e	2	.1850e	1
.9570e	2	.1780e	1

36

of the hole. At each station the tool was rotated 360° in 90° increments to obtain a minimum count rate. This was presumed to be equivalent to the minimum gap between the tool and the rock. The data were then reduced by applying a rib-and-spine algorithm for the two detector readings. The reduced data are shown graphically on figure 16. The values on the figure represent averages for the data inside and outside the chimney. The data in the chimney suggest a slightly higher geologic noise level; however, there is no measurable density contrast between the material inside and outside the chimney.

Geophone Surveys

Prior to any discussion of seismic measurements it is advisable to establish some basis for comparison of the postshot velocity data. This is done in table 7 where the average shear and compressional velocities representative of core and in situ values obtained prior to the Dining Car event are listed. Average values for core were obtained from measurements made on samples from tunnel beds 4J and 4K taken from three pre-Dining Car exploratory holes (Carroll and Cunningham, 1978). Two of these holes, U12e.14 UG-10 and U12e.15 UG-2, are shown on plate 1. The other hole was a vertical exploratory hole, UE12e#1. The core measurements were made by Terra Tek, Inc. The in situ seismic data listed in the table are the average of the seismic velocities obtained preshot from the seismic surveys nearest the Dining Car WP (fig. 17). The standard deviations of velocity listed in this report are one standard error of the slope of the time-distance plot.

DENSITY, IN MEGAGRAMS/CUBIC METERS
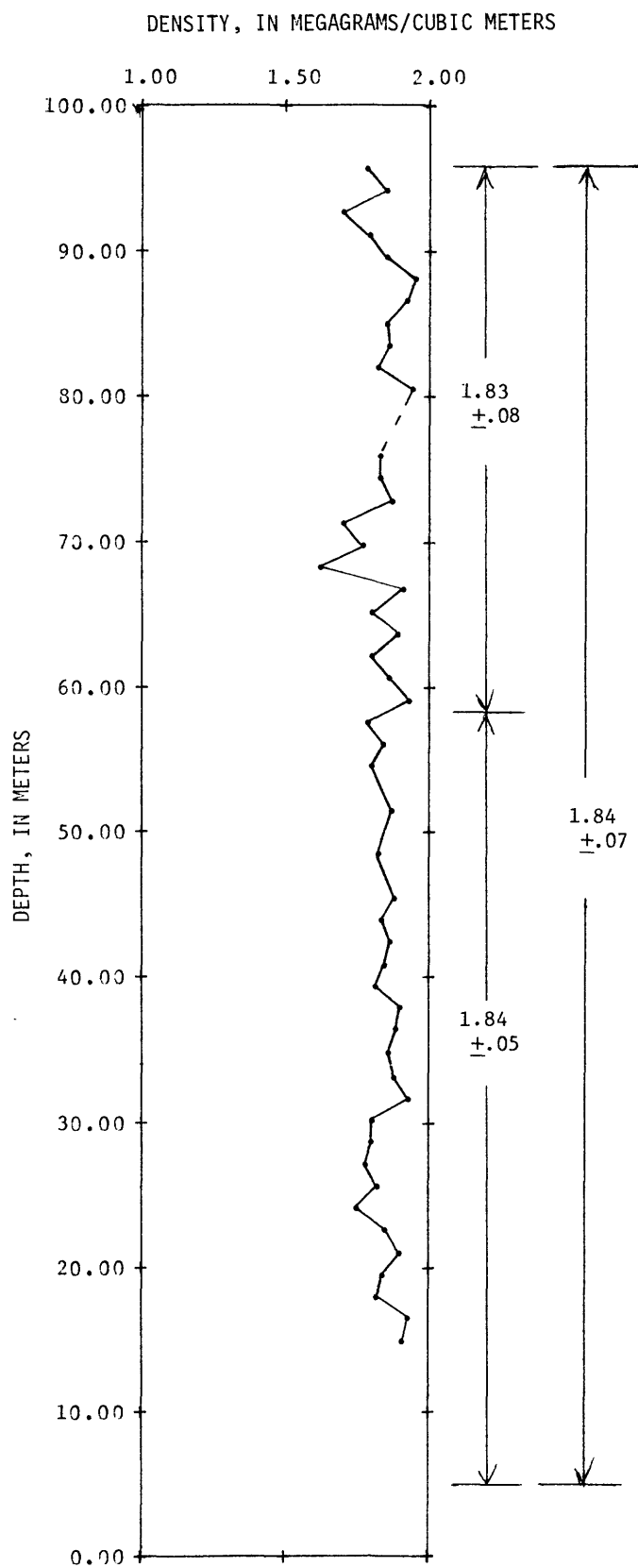
Figure 16.--Density obtained from geophysical log in
U12e.18 DNRE-1 drill hole.
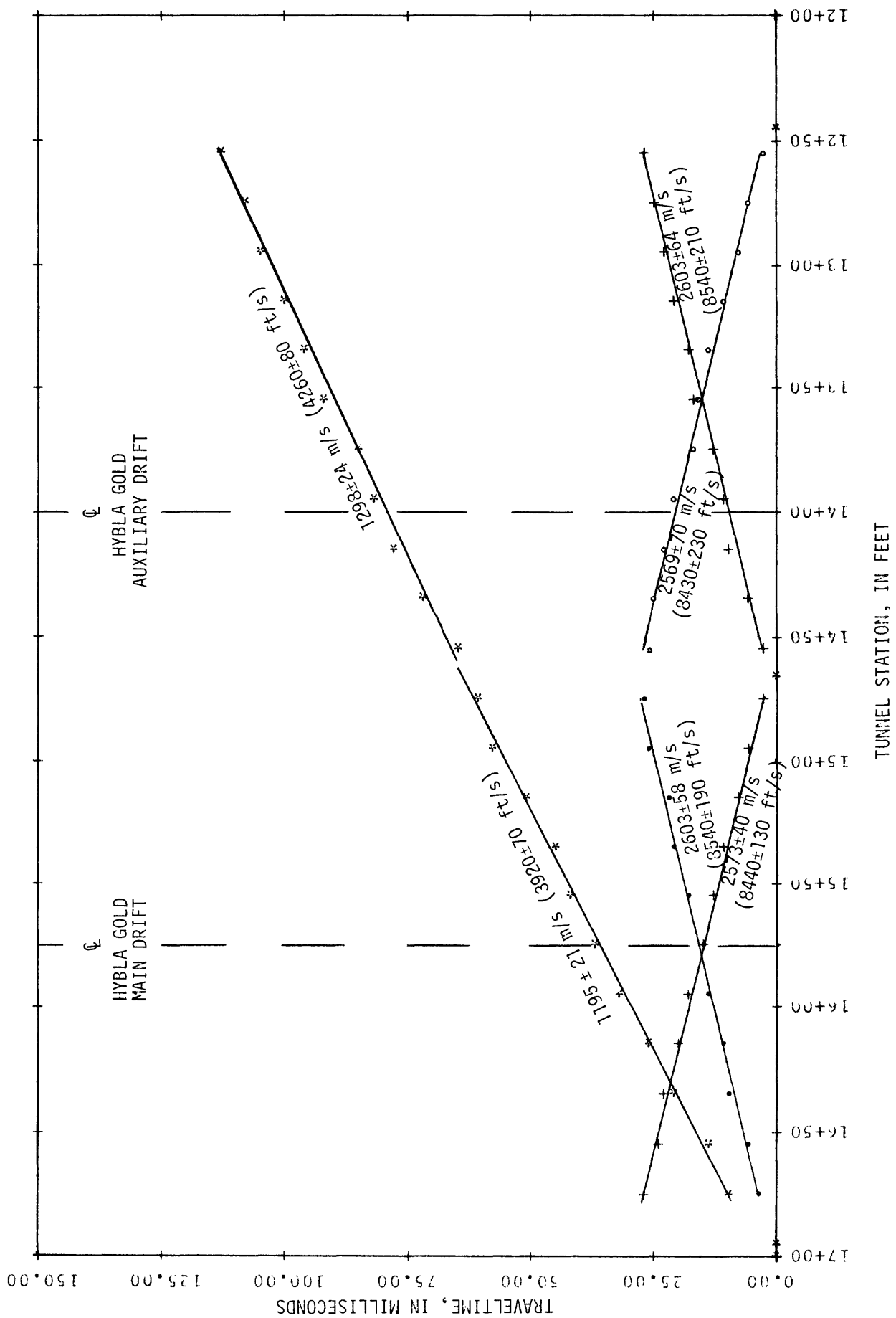
Figure 17.--Results of seismic survey in U12e.18 main drift prior to Dining Car event. The intersection of the Dining Car drift with the Hybla Gold complex occurs at CS 2+04 in the Hybla Gold main drift (from Carroll and Cunningham, 1978).

39

Table 7.--Averages of core and seismic velocities obtained prior
to the Dining Car event

	Compressional velocity (m/s)	Shear velocity (m/s)
Core	2,710 (49 samples)	1,350 (46 samples)
Seismic	2,590	1,250

The 4 percent difference in the preshot compressional velocities listed in the table is not significant. In addition, the compressional velocities showed no change on seismic surveys obtained after a 3-month period. The difference of 7 percent in the average shear velocities might be argued to suggest that there was some effect of bulk fracturing on the in situ shear data in the preshot survey. Such effects would of course not be observable in core measurements. The small differences in the preshot velocities between the two techniques makes the site an ideal one for pre- and postshot velocity comparisons. Large differences between velocities measured by the two techniques have occasionally been observed at other tunnel locations.

Core sampling was somewhat restricted in the postshot drilling because of cohesion problems with samples near the chimney. However, where sufficient core was available postshot we have an alternate method for comparison. Using core velocities one may construct a hypothetical seismic survey by integrating the times obtained from the velocity of the core. This was done with the core in three holes using the following relationship:

$$T = \sum_{n=1}^{N} \frac{d(n)-d(n-1)}{V_n} \tag{1}$$

where T is the total time of travel of a shear or compressional wave down the borehole to a depth d(n) of a core sample, V_n is the velocity of the core

sample, d(n-1) is the depth to the previous core point, and N is the total number of samples to the depth of interest. The core velocities were obtained from Terra-Tek, Inc. (Gardiner and others, 1977). Hypothetical seismic traveltime plots obtained from this procedure are shown in this report for the three holes for which data are considered adequate--U12e.20 UG-2, U12e.20 UG-3, and U12e.20 HF-5 (pl. 1).

Measurements of shear and compressional velocity were made at 11- to 12-m (36- to 40-ft) intervals in the three chimney area holes by fabricating a probe containing a geophone and preamp. The locations of the geophone stations are shown on plate 1. In the DNRE-1 hole, data were obtained by pumping the probe out of the bit and measuring at discrete intervals while 'ringing the drill rod out of the hole. In the UG-1 and UG-2 holes, the probe was placed in the open hole using sections of aluminum tubing to push the probe to the desired station. The energy source used was a 1,966 cm^3 (120 in^3) Par 1900 B air gun located in a pit in the crosscut at CS 13+25 in the Dining Car bypass drift (pl. 1). A schematic of the measuring system is shown on figure 18.

The air-gun source produces an asymmetric impulse, thereby imparting maximum energy to the ground in the shear mode. An example of a record is shown on figure 19.

The arrival times obtained in the three holes are plotted on figures 20 through 22. The results in the DNRE-1 hole were somewhat complicated by the presence of a seismic arrival coupled to the drill steel. This situation necessitated the selection of later arrivals.
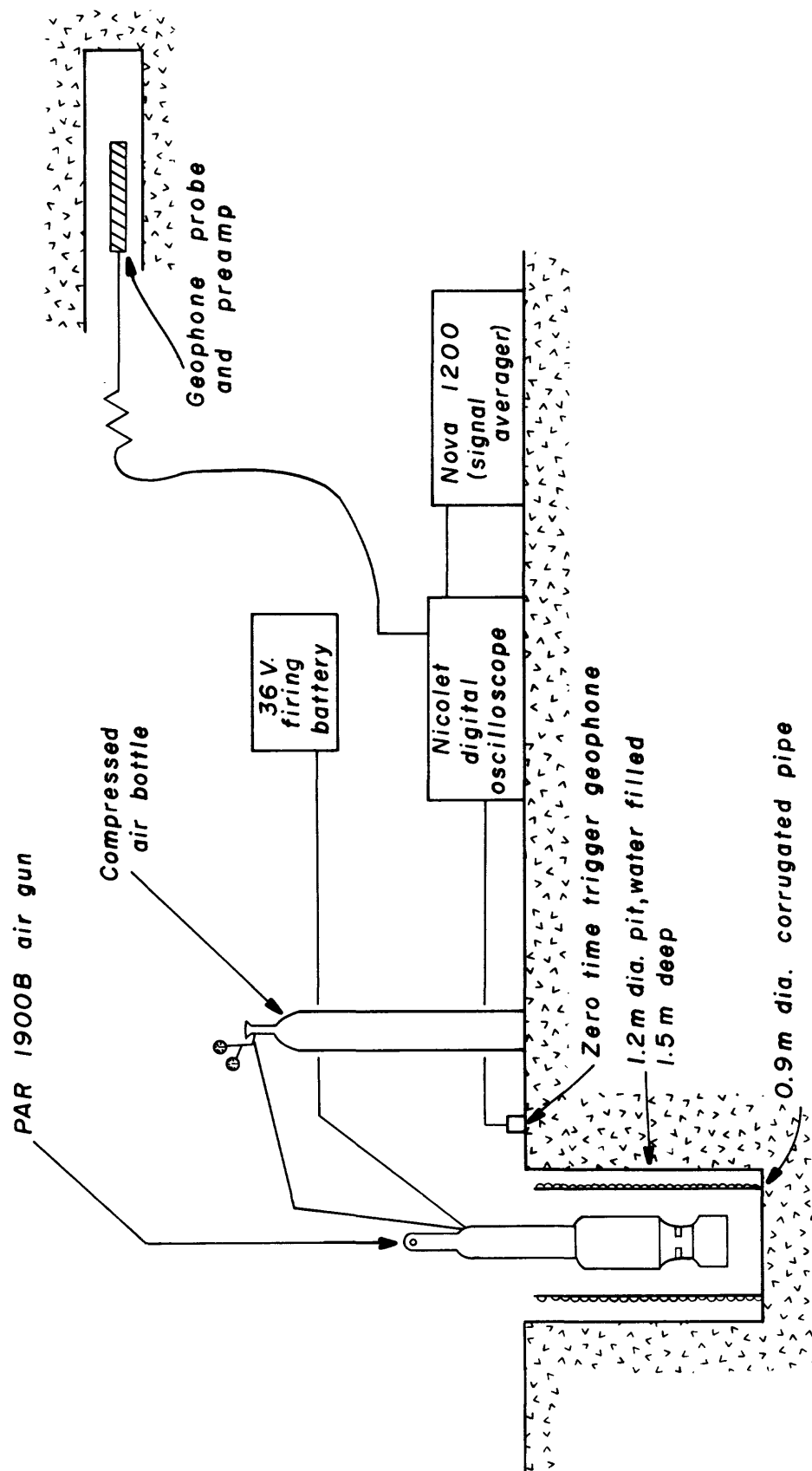
Figure 18.--Measurement system used to obtain shear and compressional velocities in horizontal drill holes near Dining Car chimney.
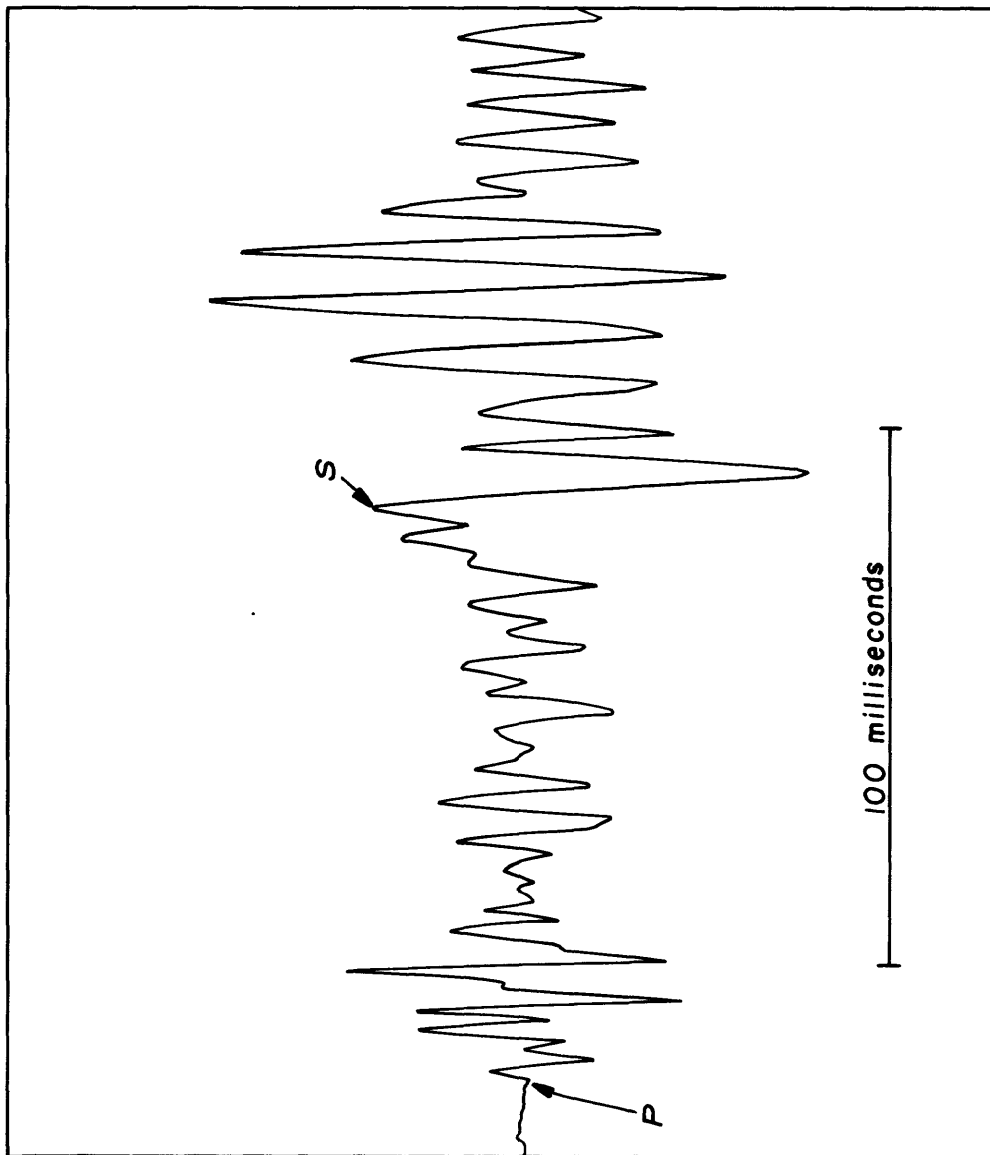
Figure 19.--Record obtained with air-gun source in U12e.20 UG-1 drill hole showing compressional (P) and shear (S) arrivals.

43
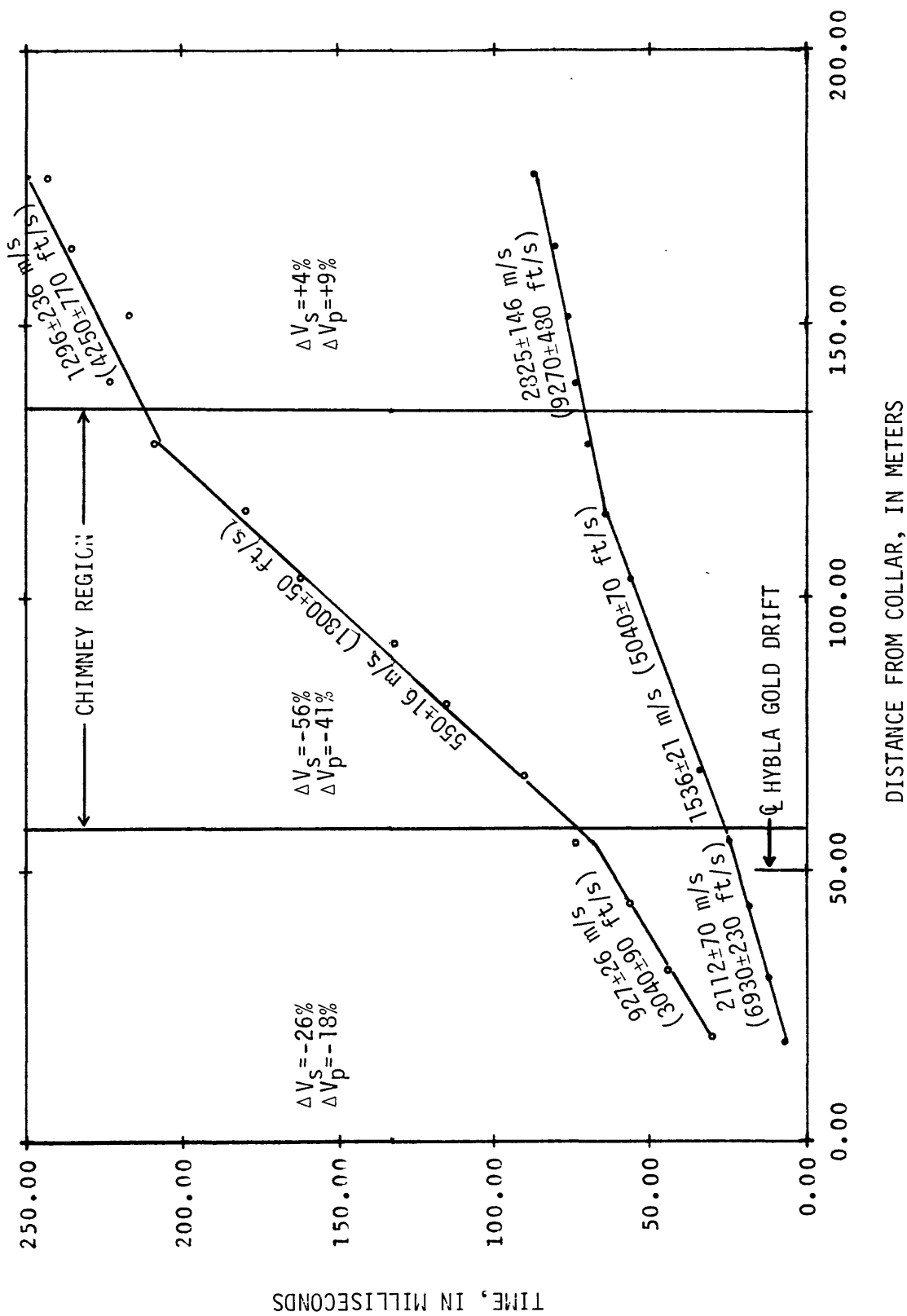
Figure 20.--Results of geophone survey in U12e.18 DNRE-1 drill hole. ΔV_p, ΔV_s refer to velocity changes referenced to preshot velocities obtained in Dining Car area.
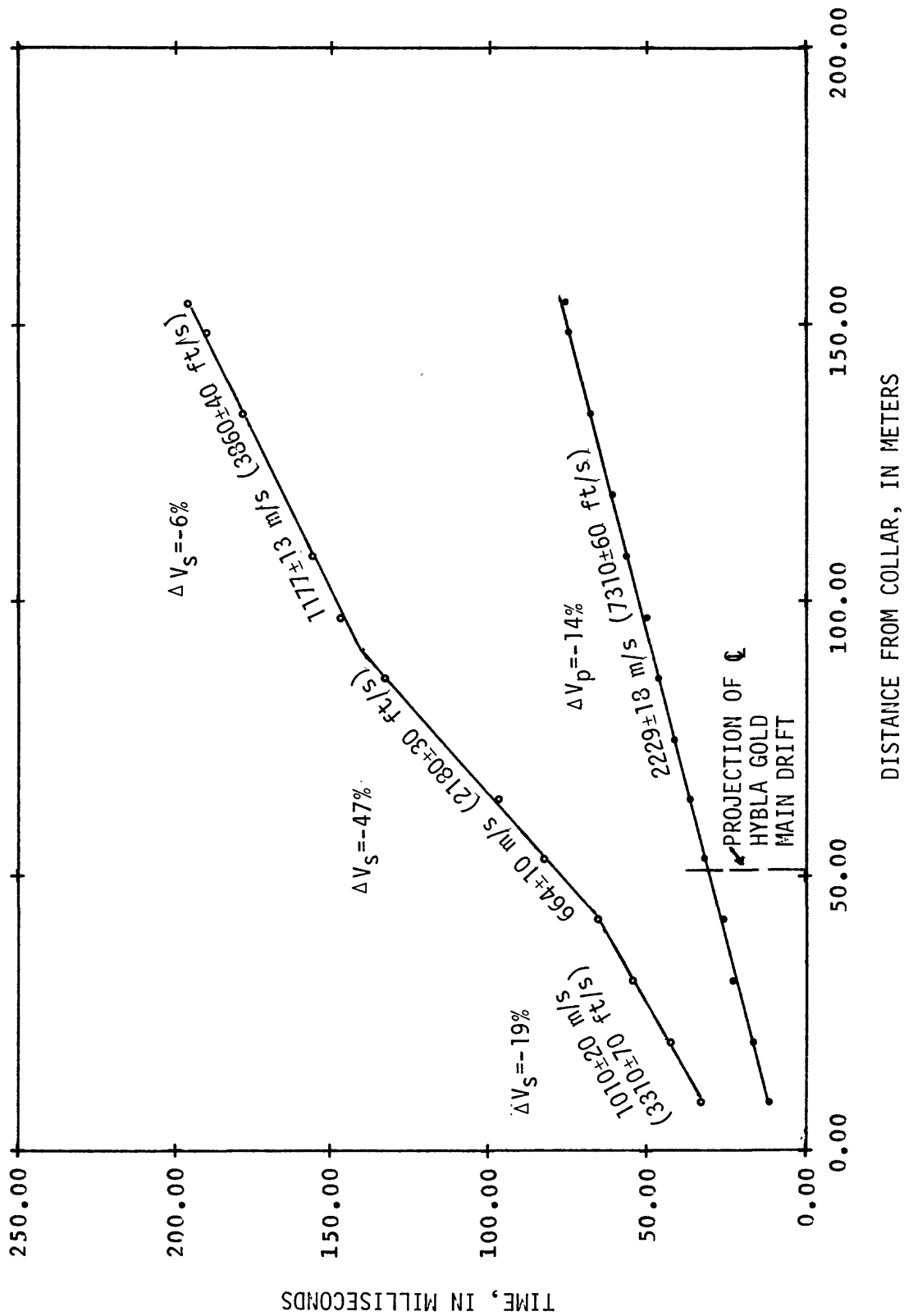
Figure 21.--Results of geophone survey in U12e.20 UG-1 drill hole. ΔV_p, ΔV_s refer to changes in velocity referenced to preshot velocities obtained in Dining Car area.

45
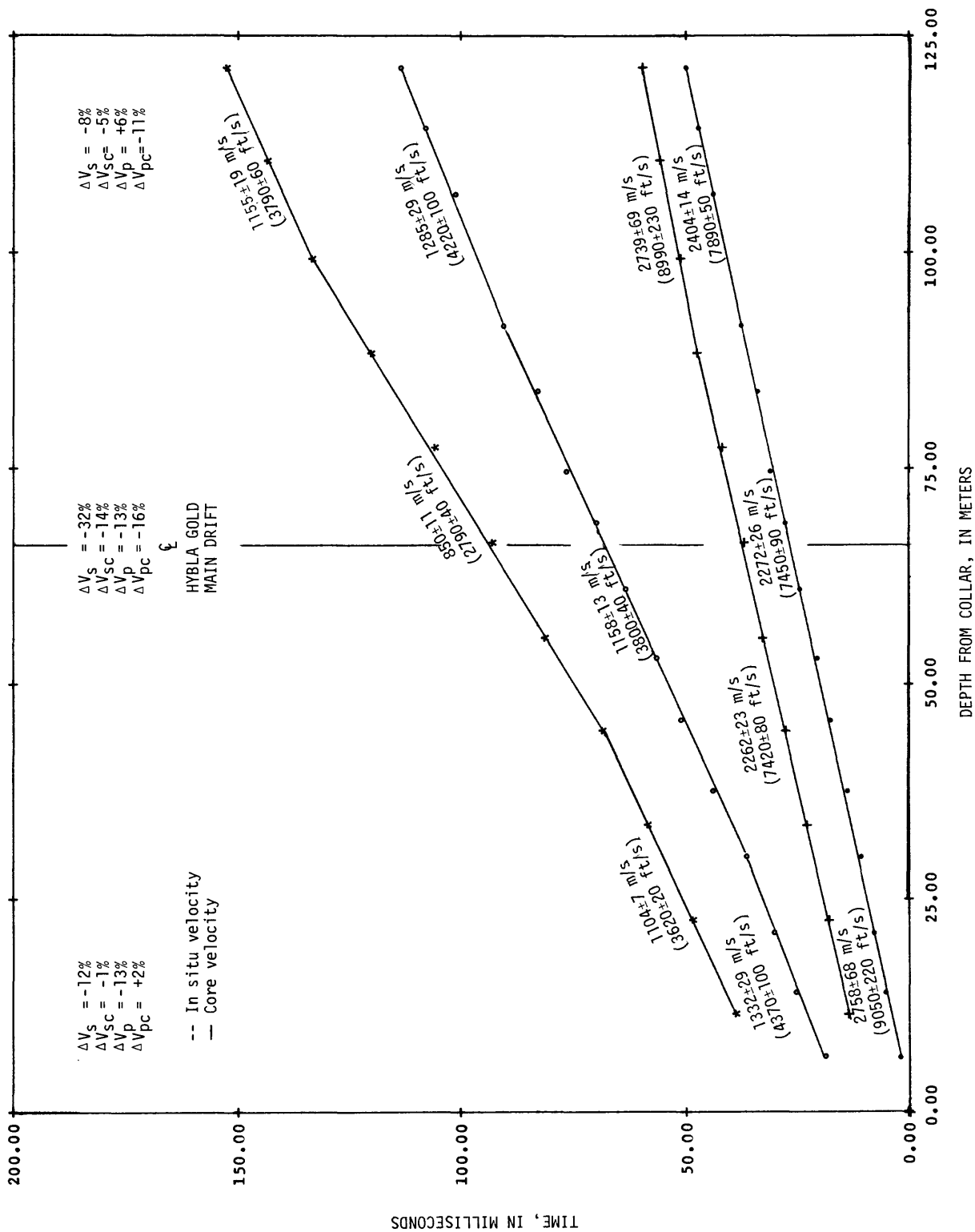
Figure 22.--Results of geophone survey in U12e.20 UG-2 drill hole compared with time-distance plots derived from core data. ΔVp, ΔVs refer to changes in velocity referenced to average preshot velocities obtained in Dining Car area. ΔVsc, ΔVpc refer to changes in average preshot core velocities.

A peculiarity exists in the compressional-velocity data from the DNRE-1 hole. The velocity at the bottom of the hole is considerably higher than one would expect for the chimney material and somewhat higher than one would expect for undisturbed ground. This suggests the probability of a refracted arrival in this region. The possibility that the hole is outside of the chimney or the chimney influence at this range is not considered tenable in light of the measurements obtained by the geophysical logs in this hole. The shear-wave velocity change on the far side of the chimney occurs near the expected location of the far boundary; however, the value of the shear velocity immediately outside the chimney beyond that range is equivalent to the shear velocity of virgin tuff. The shot offset at this range is close to 152 m (500 ft) and refractions are a distinct possibility. Note also that a distinct zone of considerably reduced shear velocity also exists in the other two holes, neither of which penetrated the chimney. In the DNRE-1 hole, the lowest velocities predictably occur in the chimney material[4]. These were also the lowest in situ velocities measured anywhere in the tunnel complex.

The low velocities observed closest to the chimney in the UG-1 and UG-2 holes (figs. 21, 22) are postulated to delineate zones where the tuff has pervasively failed under the influence of the transit of the shock wave and growth of the cavity. It is noteworthy that the velocity changes are most noticeable in the shear-wave velocity, the compressional-wave velocity being somewhat insensitive in these zones. As will be subsequently observed in the seismic velocities obtained in the Hybla Gold drifts, this insensitivity of the compressional velocity is a consistent effect.

[4]Shear- and compressional-wave velocities were also obtained by the author in the Cypress chimney. A compressional-wave velocity of 1,036 m/s (3,400 ft/s) and a shear-wave velocity of 488 m/s (1,600 ft/s) were obtained in the collapsed tuff material at that location. These represent a reduction in the average preshot velocities of approximately 60-65 percent.

The in situ velocity changes listed on the figures are based upon the data in table 7. In the UG-2 hole, the only hole wherein adequate core data were obtained, the percent changes with respect to the core values listed in table 7 are shown with a subscript "c" on figure 22.

The changes listed on the figures quantify what is visually apparent on the traveltime plots, i.e., that the Dining Car explosion has been considerably more effective in lowering the in situ shear-wave velocity than the compressional-wave velocity, particularly for the pervasively failed material outside the chimney (figs. 20, 21). The shear velocity in the tuff immediately outside the chimney is down nearly 50 percent in the UG-1 hole.

Since one would expect the explosion effects on the tuff velocity to be somewhat equally distributed around the chimney, the lack of reductions in velocity at the bottom of the UG-1 and UG-2 holes similar to those that occur near the hole collars, suggests that, as in the DNRE-1 hole, the deeper wave arrivals in these holes are not representative of direct arrivals. This may also explain why the far boundary of the zone of pervasive failure in the UG-1 hole appears much closer to the chimney than might be deduced from the results obtained in the UG-2 hole. However, the data closer to the collar of both holes, particularly the shear-wave data, are reflecting what is believed to be a zone of pervasive failure near the chimney and a zone of lesser disturbance of the tuff at greater range. This zone of lesser disturbance will be further addressed in connection with the seismic surveys in the Hybla Gold drifts discussed below.

The velocity traveltime plots derived from the core data in the UG-2 hole (fig. 22) also distinctly show the zone of pervasive failure. They differ from the in situ data as follows:

(a) The core data do not show significant changes in velocity outside the zone of pervasive failure.

(b) The shear-velocity reductions are not nearly as dramatic as the in situ data.

(c) The changes in slope of the traveltime plots occur at the same locations for both the shear and compressional data.

(d) The shear and compressional velocities are equally sensitive in defining the zone of pervasive failure.

Many of these differences in measurement are due to the inability to adequately sample the effect of bulk fractures in a core measurement of velocity. On the other hand, the in situ technique suffers from the possibility of refracted arrivals confusing the interpretation at long offsets. It is believed proven, however, that the in situ shear velocity is a highly diagnostic indicator of the explosion effects in the pervasively failed region outside the chimney, the data indicating that a 30-50 percent reduction in the preshot shear velocity of the tuff has been caused in that zone by the explosion.

We now proceed to amplify these observations by examining the velocity data obtained after the Hybla Gold complex was mined.

INVESTIGATIONS IN THE U12e.20 TUNNEL COMPLEX

The locations of the seismic-refraction lines run in the Hybla Gold main and auxiliary drifts and the geophone stations in the U12e.20 HF-5 drill hole are shown on plate 1. Electrical resistivity and magnetic field intensity measurements were also made in the main drift; however, as these data were obtained for a purpose other than documenting the effects of the Dining Car explosion they are discussed in the appendix (p. 70).

49

Compressional- and Shear-Wave Surveys in the Main and Auxiliary Drifts

Seismic-refraction surveys were run in the main drift (Apr. 25, 1977) and auxiliary drift (May 4, 1977) using the geophone locations and shotpoints shown on plate 1. Compressional waves were generated using dynamite in 1.5-m (5-ft) drill holes. Shear waves were generated using rock-bolt plates backed with primercord and detonated in ditches dug in the invert.

The results of these surveys are shown on figures 23 and 24. In the main drift we again note a distinct break in the velocity of the shear wave, and no corresponding break in compressional-wave velocity. Selection of the exact location of the break in the shear velocity is somewhat subjective, but was chosen at CS 3+10. The uncertainty is due to the fact that the shear-wave character on the records was well defined for arrivals between CS 2+06 and CS 2+94, but of poorer quality at the other geophone locations. The difficulty in selecting the exact onset of the shear wave in the general seismic wavetrain results in use of a time of arrival based on some well-developed peak or trough. Therefore, in some of the traveltime plots the shear wave does not have a zero intercept.

The compressional-velocity time-distance plot obtained from the shotpoint near the Hybla Gold WP suggests a minor break in slope near the geophones between CS 2+95 and CS 3+15. However, because of the general insensitivity of the compressional-wave velocity, the initial interpretation utilizing one velocity fit to the line was retained. Averaging comparable velocity segments, we again note that the shear-velocity changes are greatest compared with preshot velocities; 47 and 21 percent lower than preshot values as opposed to a 19 percent reduction in the compressional velocity. The dynamic moduli calculated from these averages are also shown on figure 23.

Tunnel interval (ft)	Compressional velocity (m/s)	Shear velocity (m/s)	Young's modulus (kb)	Bulk modulus (kb)	Shear modulus (kb)	Poisson's ratio
1+84–3+10	2,107	659	23.8	73.3	8.25	0.45
3+10–4+26	2,107	934	50.1	59.8	18.4	.36

TIME, IN MILLISECONDS

TUNNEL STATION, IN FEET
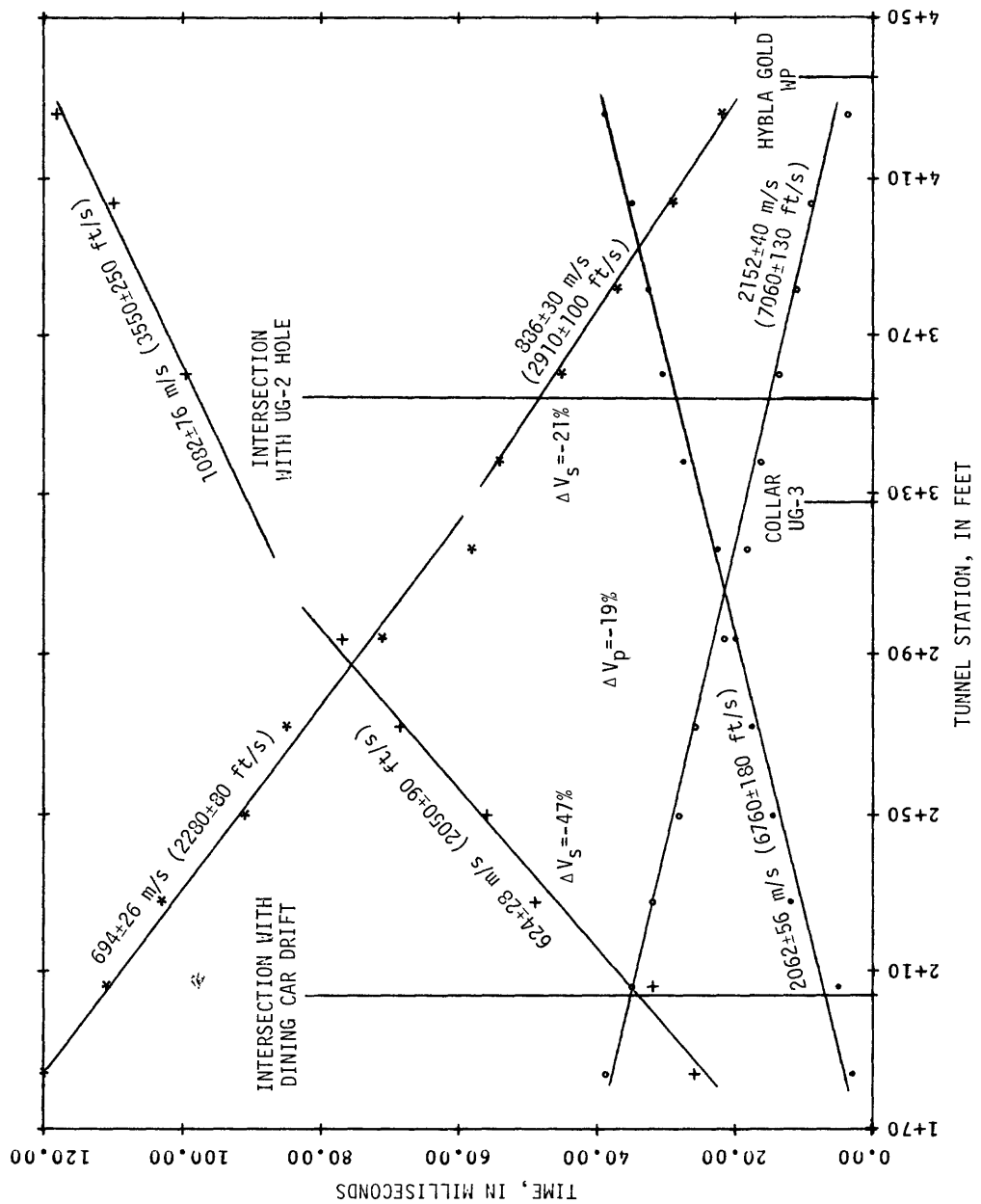
Figure 23.--Results of seismic survey in UI2e.20 tunnel, main drift. Moduli were derived using averages of velocities of equivalent segments and assuming a density of 1.9 Mg/m³.

51

Tunnel interval (ft)	Compressional velocity (m/s)	Shear velocity (m/s)	Young's modulus (Kb)	Bulk modulus (Kb)	Shear modulus (Kb)	Poisson's ratio
2+00-4+20	2,442	1,045	57.6	85.6	20.7	0.39
4+20-2+00	2,352	988	51.7	80.4	18.5	.39

$\Delta V_p = -7\%$
$\Delta V_s = -19\%$

1045±12 m/s (3430±40 ft/s)

988±18 m/s (3240±60 ft/s)

2442±34 m/s (3010±110 ft/s)

2352±45 m/s (7720±150 ft/s)

TUNNEL STATION, IN FEET

TIME, IN MILLISECONDS
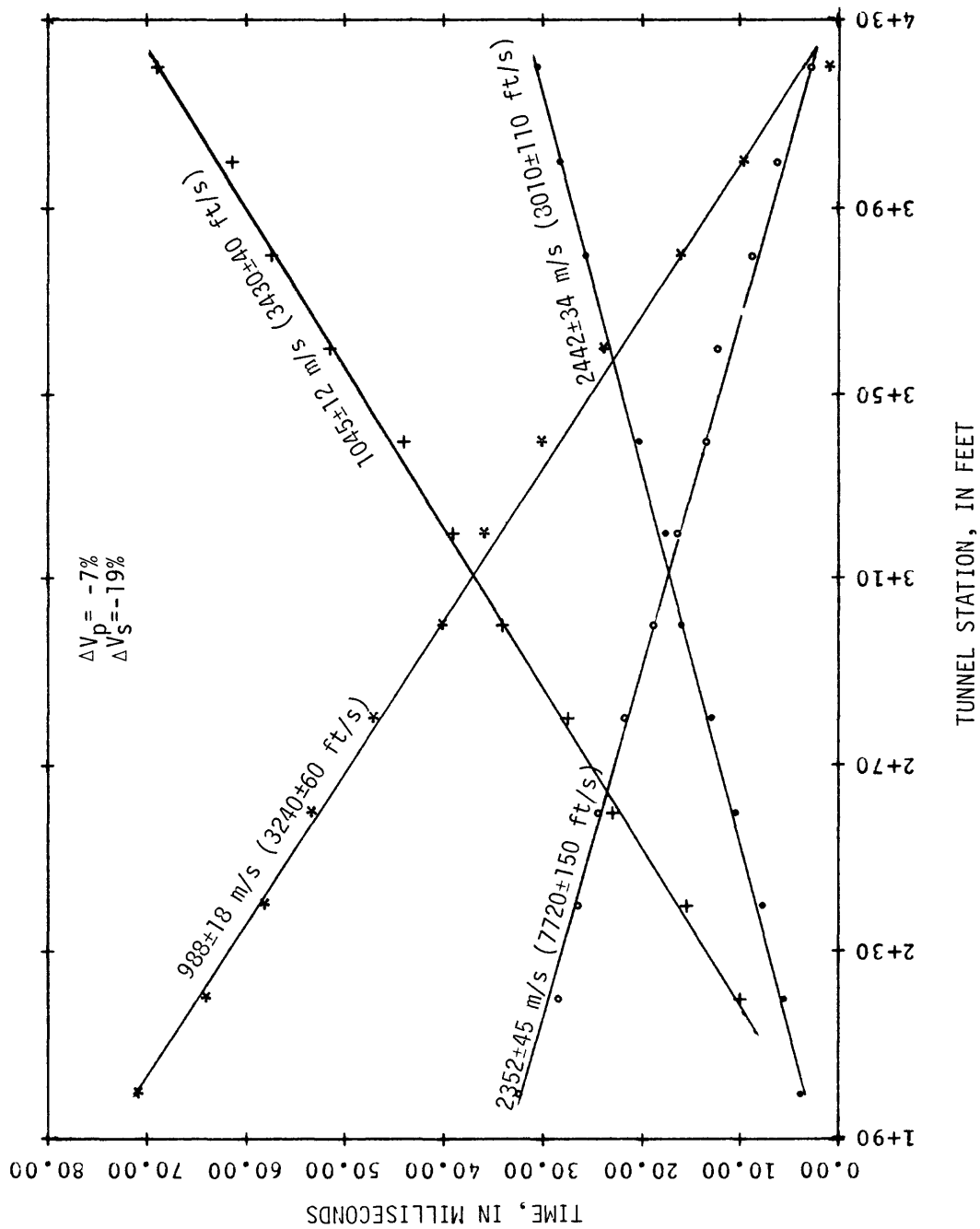
Figure 24.--Results of seismic survey in U12e.20 tunnel auxiliary drift. Moduli were derived using averages of equivalent segments and assuming a density of 1.9 Mg/m3.

52

The absence of distinct breaks in the slope of the compressional-wave time-distance plot in the main drift (fig. 23) at the same locations as the shear-wave plot is an interesting phenomenon and one for which there is no ready explanation. This is a consistent result as may be noted in the results in the UG-1 and UG-2 drill holes (figs. 21, 22). Assuming that the arrivals are travelling over equivalent paths, the implication is that the explosion-induced effects on the tuff are such that the compressional velocity is relatively insensitive to these effects. This does not mean that the compressional velocity is not reduced. We are unaware of any previous work which demonstrates such dramatic changes in shear velocity unaccompanied by similar changes in compressional velocity. "Inconsistencies" of this dramatic nature have not been observed in any preshot seismic survey in Rainier Mesa tunnels.

The seismic data obtained by the author near the Camphor chimney (unpublished data, 1981) also indicates that breaks in the two-way traveltime plot of shear velocities are consistent in terms of location but do not always coincide with breaks in the compressional-wave traveltime plot. Postshot seismic results obtained in the vicinity of the Hudson Moon chimney, however, do indicate consistency in the location of breaks in the traveltime plots of both the shear and compressional waves. Similar to the data reported here, Camphor and Hudson Moon both lowered the shear velocity to a greater extent than the compressional velocity. It is probable that with a finer spatial sampling and time resolution, a break in the compressional-wave plot could be resolved. This is certainly suggested by the results of core measurements plotted on figure 22.

A factor of possible greater significance in explaining the difference in location of changes in velocity between compressional- and shear-wave

traveltime plots is the three-dimensional environment of the tunnel coupled with the difference of almost 2:1 in wavelength of the two waveforms. Examination of the waveforms indicates a comparable frequency for the two wave types with a compressional wavelength of about 15 m (50 ft). The wavelength of the shear mode is about one-half that of the compressional. Thus, sampling effects could be quite different for the two modes of propagation.

Another notable feature of the in situ shear-velocity data is the abruptness of the shear-velocity changes on the time-distance plots. Similar strong demarcations have also been noted on the postshot seismic data obtained in the Camphor and Hudson Moon reentries. As mentioned, it is felt that these breaks represent the envelope of failure of the tuff around the chimney arising from dilation of the tuff due to shock loading. If so, the transition zone between failed and unfailed rock appears to be relatively narrow along any particular radial from the WP.

The results of the seismic survey obtained in the auxiliary drift are shown on figure 24. The data again indicate a significantly reduced shear velocity compared with preshot values. The reduction in the compressional velocity is considered of borderline significance. Based on the shear-velocity data obtained in this drift, it is concluded that at a range approaching three chimney radii, dislocations of the preshot environment are still evident. Thus, the entire Hybla Gold complex is probably within the range of seismically measurable effects from the Dining Car event[5].

[5]This is in agreement with unpublished data of the author which indicates significant changes in shear velocity in the Camphor reentry at scaled ranges which would include the Hybla Gold complex.

U12e.20 UG-3 Horizontal Drill Hole

Unfortunately, because of the mining schedule, time was not available to obtain seismic data in the UG-3 drill hole (pl. 1, fig. 23). This hole is of interest in that it is near the shear-velocity transition zone shown by the main drift seismic survey and samples a portion of the same ground as the UG-2 hole. The density of core sampling in this hole, however, was sufficiently adequate to construct a seismic time-distance plot in the manner done in UG-2. The results are shown on figure 25 and are peculiar for several reasons:

(a) The core shear velocity (1,359-1,394 m/s or 4,460-4,570 ft/s) is essentially invariant in this hole and is no different from preshot values, although one can recognize some perturbation in the shear velocity in the vicinity of 30 m. The values of core shear velocity are significantly higher (17 percent) than would be predicted based on the core results in the UG-2 hole (1,158 m/s or 3,800 ft/s) which was drilled through the same region (fig. 22).

(b) The compressional velocity of the core is consistent with the results obtained in the UG-2 hole. The value close to the collar of the hole (2,241 m/s or 7,350 ft/s) is in agreement with what was obtained in UG-2 (2,272 m/s or 7,450 ft/s). The 6 percent change in core compressional velocity in the deeper part of the hole is approaching borderline significance and cannot be argued to indicate shocked samples.

The shear-wave results in this hole are puzzling and may be due to bias in selecting competent samples. The break in the compressional velocity, occurring at about CS 3+66, is intriguing in that it was in this region, rather than at the closest approach to the chimney at CS 2+04, that the most unstable ground was encountered in mining. In addition, relatively high
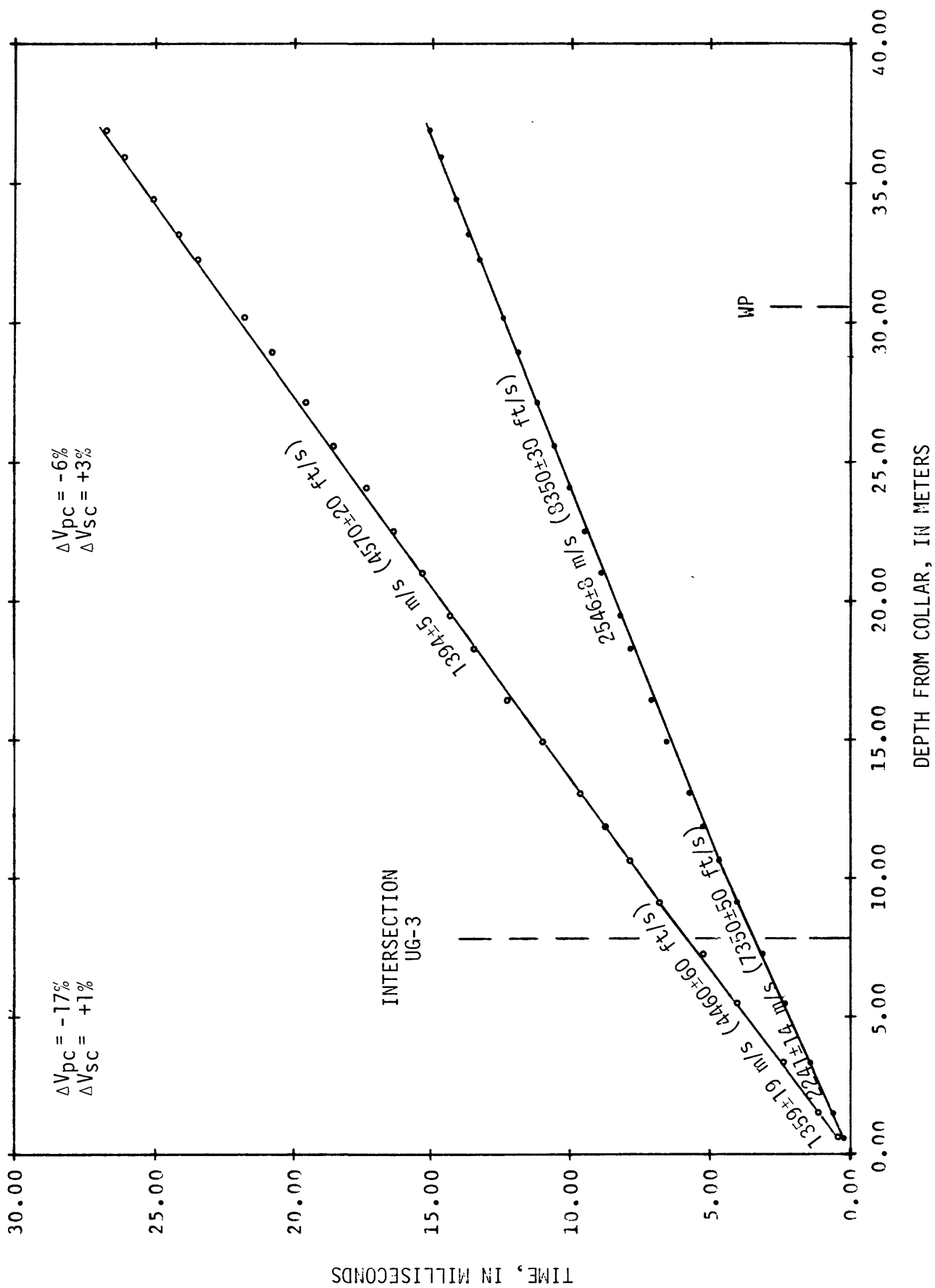
Figure 25.--Time-distance plot of integrated core shear- and compressional-velocity data obtained in U12e.20 UG-3.

values of minimum stress were obtained in this region from the hydrofracture records obtained in this hole (W. L. Ellis, written commun., 1980).

U12e.20 HF-5 Horizontal Drill Hole

The HF-5 hole was drilled to determine the location of an anticipated fault east of the WP (pl. 1). Resistivity was measured in this hole on 1.8-m (6-ft) intervals from 2.7 to 22.6 m (8.3 to 74.3 ft). The results are shown on figure 26.

Because of caving, the resistivity probe could not be pushed to the bottom of the hole. There was no core recovery in the bottom 6.1 m (20 ft) of this hole; however, the last resistivity reading in the hole is more typical of tunnel bed 4H than 4J. Excluding the last reading in the hole, the ·esistivity data average 24±3 ohmmeters, typical of tunnel bed 4J, and which is comparable to data from drill hole UE12e#1 (Carroll and Cunningham, 1978). This suggests a contact or fault between the depths 20.8 and 22.6 m (68.3 and 74.3 ft) in this hole.

Compressional-wave velocities were obtained using the inhole geophone probe with stations on 4.6-m (15-ft) intervals from the bottom of the hole 27.7-0.3 m (91-1 ft) to the collar. Unfortunately, no attempts were made to obtain shear velocities. The results are shown on figure 26. The compressional velocity of 2,417 m/s (7,930 ft/s) compares with the velocity obtained in the auxiliary drift and is sightly higher than that obtained in the main drift.

Core sampling was also sufficient in the HF-5 hole to obtain a simulated time-distance plot. The time-distance plots using the core shear- and compressional-velocity data and in situ compressional-velocity data are plotted on figure 27 along with differences in velocity by the two techniques again using the velocities in table 7 as the norm. The postshot changes in

57
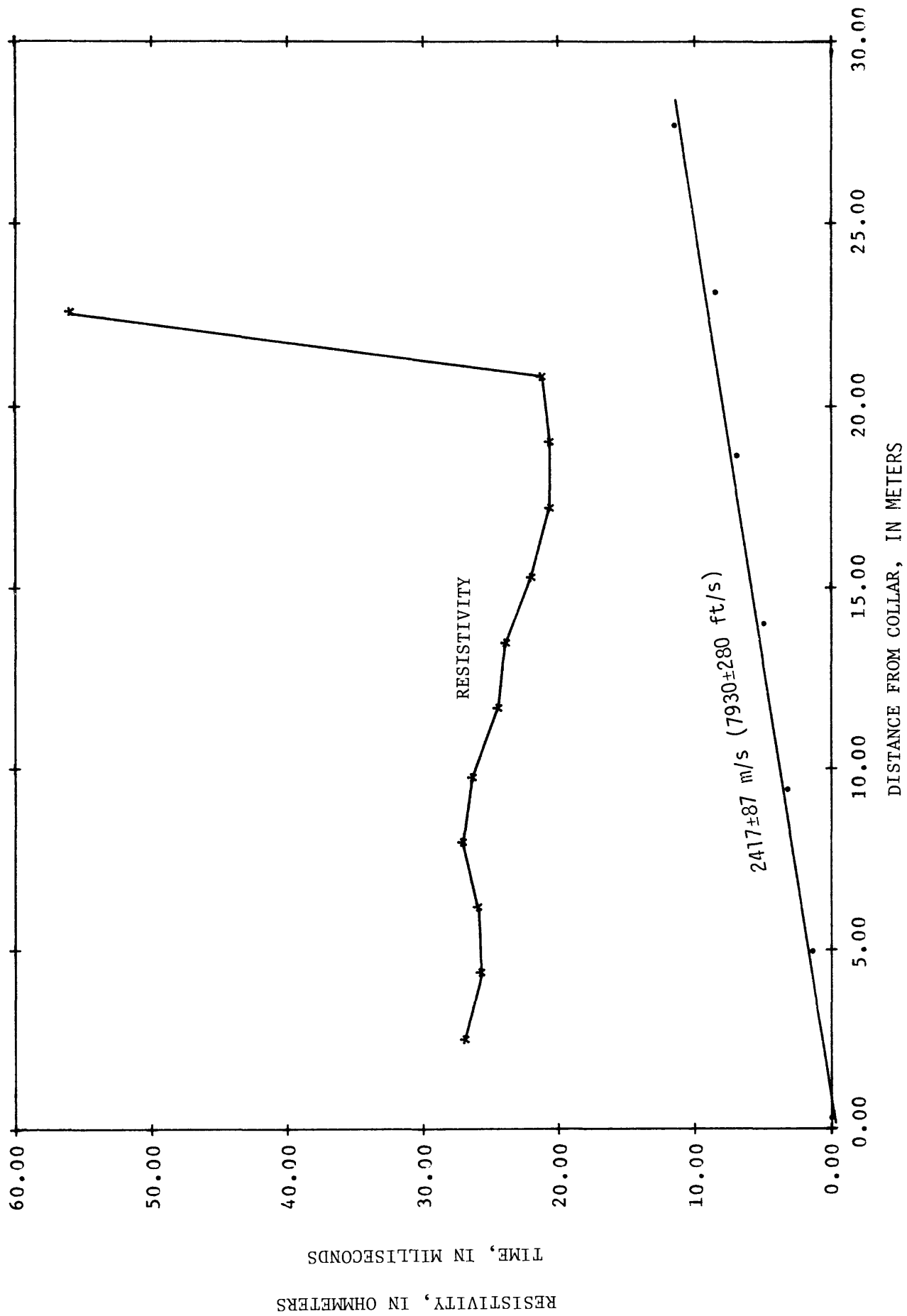
Figure 26.--Results of resistivity and seismic surveys in U12e.20 HF-5 drill hole.

DISTANCE FROM COLLAR, IN METERS

TIME, IN MILLISECONDS

RESISTIVITY, IN OHMMETERS

RESISTIVITY

2417±87 m/s (7930±280 ft/s)

58
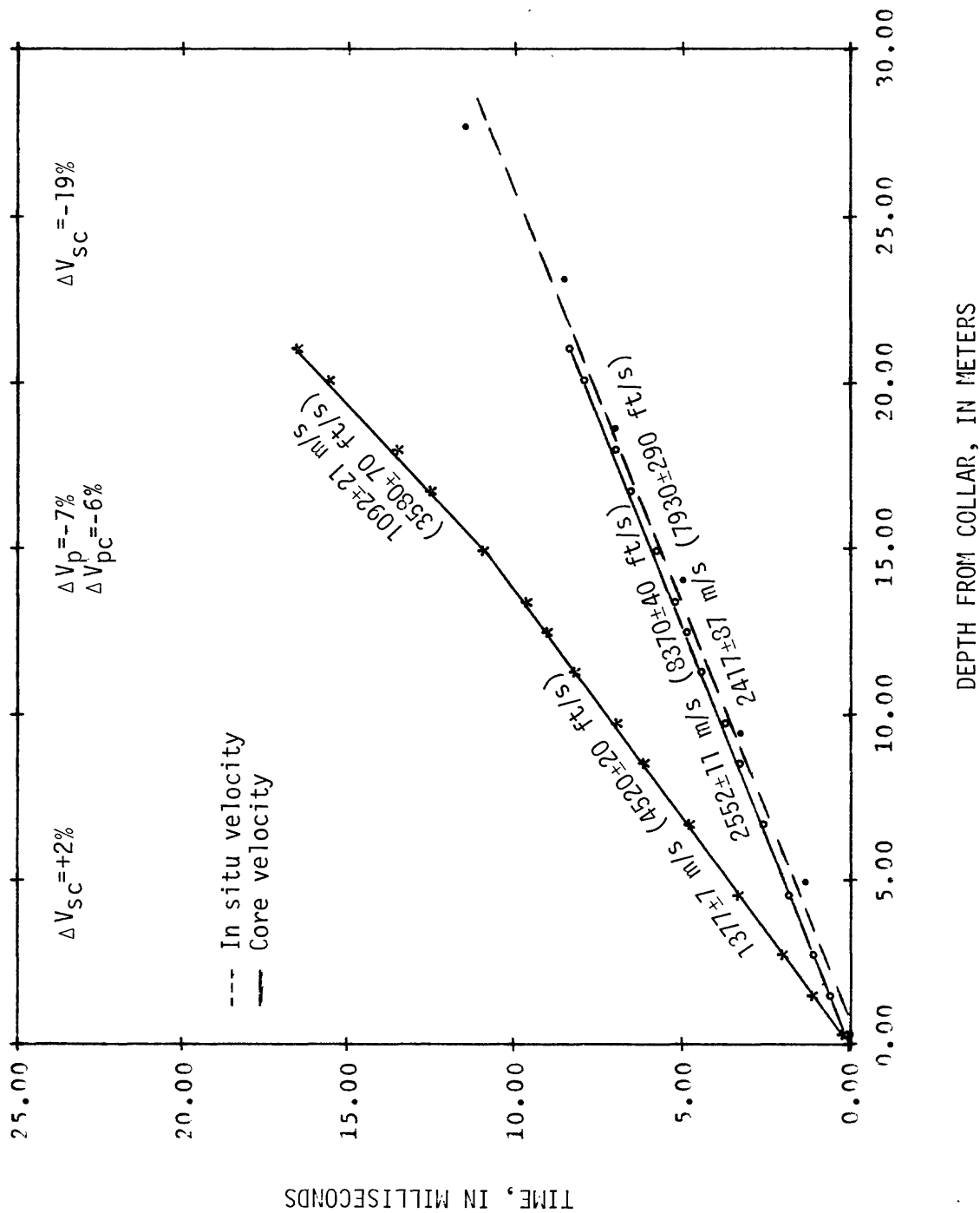
Figure 27.--Results of geophone survey in U12e.20 HF-5 compared with time-distance plots derived from core data.

compressional-wave velocities are of borderline significance and the shear-wave velocity obtained from the core is only significantly different from the preshot core data at the bottom of the hole where it is 19 percent below the expected value. However, the core from this section of the hole is highly broken and the fault previously mentioned is the dominant geologic feature. It is possible that the low core shear velocity is a reflection of microcracking associated with fractures near the fault. On the other hand, one might argue that the consistent bias of the compressional velocities toward lower values is consistent with the magnitude of changes seen in the auxiliary drift where shear velocities were significantly lowered. The absence of in situ shear-velocity data in this hole renders the results inconclusive with respec: to any event-induced changes in seismic velocity.

Comparisons with Velocities in Other Tunnels

A further perspective on the magnitude of the in situ velocity changes may be gained by examining the velocity data with respect to velocities obtained in undisturbed ground in other tunnels. These data are shown on the histograms on figures 28 and 29. These histograms depict the results of preshot seismic surveys in 15 other tunnels in the Rainier Mesa area in which shear- and compressional-wave velocities have been obtained in situ. The average results of the postshot seismic surveys in the main and auxiliary drifts in Hybla Gold and in the Dining Car chimney rubble are also shown on the figures. The two zones determined for the shear velocity in the Hybla Gold main drift are shown independently. The inner zone is considered the region of pervasive failure due to the shock wave exceeding the strength of the tuff.

Note on the figures that the average postshot shear-wave velocities obtained in the Dining Car area are outside experience for any tunnel shear

60
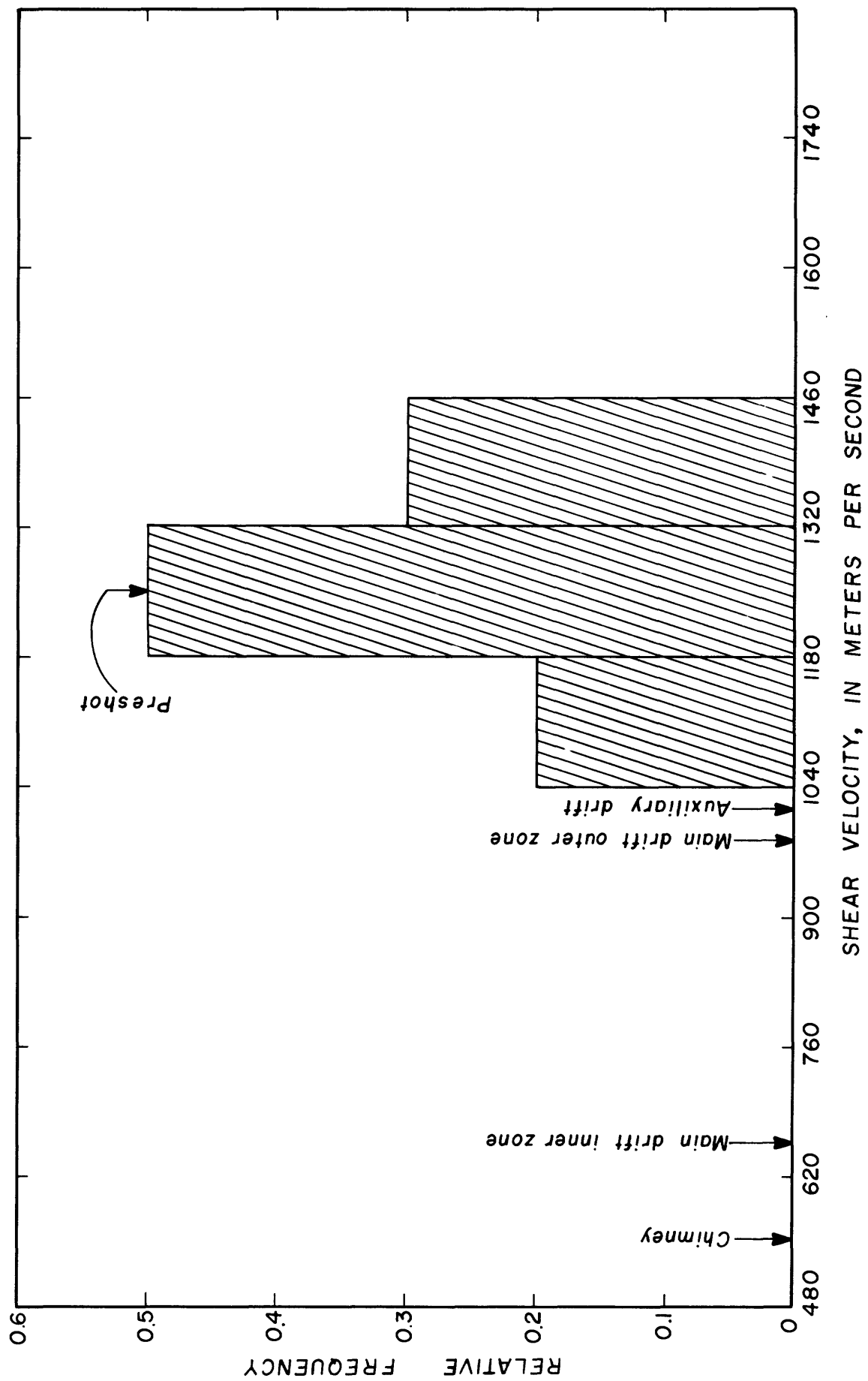
Figure 28.--Histogram of shear velocity measured preshot in 15 tunnels compared with shear velocities measured in the Dining Car/Hybla Gold complex.
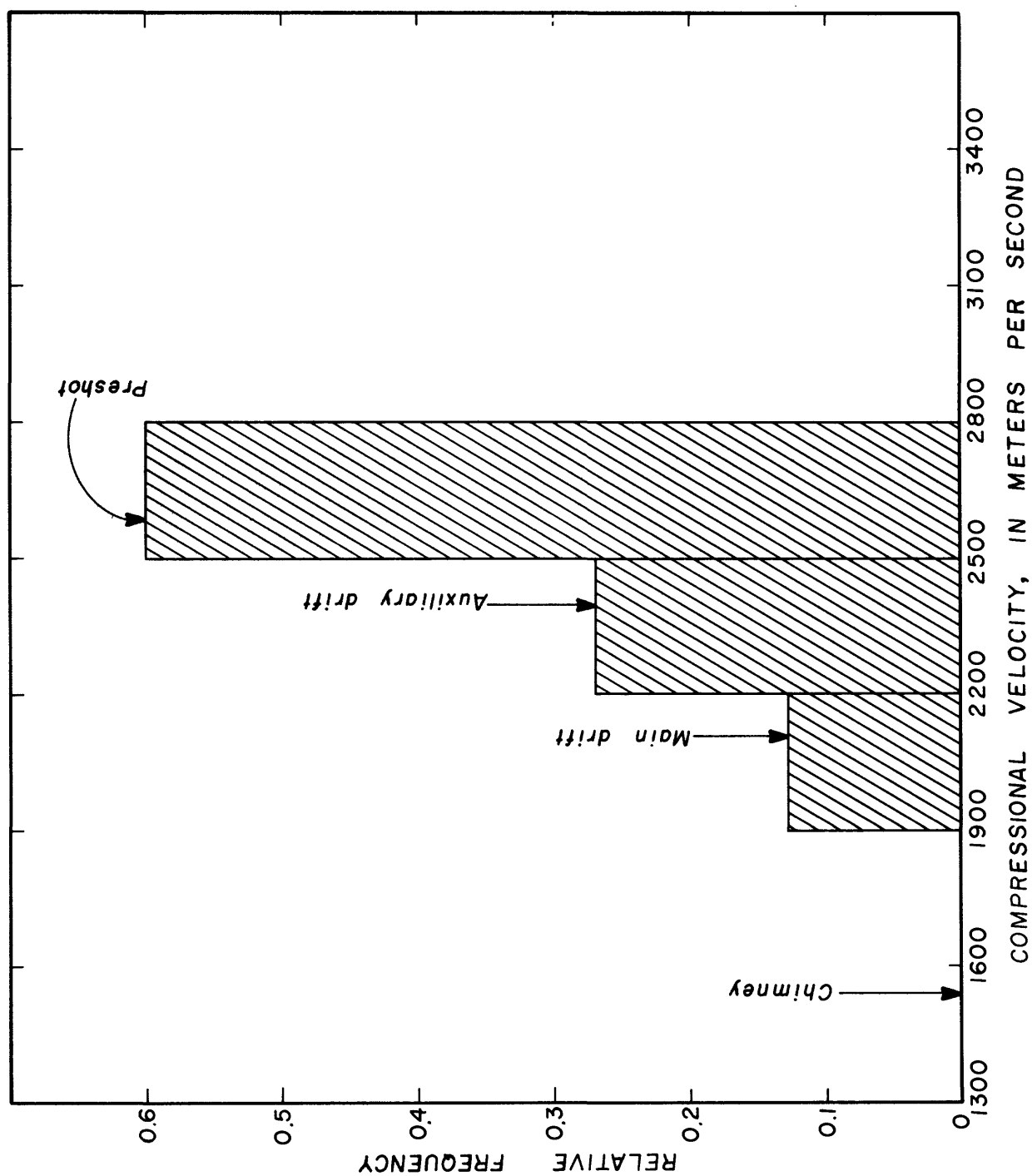
Figure 29.--Histogram of compressional velocity measured preshot in 15 tunnels compared with compressional velocities measured in the Dining Car/Hybla Gold complex.

velocity measured in virgin ground. On the other hand, the compressional-wave velocity is relatively undisturbed with the predictable exception of the velocity of the chimney material suggesting again that the major effect of the explosion has been a reduction in shear strength of the tuff.

DISCUSSION OF RESULTS

It would have been desirable to obtain additional seismic data in the Dining Car/Hybla Gold region; however, the press of mining and event scheduling did not allow this. When coupled with previous experience, however, it is felt that the data obtained are quite adequate for the conclusions made.

The results of the in situ seismic data indicate abrupt boundaries over ·'hich the shear velocity markedly changes. The approximate locations where these boundaries exist in the seismic data and core are shown on plate 1. It is difficult to say to what extent these boundaries are of significance in defining distinct effects around the explosion point without some independent material property, such as shear strength, with which to correlate the results. Two effects which may interact to cause dilation and failure of the tuff medium near the explosion are the passage of the shock wave and the growth of the cavity. However, mining of the Hybla Gold complex exposed no gross visual indications of rock failure. Although the ground was soft and slabby, large and obviously shock-induced throughgoing fractures were absent. The major visual effect was the tendency of the tuff to disaggregate into sandlike material as one approached the chimney. A similar observation was made during the Rainier reentry where it was correlated with a systematic decrease in microcracking (observed in thin sections of the rock) as one progressed outward from the edge of the chimney (Wilcox and Wilmarth,

1959)[6]. Thus, the presence of a boundary of rock material which failed on a microscopic scale has precedent. Microcracking was also observed in samples obtained in the Hybla Gold/Dining Car region (Gardiner and others, 1977); however, no systematic attempt was made to determine the range limit of this effect. It is believed that the more dramatic close-in changes in shear velocity are reflecting this pervasive microfailure of the tuff. However, superimposed upon this microscopic failure is seismic evidence of macroscopic failure due to gross dislocations on a larger scale than can be adequately sampled by core velocity data[7]. Based on shear-velocity data obtained in the auxiliary drift, these larger dislocations are present throughout the entire Hybla Gold complex. The geometry of the complex did not allow definition of the limit of this outer zone from the seismic data. The zone extends to at least three chimney radii.

It is inferred, therefore, that the region of microfailure of the medium is defined by the range limit within which core shear velocity, as well as in situ shear velocity, have been reduced. This range is about two chimney radii from the WP.

The presence of a microfailure and macrofailure zone around the chimney appears, on first glance at the data, to be demarcated by a well-defined change in the shear-wave velocity. The locations where boundaries are indicated by the results of the shear-wave refraction surveys (figs. 19-21,

---

[6]The particulars on the Rainier event along the tunnel radial from the WP in which these data were obtained were a chimney boundary 18-21 m (60-70 ft) from the explosion and microcracking observable to about 40 m (130 ft) in thin sections. The boundary of microcracking was closely coincidental with changes in strength and velocity of core. In situ compressional velocities showed approximately 70, 40, and 10 percent reductions in the chimney, inner and outer zones respectively; unfortunately no shear velocities were recorded.
[7]Core velocities are measured on a 2.5-cm-length sample, whereas the sample size (geophone spacing) of the in situ seismic is 2-2 1/2 orders of magnitude larger.

23) or by the integrated core-velocity data (figs. 21, 25) are shown on plate 1. The locations are shown coincidental with breaks in the time-distance plots; however, the exact locations could vary by as much as the geophone or sample spacing. In addition, because of the previously discussed possibility of other than direct arrivals at the larger ranges in the horizontal holes, those breaks nearest the hole collars are considered more reliable indications of the range of effects from the explosion. The breaks noted in the DNRE-1 hole correspond to the velocity changes at the edge of the chimney. The geophone spacing was inadequate to define the edge of the microfractured zone near the collar of the hole. Aside from this the data appear to roughly satisfy symmetry about the chimney. In terms of relative magnitudes of the velocities involved, however, anomalies exist. The low shear-velocity zone in the UG-2 hole is roughly equivalent in magnitude (850 m/s or 2,790 ft/s) to the shear velocity of the main drift segment farthest from the chimney (984 m/s or 3,230 ft/s). This is reasonable since the seismic lines intersect common ground. However, the author's interpretation of the data places the velocity change in the UG-2 hole as representative of the zone of microfailure and the velocity segment recorded in the main drift nearest the Hybla Gold WP as representative of macrofailure. This is a contradiction if we assume similar values of shear velocity should equate to similar effects. On the other hand, the shear velocity of the low-velocity material in the UG-1 hole (664 m/s or 2,180 ft/s) is equivalent to the velocity of the segment recorded nearest the chimney in the main drift (659 m/s or 2,160 ft/s). These data are consistent but significantly lower in velocity than the velocity obtained in the UG-2 hole. The results in the DNRE-1 drill hole show agreement with the UG-1 hole although the shear velocity (927 m/s or 3,040 ft/s) is based upon only three geophone stations.

One explanation for the differences in velocity may be the difference in rock type. The break in the time-distance plot obtained in the main-drift shear-wave survey occurs at approximately the boundary between tunnel beds 4J and 4K, the lower velocities being in tunnel bed 4K, the unit nearest the chimney. The lower velocities in the UG-1 hole also occur in the same geologic unit. Thus, the lower velocities in the 4K bed may be a reflection of the difference in the effect of shock-wave loading in this tunnel bed as opposed to tunnel bed 4J. Alternately, the zone nearest the cavity may be affected by plastic deformation arising from cavity growth as well as shock loading, thereby lowering the shear-wave velocity beyond that normally expected in the microcracked region.

T'ie near 50 percent reduction in shear velocity near the chimney (75 percent reduction in shear modulus) and the resulting inference that the major effect of the explosion on the rock has been a reduction in shear strength makes desirable some estimate of the magnitude of strength reduction. An empirical study of the relationship between the shear velocity of 471 tuff samples and failure at 4 kb indicates the best fit is one relating strength to the square of shear velocity (Duff, 1978)[8]. This implies a probable linear relationship to shear modulus. Thus, the reduction in shear strength is assumed to be possibly 50-75 percent in the zone of microfailure. In the zone of macrofailure, the question of whether we can assume a relationship between shear velocity and shear strength is considerably more speculative. This is because there are at present no quantitative techniques for assessing the effect of fractures, fracture orientation, and fracture spacing on rock

[8]The correlations in this study were poor; however, core velocities were measured in the unloaded state. It is the author's experience that correlation coefficients involving the velocity of tuff as against, for example, porosity, can often be raised 0.1-0.2 unit over the unloaded regression when the core is loaded to in situ stress levels.

velocity and strength. There is probably some level of fracture frequency above which a strong relationship exists between velocity and strength. The fact that the inner zone of lowered shear velocity near the Dining Car chimney can be considered pervasively fractured on the microscopic level suggests that the assumption that we are within this threshold in that region might be a reasonable one. Further research is required to quantify these relationships.

CONCLUSIONS

The mechanisms resulting from a nuclear detonation result in failure and dislocation of the rock media to some distance from the detonation point. Results of seismic investigations pre- and post-Dining Car indicate the following about the effect of that event on the surrounding rock:

1. The medium around the WP is characterized by three zones of altered velocity: the chimney; a zone of pervasive failure of the rock outside the chimney inferred to be failed on a microscopic (microfractured) scale; and a zone of gross dislocations along bedding planes, joints, and other features. The failed zones outside the chimney are not strikingly visual on mining but are strongly reflected in the in situ seismic data.

2. The major disruption in velocity is predictably in the chimney collapse material where compressional velocities have been reduced over 40 percent and shear velocities have been reduced close to 60 percent of their preshot values.

3. The tuff outside the chimney exhibits percentage reductions in shear velocity of $2\frac{1}{2}$ times that of the reduction in compressional velocity. The maximum reduction in velocity for the shear wave is about 50 percent in the material adjacent to the chimney as opposed to a reduction of 20 percent of preshot values for the compressional velocity.

4. The reductions in average shear velocity measured in situ outside the chimney are sufficient to render the magnitude of the velocity outside any previous experience for shear velocity measured in 15 tunnels in virgin ground. The compressional velocity, on the other hand, while lowered from preshot values is not lowered to the extent of being anomalous for in situ measurements in virgin tuff.

5. There are pronounced differences in velocity when comparing core velocities with in situ velocities. The sensitivity of the in situ seismic measurement to shear velocity changes is about twice that of the core over comparable intervals. It is concluded that this is because core data do not sample the gross dislocations along joints and bedding planes and only reflect the inner zone of microscopic failure near the chimney. This zone near the chimney is also seen by the in situ seismic measurements and the data indicate the outer boundary of this zone is at a range of about two chimney radii from the detonation point. Beyond this range, core data suggest no changes in the seismic velocities of the tuff. The in situ velocities, particularly the shear velocity, however, indicate that macrodislocations have occurred in the tuff throughout the entire Hybla Gold complex, i.e., to at least a range of three chimney radii.

6. The difference in the velocities measured by the two methods is believed due to the presence of both microfractures (microfailure) and gross dislocations (macrofailure) of the tuff. Both are sensed by the in situ shear velocity; however, only the former is sensed by the core measurement. The boundary between these two effects is strongly demarcated by either technique. The boundary between macrofailure and virgin tuff was not within the in situ measurement geometry and its nature has yet to be investigated.

68

REFERENCES CITED

Carroll, R. D., and Cunningham, M. J., 1978, Geophysical investigations, in U.S. Geological Survey investigations in connection with the Dining Car event, U12e.18 tunnel, Rainier Mesa, Nevada Test Site: U.S. Geological Survey Report USGS-474-246, 68 p.; available only from U.S. Department of Commerce, National Technical Information Service, Springfield, VA 22161.

Carroll, R. D., Cunningham, M. J., and Muller, D. C., 1979, Geophysical investigations, in U.S. Geological Survey investigations in connection with the Mighty Epic event, U12n.10 tunnel, Nevada Test Site: U.S. Geological Survey Report USGS-474-228, 191 p.; available only from U.S. Department of Commerce, National Technical Information Service, Springfield, VA 22161.

Duff, R. E., 1978, Comments on the strength of Area 12 tuff: Defense Nuclear Agency Report DNA 4526T, 28 p.

Gardiner, D. S., Enniss, D. O., Butters, S. W., and Jones, A. H., 1977, Material properties of Nevada Test Site tuff and grout--with emphasis on the Diablo Hawk and Hybla Gold events: Defense Nuclear Agency Report DNA 4528F, 282 p.

Wilcox, R. E., and Wilmarth, V. R., 1959, Textural and chemical changes, in Geologic effects of the Rainier underground nuclear explosion: U.S. Geological Survey Open-File Report TEI-355, p. 7-1 to 7-7.

APPENDIX

APPENDIX

Magnetic Intensity and Electrical Resistivity

Electromagnetic pulse experiments were carried out in connection with the Hybla Gold event. As input data to these experiments the USGS was requested to perform measurements of the direction and intensity of the Earth's magnetic field in the main drift and to obtain measurements of the resistivity of the concrete in the invert.

Measurements of the direction and intensity of the Earth's magnetic field were made by Gordon Bath of the USGS at 34 stations in the main drift between stations CS 4+28 and CS 1+64. The readings were taken along the left rib corresponding to the pipe axis at a distance of 0.50 m (1.64 ft) from the grout floor in the vertical plane perpendicular to the drift. The bearing of the vertical plane is N. 17° W. (drift bearing N. 73° E.). The averages and standard deviations for these 34 measurements yield:

Inclination (degrees downward from horizontal)	Intensity (10^3 gammas)
63.7±1.8	49.8±1.0

The presence of rock bolts and wire mesh caused some of the variations in the readings. Published charts for this area indicate an inclination of 66.4° and an intensity of 50,300 gammas would be expected in the absence of anomalous magnetic effects.

Electrical resistivity measurements were made to determine the in situ resistivity of the concrete pad on the tunnel floor and the resistivity of the concrete on the A-box wall. Resistivities were measured using a 20-cm (8-in.) Wenner array. Based upon 12 measurements on the concrete pad, from CS 0+76T

in the tail drift to CS 4+05, and two other measurements, the following average resistivities were determined:

Concrete pad	A-box wall
4.2±0.8 ohmmeters	5.1 ohmmeters

IN SITU STRESS INVESTIGATIONS

By

W. L. Ellis and J. E. Magner

ABSTRACT

Overcoring and hydrofracturing techniques were used to obtain estimates of in situ stress conditions within 100 m (328 ft) of an expended underground nuclear detonation, the Dining Car event. The measurements, conducted approximately 2 years after the Dining Car event, were part of the geotechnical site characterization effort for the Hybla Gold event, located 83 m (272 ft) from the Dining Car site. Unfavorable rock conditions, primarily due to shock damage from the Dining Car event, compromised the quantitative value of the data. Nonetheless, results demonstrate that the "residual stress cage" believed to form around nuclear explosion-induced cavities had dissipated in the 2 years following the Dining Car event. The pattern of apparent remnant stress changes, however, suggests that a "residual stress cage" qualitatively similar in character to computer-model predictions may have once existed in the vicinity of Dining Car.

INTRODUCTION

During the last several years the determination of in situ stress conditions at the WP of proposed underground nuclear tests within Rainier Mesa has been a routine practice. The Hybla Gold investigations were unique, however, in that the WP was located within about 83 m (272 ft) of an expended underground nuclear test, the Dining Car event. This proximity, coupled with the test design of the Hybla Gold event, made some knowledge of the distribution of stress in the vicinity of, and especially between, the two sites necessary. Therefore, the Hybla Gold investigations provided the

opportunity to obtain field data concerning explosion-induced stress effects in the vicinity of an expended event. The state of stress determined at the Dining Car WP (Miller and others, 1975) prior to execution of that event provided the reference to which the Hybla Gold data could be compared.

It is important to note that in this report references to Dining Car stress effects unavoidably includes the unknown effects of time. Approximately 2 years had elapsed between the execution of the Dining Car event and the Hybla Gold investigations. Consequently, stress data collected for the Hybla Gold event represented a complex superposition of the explosion-induced and preexisting stress state modified by time-dependent dissipation and alteration. In addition, the presence of the rubble-filled Dining Car chimney undoubtedly had some influence on stress distribution in its immediate vicinity.

Two methods were used to obtain the stress data for this investigation-- the USBM (U.S. Bureau of Mines) overcore method and hydrofracturing. The overcore method was used to determine the complete state of stress at the Hybla Gold WP and the horizontal stress component(s) at two other locations in the U12e.20 drift complex. A portable hydrofracture system, developed by the USGS and DNA, was used to obtain estimates of minimum stress magnitudes at various locations. A total of 38 hydrofracture tests were conducted in 14 NX-diameter drill holes within the tunnel complex, with the majority of these tests conducted in the area between the Hybla Gold WP and the Dining Car chimney. The hydrofracture data was obtained in order to "map" the distribution of minimum stress magnitudes. No efforts were made to determine the orientation of induced fractures.

As might be expected, conditions for obtaining stress data in the Hybla Gold workings were less than favorable, especially for the overcoring method and particularly at locations nearer the Dining Car chimney. As a result, there is less confidence than normal in the reliability of the calculated stress magnitudes from the overcore data. The results, however, do appear quite reasonable and the indicated directions of the principal and secondary principal stress components are considered reliable in that they are derived directly from the borehole deformation measurements. The hydrofracture measurements also appeared to be influenced by rock conditions in that test results were quite variable over short distances. Presumably, this variability occurred as a consequence of the proximity to the Dining Car vent, although the reasons for it are uncertain. Despite the variability of the hydrofracture test results, however, definite trends in the distribution of pumping pressures and shut-in pressures were apparent.

This report summarizes the results of the Hybla Gold stress investigations and discusses the apparent effects of the Dining Car event on the local stress field. An effort, requiring considerable subjectivity, is made to evaluate the results in context with the present theory of nuclear containment.

FIELD MEASUREMENTS AND RESULTS

USBM Overcore Method

The well-documented USBM overcore method (Hooker and Bickel, 1974) was used to determine the complete state of stress at the Hybla Gold WP and to determine horizontal stress components at two other locations in the U12e.20 drift. Attempts to obtain horizontal stress data at a fourth location were unsuccessful. The locations of these overcore drill holes are shown on figure 30, which is a map of the final configuration of the U12e.20 drift complex showing the location and approximate boundary of the Dining Car chimney. The overcore drill holes are designated as ISS (in situ stress) holes. The ISS-1, -2, and -3 holes were located at the Hybla Gold WP, ISS-7A was in the auxiliary drift at a range of 93 m (305 ft) from the Dining Car WP and ISS-9 was located in the tail drift at a range of 44 m from the Dining Car WP. Holes ISS-4A and -8, from which no successful data were obtained, were located in the main drift at a range of about 48 m (144 ft) from the Dining Car WP.

A major problem encountered in all of the overcore work concerned the determination of the elastic modulus of the overcore samples. The elastic modulus is used in converting the borehole deformations to stress values. Normally, the moduli of the overcore samples are determined using a biaxial pressure chamber and the USBM three-component borehole deformation gage (Fitzpatrick, 1962; Aggson, 1977). This procedure proved unsuccessful, however, because of sample failure either during retrieval from the drill hole or during the biaxial test attempts. In order to arrive at an elastic-modulus estimate for use in the stress calculations, samples from each overcore hole were submitted to Terra Tek, Inc., Salt Lake City, Utah, for triaxial testing. At Terra Tek, a 5.10-cm (2.0-in.) diameter by 6.35-cm (2.50-in.) long cylindrical test specimen was recored from each sample. These

76
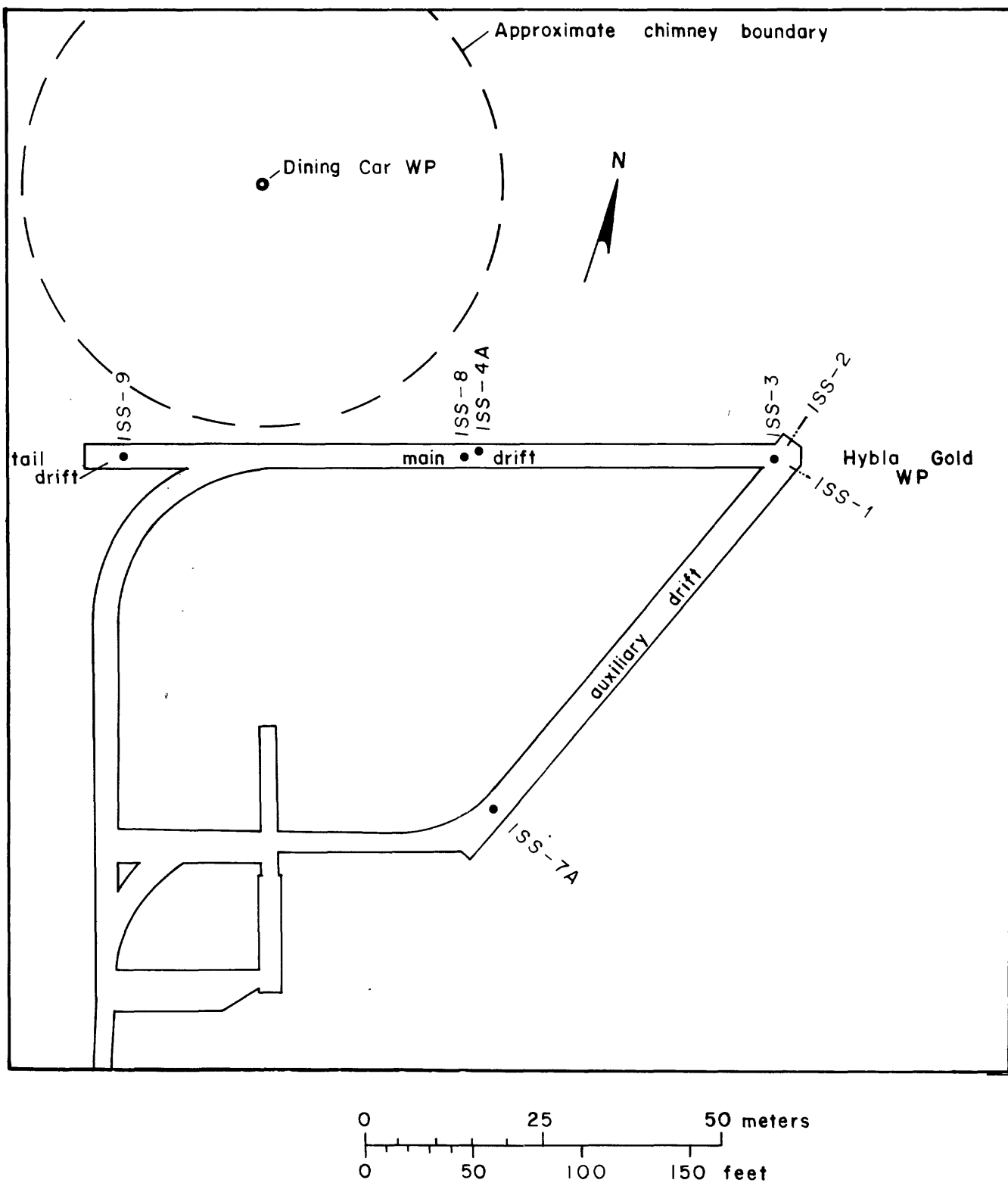
Figure 30.--U12e.20 (Hybla Gold) drift complex showing location of
overcore stress determination (ISS) drill holes.

cylindrical samples were then tested triaxially at 3.5 MPa confining pressure and the elastic moduli scaled directly from the stress-strain curves. Results of these tests are listed in table 8 (D. S. Gardiner, written commun., 1977). The ISS-2, -3, and -7A samples gave mutually consistent results which average 14 Kb, while the ISS-1 and -9 samples gave unrealistically low results of 3.85 Kb and 0.40 Kb, respectively. Overcore samples obtained from the ISS-1, -2, -3, and -7A holes were very similar in physical appearance, drilling characteristics, and behavior during biaxial test attempts. The low result for the ISS-1 sample therefore probably represents a weakness in the cylindrical test sample not representative of the larger overcore from which it was recored. The 14 Kb value was chosen to be the best available estimate for the elastic modulus of overcores obtained at the Hybla Gold WP and from the ISS-7A location. The WP stresses calculated using this elastic modulus value are in good agreement with the vertical stress expected from overburden and compare very well with the minimum stress estimate from hydrofracture data, as will be shown later.

The conditions for arriving at an elastic-modulus value for the ISS-9 overcores were even less favorable. The overcore samples from this hole were significantly different in appearance and behavior from those at the WP and ISS-7A site. The rock was much less competent and tended to moderately disaggregate during overcoring, requiring a modification to normal overcoring procedures. A reasonable estimate of the elastic modulus of the overcore samples could not be made with any degree of confidence. The Terra Tek triaxial test result of 0.40 Kb is unrealistic for stress calculations, although it was probably quite indicative of the condition or behavior of the rock after its removal from the confined in situ state. It is almost certain

Table 8.--Results of Terra Tek, Inc., triaxial compression tests for determination of elastic modulus from over-core samples (3.45 MPa confining pressure)

[Leaders (---), indicate data not measured]

Overcore drill-hole No.	Depth meters (feet)	Elastic modulus (Kb)	Poisson's ratio[1]
ISS-1	2.1 (6.9)	3.85	0.44
ISS-2	4.3 (14.1)	14.81	0.16-0.21
ISS-3	1.2 (3.9)	13.79	0.18-0.20
ISS-7A	2.4 (7.9)	13.33	0.16-0.18
ISS-9	---	0.40	---

[1]Range was derived from difference in the two lateral strain measurements.

that the 0.40-Kb value was not representative of the stress-strain behavior of the rock during the overcoring operation.

Extreme degradation of strength and modulus properties of tuff near an underground nuclear detonation was observed in postevent studies of the Rainier event (Diment and others, 1959). This degradation of mechanical properties was attributed primarily to the presence of extensive microfracturing induced by the shock loading of the rock. The Rainier event experience indicated the microfracturing to be most intense near the chimney boundary and to decrease in intensity with increased distance from the chimney. Microfracturing was also observed in rock samples from the vicinity of the Dining Car event and were cited as a causitive factor in apparent rock-streng'h reduction (Gardiner and Butters, 1977). Because the ISS-9 drill hole was located within about 10 m (32.8 ft) of the Dining Car chimney, it is reasonable to assume that the rock at the location was extensively microfractured. If so, then the process of stress relief from overcoring would allow dilation of the microfracture and would result in a gross change in the structural and behavioral characteristics of the overcore sample. The rock would thus not obey the laws of elasticity, and subsequent laboratory testing of the sample would not produce a modulus parameter representative of the load-deformation response of the rock during the initial stress-relief overcoring. Apparently, such a situation existed at the ISS-9 location as suggested by the physical deterioration of the core and the triaxial test result.

Because of the inability to determine a modulus value considered representative of the deformational behavior of the rock during overcoring, the magnitude of the stresses at this location could not be reliably determined. The quality of the borehole deformation data obtained during

overcoring appeared quite good, however, and at least provided information regarding the orientation of the horizontal stress components as well as the ratio of their relative magnitudes. Presumably, an appropriate elastic-modulus value for conversion of the borehole-deformation data to secondary principal stresses lies somewhere between a minimum of a few kilobars to a maximum of about 14 Kb; the value used for the more competent rock at the WP. For purposes of this report, the 14 Kb elastic-modulus value was arbitrarily chosen for conversion of the borehole deformations to stress values. The stresses thus calculated should provide a reasonable upper limit estimate of the horizontal stress magnitudes at the ISS-9 location.

Hybla Gold Working Point

Overcoring borehole deformation obtained from drill holes ISS-1, -2, and -3 were used to determine the complete state of stress at the Hybla Gold WP. Figure 31 is a map showing the U12e.20 drift configuration at the time the measurements were made and showing the location of the overcore holes.

Three overcores were obtained in each drill hole, providing a total of 27 borehole-deformation measurements for use in the stress calculations. Because of time constraints and minor difficulties imposed by rock conditions, the measurements were made at relatively shallow drill-hole depths. The drift diameter at the time of overcoring was approximately 3.3 m (11.0 ft), and overcoring measurements were made between drill-hole depths of 1.5 m (4.9 ft) and 4.7 m (15.4 ft). The majority of the data were therefore obtained within one diameter of the drift opening, and as such were subject to the influence of the drift opening. Indications are, however, that this influence did not greatly affect the final results. Good agreement between the calculated vertical stress component and that expected from overburden, as well as the excellent agreement between the minimum stress magnitude and hydrofracture

81
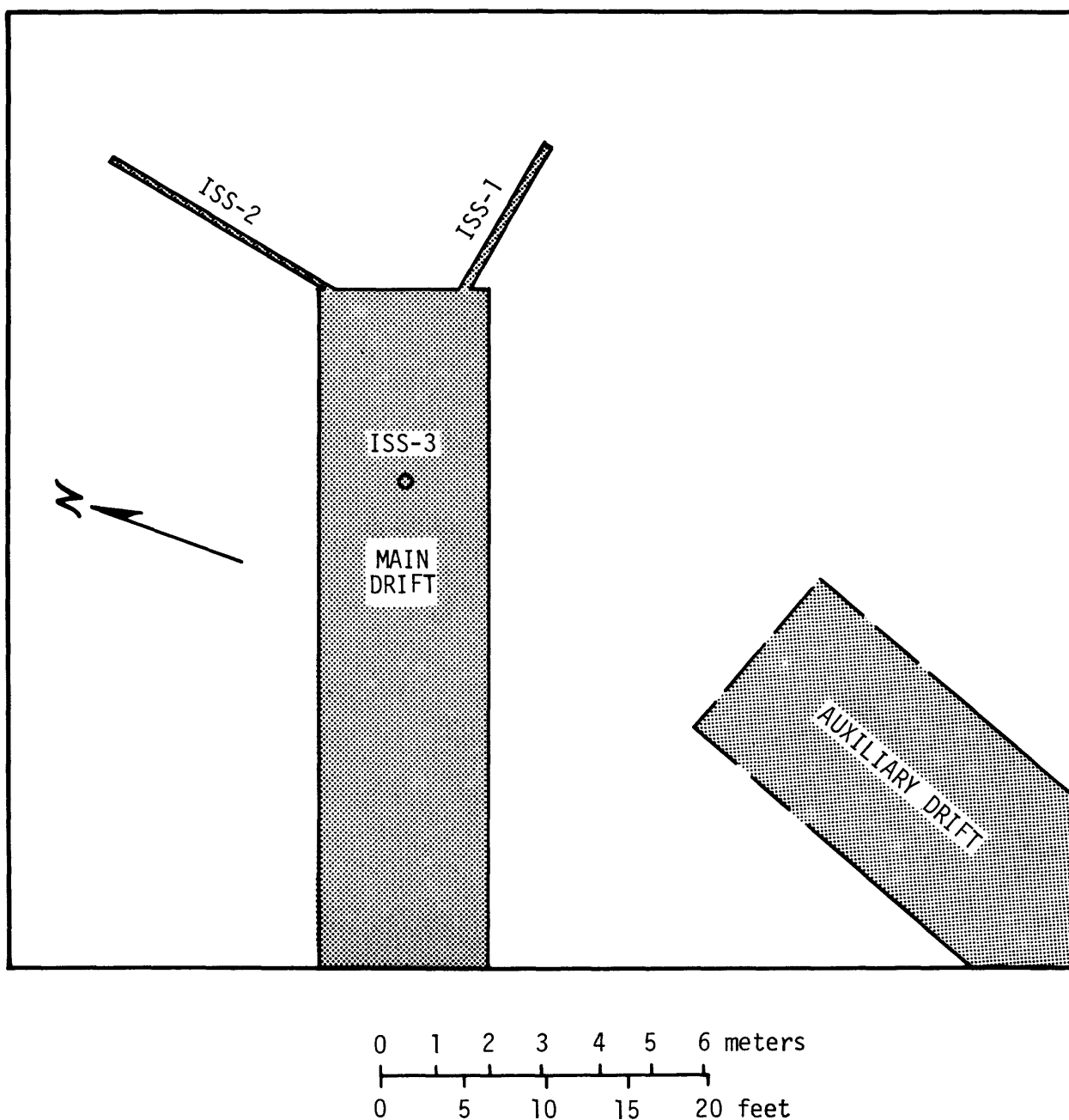
Figure 31.--Hybla Gold WP area, showing location of ISS-1, -2, and -3
   overcore drill holes and drift configuration at time of measure-
   ments in ISS-1 and -3 holes.

data, suggested that the calculated stresses were reasonably representative of the free-field stresses.

Results of the WP stress calculations are shown in table 9 and figure 32 is a graphical representation of the principal stress axes. The vertical-stress component (σ_z in table 9) of 6.4 MPa compares well with the expected vertical stress of 7.1 MPa from the 385 m (1,263 ft) of overburden (average density of 1.89 Mg/m^3).

The minimum principal stress (S_1 in table 9) of 3.2 MPa is in agreement with the minimum stress estimate of 3.2 MPa derived from hydrofracture data obtained in a drill hole penetrating the WP area prior to completion of mining of the drift (p. 100). The calculated standard deviations of the principal stress components (S_1, S_2, S_3) are greater, in percent, than normally expected in cases where conditions are not complicated by geologic or other factors. These relatively high standard deviations most likely are the result of the measurements being obtained within a zone of stress gradient caused by the drift opening. As a consequence, there is a greater degree of uncertainty in the calculated mean-stress magnitudes than if the measurements had been obtained in a uniform stress field.

The stress magnitudes determined at the Hybla Gold WP are very similar to those determined at the Dining Car WP prior to execution of that event. There is, however, a significant difference in the orientation of the stress components. A comparison and examination of the differences in these two stress determinations will be discussed later in this report.

Horizontal Secondary Principal Stresses

In addition to the WP site, data for determination of horizontal stress components was obtained at two other locations in the U12e.20 drift. Three overcores each were obtained from vertical holes ISS-7A in the auxiliary drift

Table 9.--State of stress determined at Hybla Gold WP

[---, not applicable]

	Stress magnitude MPa	Standard deviation MPa	Bearing	Inclination + degrees above horizontal - degrees below horizontal
Principal stresses				
(+, compression)				
S_1 (minimum)	3.2	±1.6	N. 70° E.	+7°
S_2 (maximum)	6.6	±1.5	N. 4° W.	-68°
S_3 (intermediate)	5.6	±1.0	N. 23° W.	+21°
Normal stress components in X, Y, Z (east, north, vertical) coordinate system				
(+, compression)				
σ_x	3.5	±0.4	East	Horizontal
σ_y	5.4	±0.4	North	Horizontal
σ_z	6.4	±0.4	---	Vertical
Shear stress components in X, Y, Z coordinate system[1]				
τ_{xy}	-0.8	±0.3	---	---
τ_{yz}	-0.5	±0.4	---	---
τ_{zx}	-0.2	±0.4	---	---

[1]Positive or negative sign on shear stress magnitude indicates direction of shear stress with respect to X, Y, Z coordinate system.

$S_1 = 3.2\ MPa \quad N.70°E. + 7°$

$S_2 = 6.6\ MPa \quad N.04°W. - 68°$
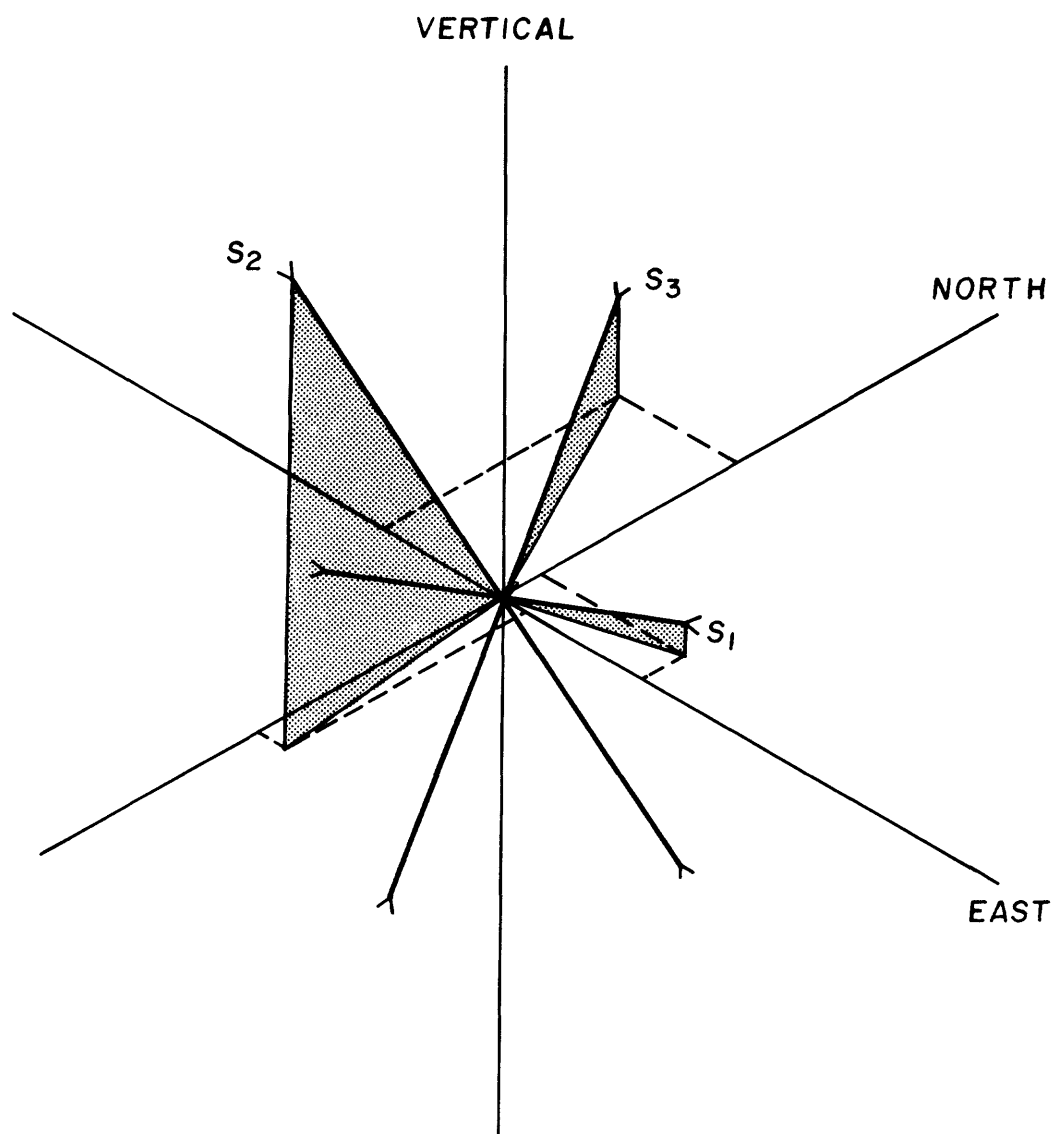
$S_3 = 5.6\ MPa \quad N.23°W. + 21°$

Figure 32.--Graphical representation of principal stress axes, Hybla Gold WP.

and ISS-9 in the tail drift (fig. 30). Attempts were made to obtain data at a fourth location (holes ISS-4A and -8), but they proved unsuccessful owing to poor rock conditions.

Rock and overcoring conditions at the ISS-7A location were very similar to those at the Hybla Gold WP. Three overcores were successfully obtained between drill-hole depths of 2.0 and 2.8 m (6.6 and 9.2 ft).

At the ISS-9 location overcoring conditions were very difficult owing to the unfavorable rock conditions. To obtain borehole-deformation data at this site it was necessary to improvise modifications to the overcoring procedure. To prevent gross failure of the rock during overcoring a 30-cm (12.0-in.) diameter core barrel was used rather than the normal 15-cm (6.0-in.) diameter barrel. The use of the larger core barrel should theoretically have no adverse effect on the borehole-deformation data (Panek, 1966). Rock conditions also adversely affected the EX-diameter pilot hole into which the deformation gage was emplaced prior to overcoring. The pilot hole tended to be oversized and the soft nature of the rock allowed the sensor pistons of the gage to scour the pilot-hole walls during gage setting. As a result, it was not possible to attain a sufficient preload on the gage. The problem was overcome by emplacing a thin grout lining around the inside of the EX pilot hole. This was accomplished by emplacing grout and an EX drill rod into the oversized pilot hole. After setup of the grout, the drill rod was broken free by applying torque and was removed from the hole. The thin grout lining that remained brought the hole into proper dimensions and provided a bearing surface for the deformation gage sensor pistons. The grout lining was less than 0.32 cm (0.13 in.) in thickness, and as such, should have had no significant effect on the borehole-deformation data, even though the grout modulus (not measured) was greater than that of the rock.

Table 10 lists the horizontal secondary principal stresses calculated
from the borehole-deformation measurements made in holes ISS-7A and -9. Also
listed in the table are the principal horizontal stress components calculated
from the complete stress determination at the Hybla Gold WP. The ISS-7A and
-9 stress calculations were done assuming plane strain conditions. A 14-Kb
elastic-modulus value was used in the calculations. As previously discussed,
there is considerable doubt concerning this modulus value for the ISS-9
location, and the stress magnitudes calculated using this value at the
ISS-9 site are considered an upper limit estimate. Because of this
uncertainty the ISS-9 stress values are queried (?) in table 10 and throughout
this report.

Also shown in table 10 are the mean horizontal secondary principal
stresses for the ISS-7A and -9 sites. These mean stresses were arrived at by
averaging common stress components $(\sigma_x, \sigma_y, \tau_{xy})$ of the two most <u>directionally</u>
consistent overcores from each drill hole. These average stress components
were then used to resolve the mean horizontal secondary principal stresses for
each site. These mean horizontal principal stresses and those at the Hybla
Gold WP, are plotted at their respective locations on figure 33. The
horizontal principal stresses determined at the Dining Car WP prior to the
Dining Car event are also shown on figure 33.

It is apparent from figure 33 that the Dining Car event has had an effect
on the distribution of horizontal stresses in the area as shown by the
directional variations of the maximum and minimum horizontal stress
components. These variations, and how they apparently relate to the Dining
Car event and original stress field, are presented in "Discussion of Results".

Table 10.--Horizontal secondary principal stresses determined in U12e.20 drift complex

[Query (?) indicates considerable uncertainty in elastic modulus value used to calculate stresses. Values are considered to be an upper limit estimate of actual stress magnitudes. Leaders (---) indicate not applicable.]

Hole No.	Location	Orientation	Overcore number	Depth meters (ft)	Secondary principal stresses Maximum (MPa)	Minimum (MPa)	Orientation
ISS-7A	U12e.20 auxiliary drift	vertical	1	2.0 (6.6)	5.1	3.2	N. 3° W.
			2	2.4 (7.9)	5.0	4.2	N. 35° E.
			3	2.8 (9.2)	4.9	4.0	N. 52° E.
			average[1] 2 and 3		4.9	4.1	N. 44° E.
ISS-9	U12e.20 tail drift	vertical	1	1.8 (5.9)	5.1(?)	3.5(?)	N. 86° W.
			2	2.2 (7.2)	4.9(?)	4.0(?)	N. 26° W.
			3	2.6 (8.5)	4.7(?)	3.7(?)	N. 76° W.
			average[1] 1 and 3		4.9(?)	3.6(?)	N. 82° W.
---	Hybla Gold[2] WP	---	---	---	5.7	3.2	N. 19° W.

[1]Average determined from two most directionally consistent overcores.
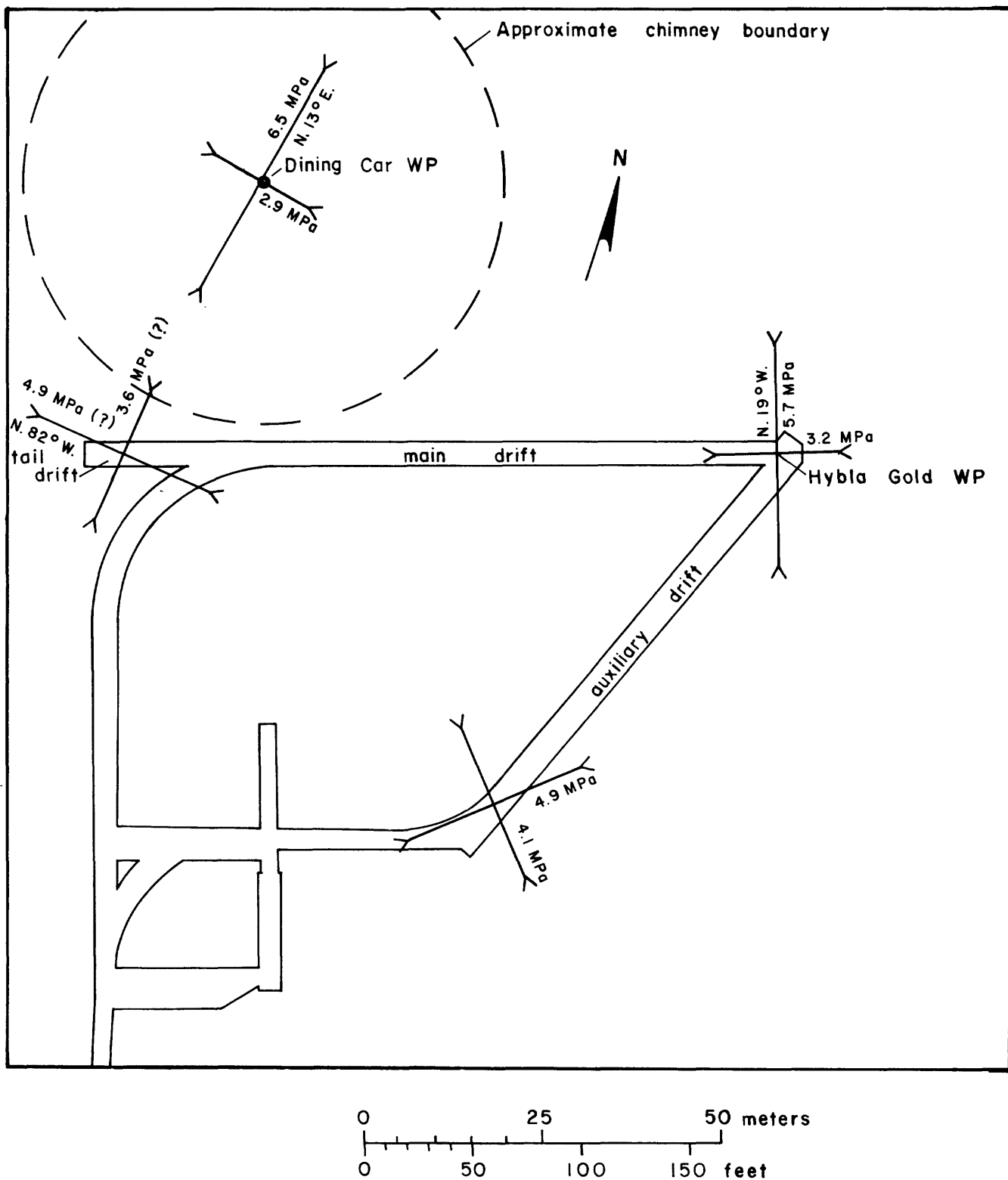[2]Determined from complete stress determination at Hybla Gold WP.

Figure 33.--Mean horizontal secondary principal stresses determined in
the U12e.20 drift complex.

89

Hydrofracture Measurements

The proximity of the Hybla Gold drift and WP to the Dining Car chimney initiated interest in the distribution of minimum stress magnitudes in the vicinity of, and especially in the area between, the Hybla Gold WP and the Dining Car chimney. Hydrofracturing proved to be a practical method for obtaining this information.

The theory of the hydrofracture method of stress evaluation is widely published (Haimson, 1977) and will only be discussed briefly. The method consists of isolating a section of drill hole by use of an inflatable straddle-packer assembly. The isolated section, called the test zone, is then pressurized with a hydraulic fluid, in this case water. The pressure in the test zone is continuously recorded on a strip-chart recorder during pressurization, and for some time afterwards, such that three distinct pressures can normally be determined. If there is no preexisting fracture within the test zone, then at some critical pressure, called the breakdown pressure, the rock surrounding the test zone will rupture forming a tensile fracture. The fracture can be further propagated by continuous pumping at the "formation acceptance" pressure, more commonly called the crack propagation pressure. The pressure required to keep the fracture open without further propagation, the shut-in pressure, occurs after pressurization or pumping is stopped and the test zone is isolated, or shut in. The basic premise of hydrofracturing is that the induced fracture will initially form, or quickly aline itself, normal to the least principal stress component. As such, the shut-in pressure is considered to be a good estimate of the minimum in situ stress magnitude.

A major concern in the practical application of hydrofracture testing is the potential influence of preexisting fractures or joints on the test

results. If conditions are such that the pressurizing fluid, rather than inducing a fracture, enters a preexisting fracture not alined normal to the minimum stress, then the shut-in pressure should be greater than the minimum stress magnitude. Whether or not a preexisting fracture would be pressurized depends on a complex interrelationship of such factors as stress difference, drill-hole orientation, fracture orientation and tensile strength of the rock. The authors are not aware of any definitive study undertaken to examine this potential problem in a field environment. The problem is usually circumvented by simply testing in competent, unfractured sections of drill hole. In many environments, including Rainier Mesa, this option is often not available.

The approach to the USGS/DNA hydrofracture program in Rainier Mesa has been to conduct tests whenever possible in designated drill holes (from tunnel level) without preselection of test zones. The rationale behind this approach is that the composite test results, while perhaps more qualitative, offer a better measure of relative stress conditions in the rock mass than if tests were conducted only in unfractured zones. This approach was dictated largely by the fact that rarely is a potential test zone of sufficient length encountered that contains no fractures or joints. Experience with hydrofracture testing in Rainier Mesa would seem to indicate that drill-hole orientation, and by implication random orientation of fractures with respect to the drill hole, has no obviously consistent effect on test results. A possible explanation for this may be the low tensile strength of the tuffs, which increases the probability that new fractures normal to the minimum stress will be induced before attaining pressures sufficient to open preexisting fractures oriented significantly non-normal to the least stress component.

This approach to hydrofracturing in Rainier Mesa has indicated that when several tests are conducted in an area, the mean value of the test results compare favorably (within 20-30 percent) to the minimum stress magnitude determined by the overcoring method. Based on this experience it appears that hydrofracture testing in Rainier Mesa provides a reasonable estimate of the minimum stress magnitude and that possible adverse effects of preexisting fractures are not normally a serious concern.

The hydrofracture data for Hybla Gold was obtained using a portable system developed by the USGS and DNA for use in NX (7.62 cm) (3.0 in.) diameter drill holes drilled from underground workings. The test-zone length (distance between straddle packers) was set at 103 cm (40.6 in.) for all tests. Downhole test-zone pressures were monitored with a pressure transducer mounted in the rear of the straddle-packer assembly and were plotted versus time on a strip-chart recorder. Volume output of the system was approximately 2.0 L/min.

A total of 38 hydrofracture tests were conducted in 14 horizontal drill holes located at various positions around the Hybla Gold workings (fig. 34). Results of these tests are listed in table 11. It is noted that the U12e.20 UG-3 drill hole (fig. 34) was drilled and tested along its entire length prior to completion of mining of the main drift. Figure 35 is a plot of the results from table 11 versus radial distance from the Dining Car WP. Figure 36 is a similar plot for the data from only the UG-3 and HF-5 drill holes. The results beyond the 55-m (180.0-ft) range from the Dining Car WP were quite erratic with alternating zones of relatively high and low test results. It is uncertain why this variability occurred, other than the fact that the tests were conducted in a rock mass which had been subjected to gross disturbance from the Dining Car event. Mechanical-properties data from core samples in
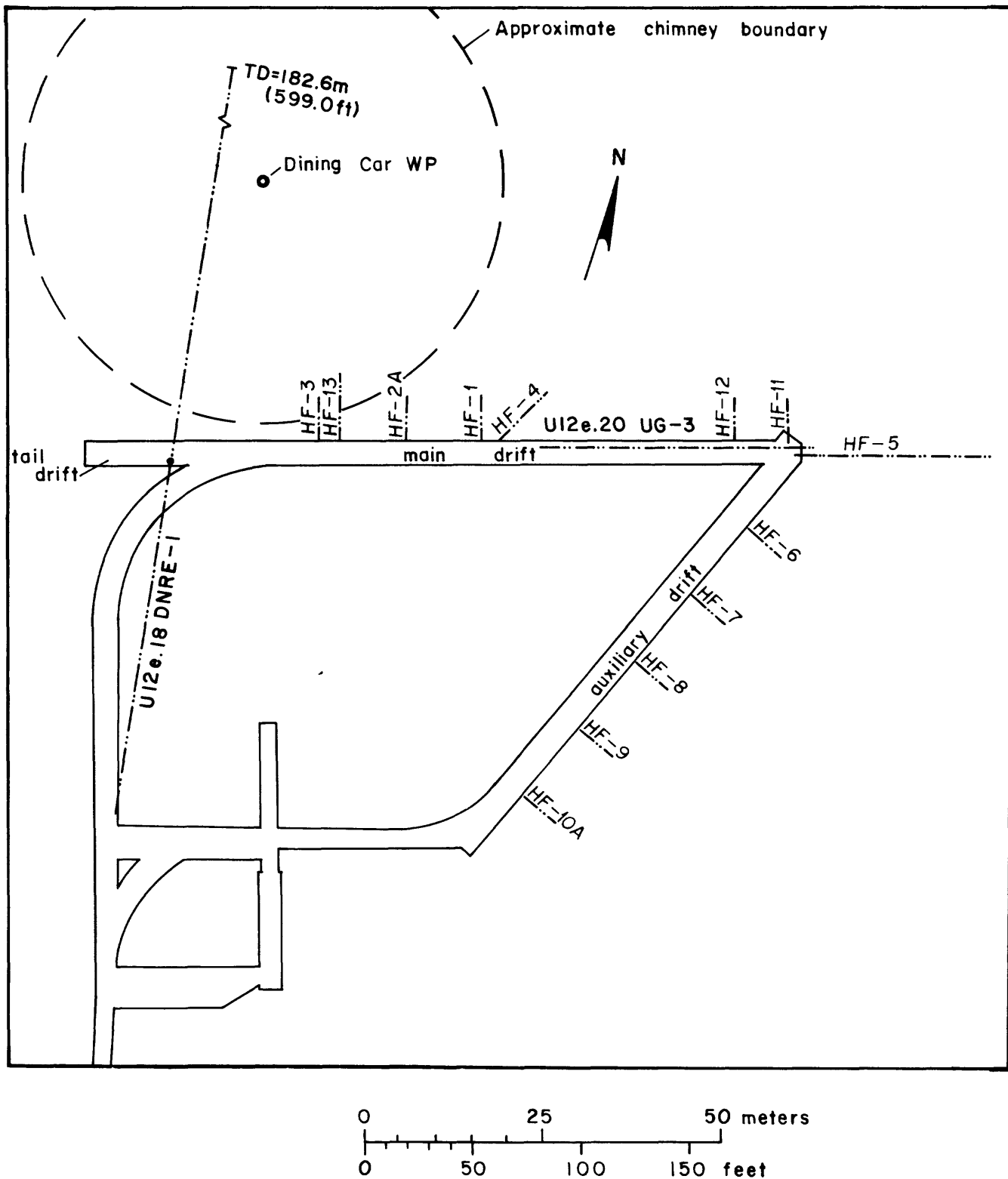
Figure 34.--Location of hydrofracture test holes in U12e.20 drift complex.

Table 11.--Results of hydrofracture tests in U12e.20 drill holes
[Leaders (---) indicate breakdown pressure did not occur or was less
than formation acceptance pressure. Query (?) indicates shut-in
pressure could not be estimated.]

| Hole No.	Depth from collar m (ft)		Range from Dining Car WP m (ft)		Breakdown pressure (MPa)	Formation acceptance pressure (MPa)	Estimated shut-in pressure (MPa)
U12.18 DNRE-1	11.7	(38.4)	78.5	(257.5)	---	3.1	1.9
U12e.20 UG-3	3.5	(11.5)	56.0	(183.7)	4.9	3.6	2.4
	6.6	(21.7)	58.5	(191.9)	3.6	3.0	2.5
	9.6	(31.5)	61.0	(200.1)	6.6	5.1	3.4
	12.7	(41.7)	63.5	(208.3)	4.1	2.9	2.8
	15.7	(51.5)	65.5	(214.9)	4.4	3.0	2.9
	18.8	(61.7)	68.0	(223.1)	6.8	6.1	6.1
	21.8	(71.5)	70.5	(231.3)	7.9	6.8	6.6
	24.9	(81.7)	73.0	(239.5)	5.6	3.7	3.1
	27.9	(91.5)	76.0	(249.3)	---	5.8	?
	30.9	(101.4)	78.5	(257.5)	5.8	3.9	3.3
	34.0	(111.5)	81.0	(265.7)	---	4.2	3.9
	36.9	(121.1)	83.2	(273.0)	---	2.9	2.5
U12e.20 HF-5	1.6	(5.2)	84.4	(276.9)	---	4.1	3.6
	4.6	(15.1)	86.9	(285.1)	---	5.6	4.6
	10.7	(35.1)	92.7	(304.1)	7.7	5.8	4.6
	13.7	(44.9)	95.4	(313.0)	---	6.5	5.2
	16.8	(55.1)	98.1	(321.9)	12.7	4.1	3.6
	19.8	(65.0)	101.2	(332.0)	6.5	5.8	3.7
	22.9	(75.1)	103.9	(340.9)	---	3.4	3.0
	25.9	(85.0)	106.7	(350.1)	5.2	4.3	3.9
U12e.20 HF-2A	3.0	(9.8)	38.5	(126.3)	2.6	2.3	1.6
	4.6	(15.1)	37.0	(121.4)	2.6	1.5	1.3
U12e.20 HF-3	2.8	(9.2)	34.0	(111.5)	---	1.7	1.4
	4.3	(14.1)	32.0	(105.0)	---	1.4	1.2
U12e.20 HF-4	3.2	(10.5)	47.8	(156.8)	---	2.9	2.6
	6.2	(20.3)	47.8	(156.8)	3.7	3.1	2.9
	7.8	(25.6)	48.0	(157.5)	3.1	2.3	2.1
U12e.20 HF-6	3.3	(10.8)	86.3	(283.1)	5.9	4.8	2.8
U12e.20 HF-7	2.8	(9.2)	85.6	(280.8)	9.5	7.2	4.5
U12e.20 HF-8	4.5	(14.8)	89.0	(292.0)	---	8.3	6.6
U12e.20 HF-9	4.6	(15.1)	92.4	(303.1)	---	8.6	6.6
U12e.20 HF-10A	4.8	(15.7)	97.2	(318.9)	7.6	6.6	5.5
U12e.20 HF-11	4.7	(15.4)	79.2	(259.8)	3.2	2.5	2.3
U12e.20 HF-12	4.3	(14.1)	73.8	(242.1)	4.6	4.1	3.8
U12e.20 HF-13	1.7	(5.6)	35.7	(117.1)	2.7	2.2	1.7
	4.7	(15.4)	33.1	(108.6)	1.8	1.7	1.5
	7.4	(24.3)	30.5	(100.1)	1.8	1.5	1.1
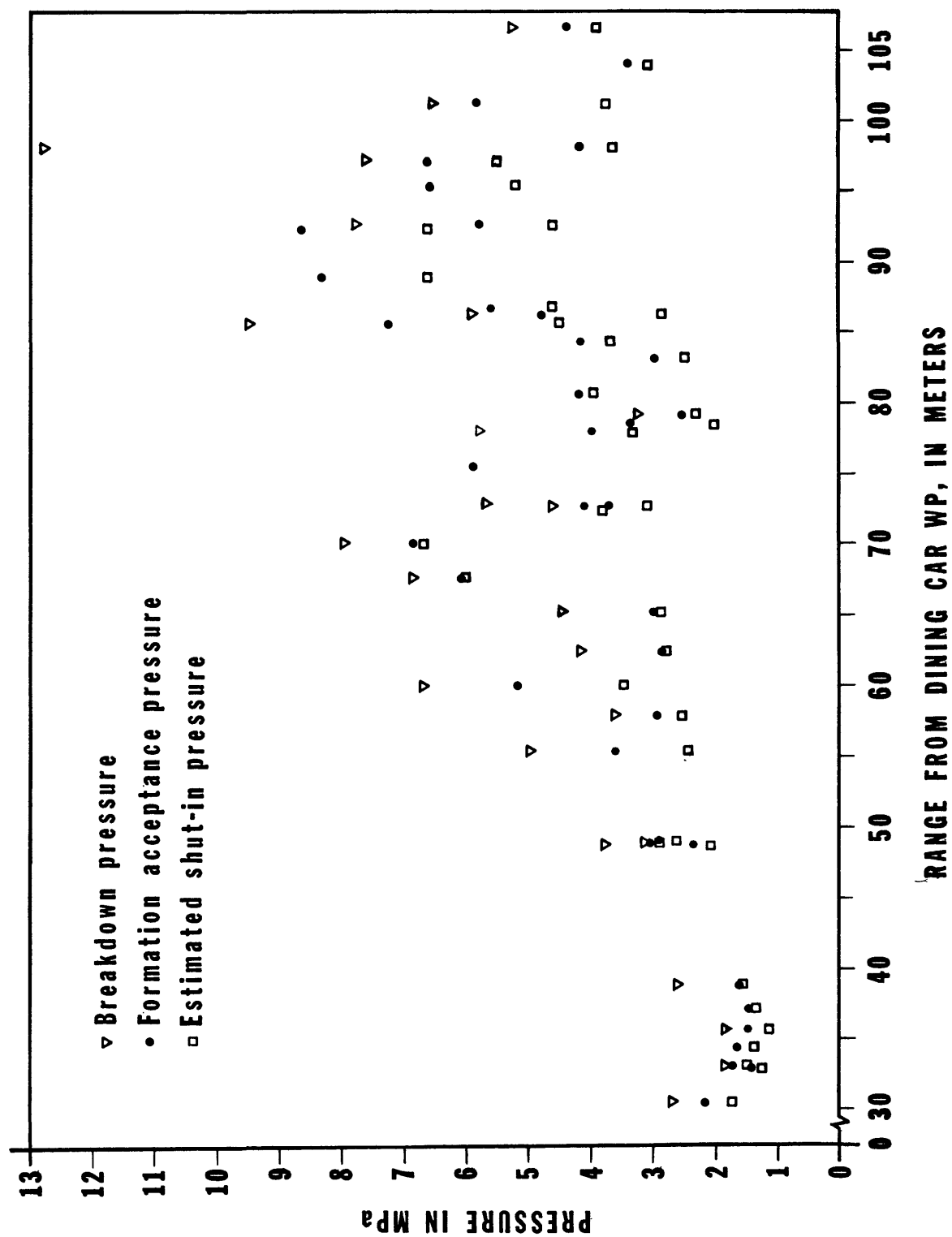
Figure 35.--Hydrofracture test results versus range from Dining Car WP.
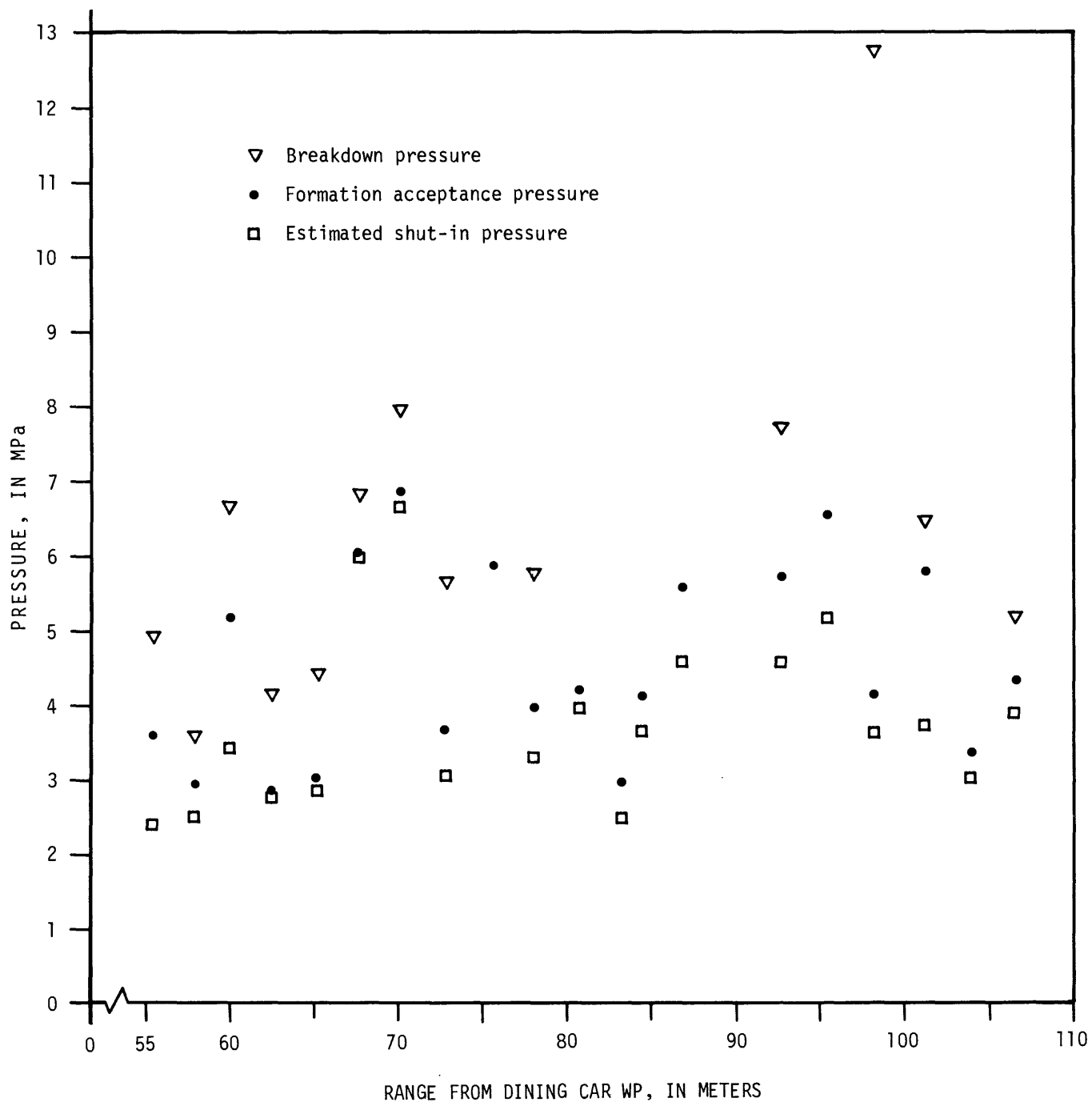
95

Figure 36.--Hydrofracture test results versus range from Dining Car WP, HF-5 and UG-3 drill holes.

the area also exhibit a high degree of variability. For example, figures 37a and 37b are plots of dynamic Young's modulus and dynamic bulk modulus versus range from the Dining Car WP for core samples obtained from the UG-3 and HF-5 drill holes. These values exhibit a variability similar to that of the hydrofracture data. The variability in mechanical property and hydrofracture data may have occurred as a result of the presence of numerous and closely spaced zones of weakness in the rock mass. During mining of the main drift with a continuous miner, extensive slabbing of rock from the tunnel heading was observed, indicating planes of weakness that were otherwise not visually obvious.

There appears to be a correlation between variability in mechanical properties of the rock mass, tunnel observations of extensive slabbing, and the scatter in the hydrofracture test results. The mechanism by which these apparent rock inhomogeneities influenced the hydrofracture test results is not completely understood. In the evaluation of the Hybla Gold hydrofracture data, however, it is assumed that the variability of test results is due to real variations in minimum stress magnitude. Because these stress variations are apparently very localized, any individual test result would not be representative of the greater rock mass. To obtain the best estimate of the minimum stress distribution in the vicinity of the Dining Car event, therefore, requires that an averaging technique be applied to the hydrofracture data.

Even with the variability of the hydrofracture data, the plots of figures 35 and 36 indicate an underlying trend in the distribution of values. In order to emphasize this trend and present a much better indication of the general distribution of minimum stress magnitude in the rock mass, a three-term moving-average filtering technique (Davis, 1973) was applied to the data. The results of this averaging technique are shown on figure 38 for all

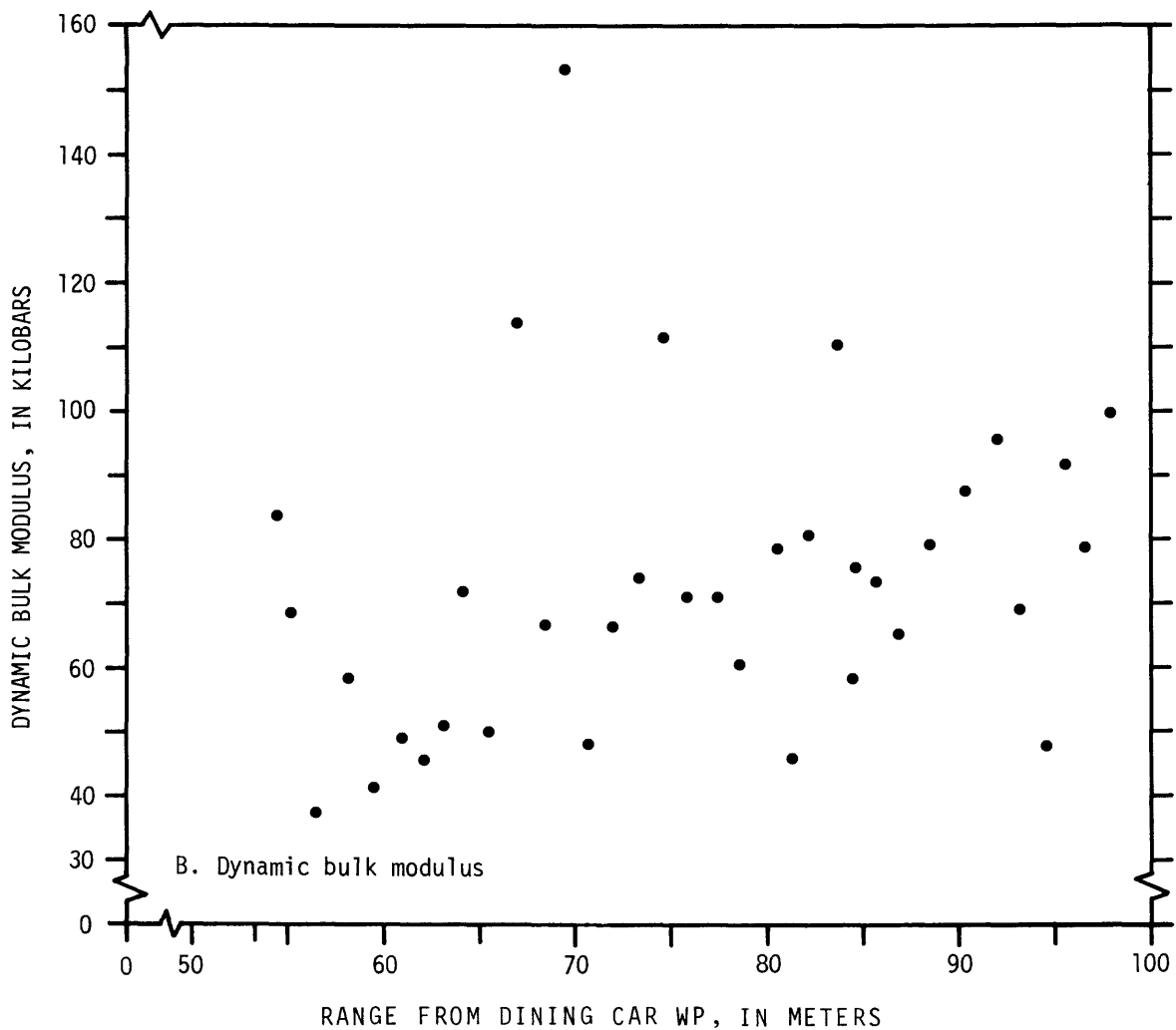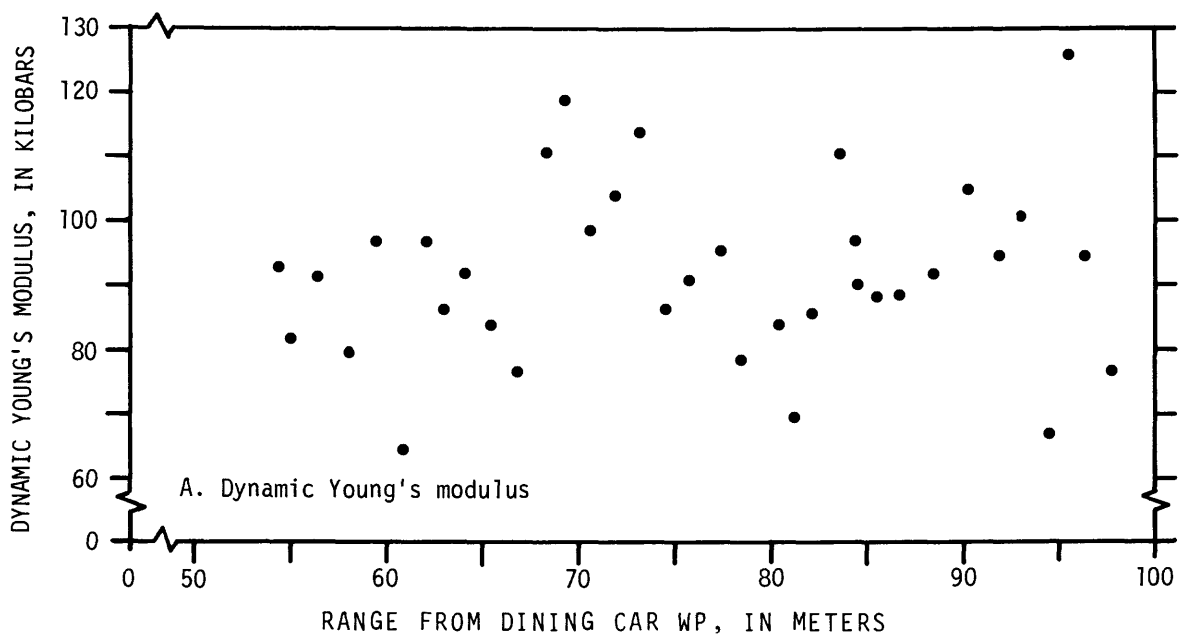Figure 37.--Plot of dynamic modulus (A, Young's; B, bulk) of core
     samples from U12e.20 UG-3 and U12e.20 HF-5 drill holes
     versus range from Dining Car WP.

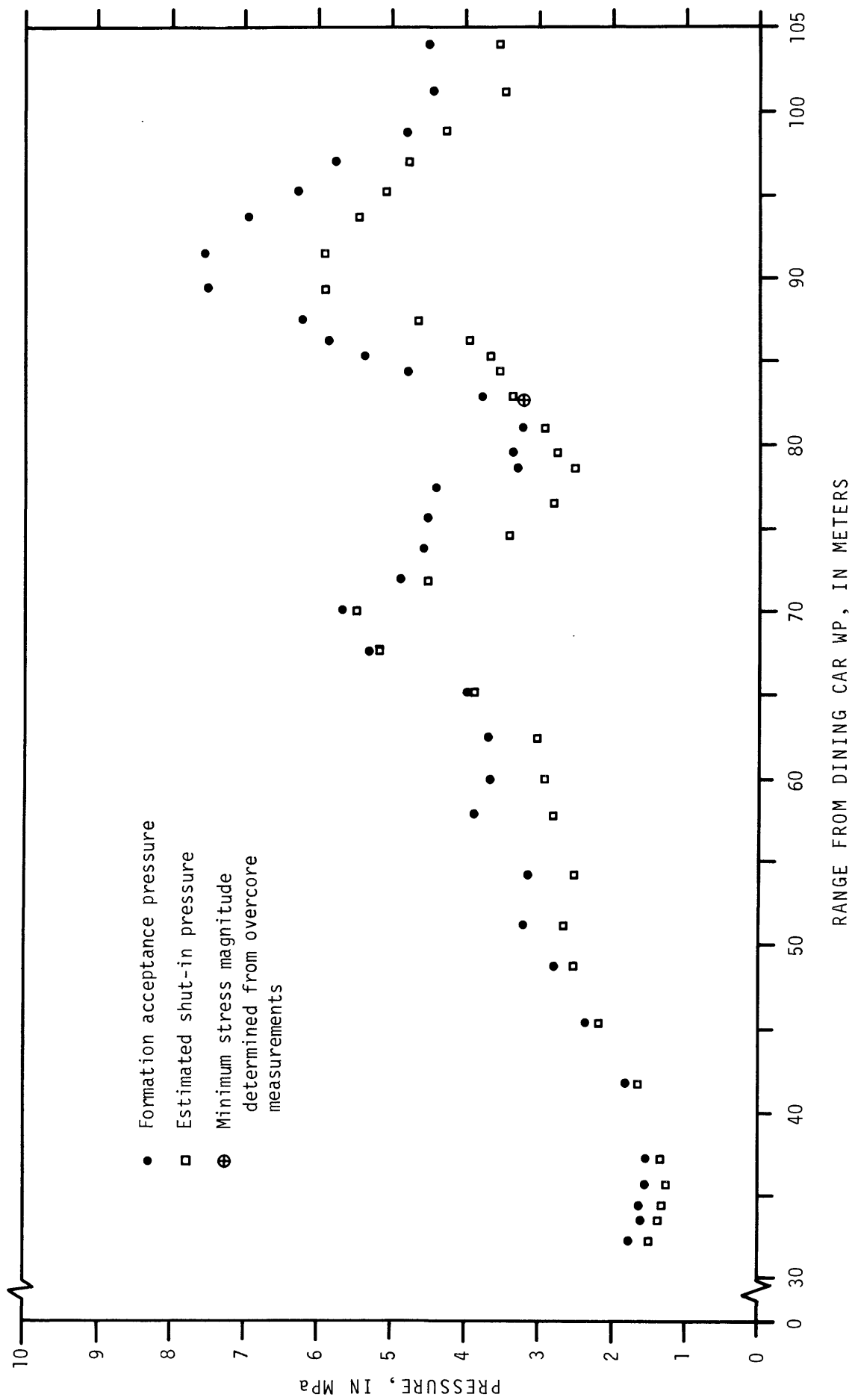Figure 38.--Hydrofracture results versus range from Dining Car WP using three-term moving average filtering technique.

Legend:
- Formation acceptance pressure
- Estimated shut-in pressure
- Minimum stress magnitude determined from overcore measurements

of the data points, and figure 39 for the data from the UG-3 and HF-5 drill holes. Only average formation acceptance pressures and shut-in pressures are shown, as breakdown pressures did not occur in all tests. It is important to note that these plots represent estimates of the minimum stress magnitude only, and that it should not be implied that the minimum stress orientation is constant.

The plot of the filtered data on figures 38 and 39 indicate an interesting distribution of minimum stress magnitude. Beginning at 32-m (105.0-ft) range from the Dining Car WP (fig. 38), the data indicate a gradual increase in minimum stress magnitude out to a range of about 62 m (203.4 ft). The most notable feature of the plots, however, is the two zones of relatively high minimum stress magnitude centered at about 69- and 90-m (226.4 and 295.3-ft) range from the Dining Car WP.

For purposes of examining the minimum stress profile versus range from the Dining Car WP, the data from the UG-3 and HF-5 drill holes (fig. 39) are most appropriate. The reason is that the post-Dining Car state of stress is theoretically a result of the superposition of spherically symmetrical explosion-induced stresses upon a deviatoric preexisting stress field with constant orientation. The resultant minimum stress magnitude is therefore a function of both range and direction from the Dining Car WP. By using only the data from the UG-3 and HF-5 drill holes, this directional influence is minimized. It is noted that at a range of 81 m (265.7 ft), which corresponds to the Hybla Gold WP, the shut-in pressure curve on figure 39 indicates a minimum stress magnitude of 3.2 MPa. This is in agreement with the minimum stress magnitude of 3.2 MPa determined at the Hybla Gold WP by the overcoring method (table 9).
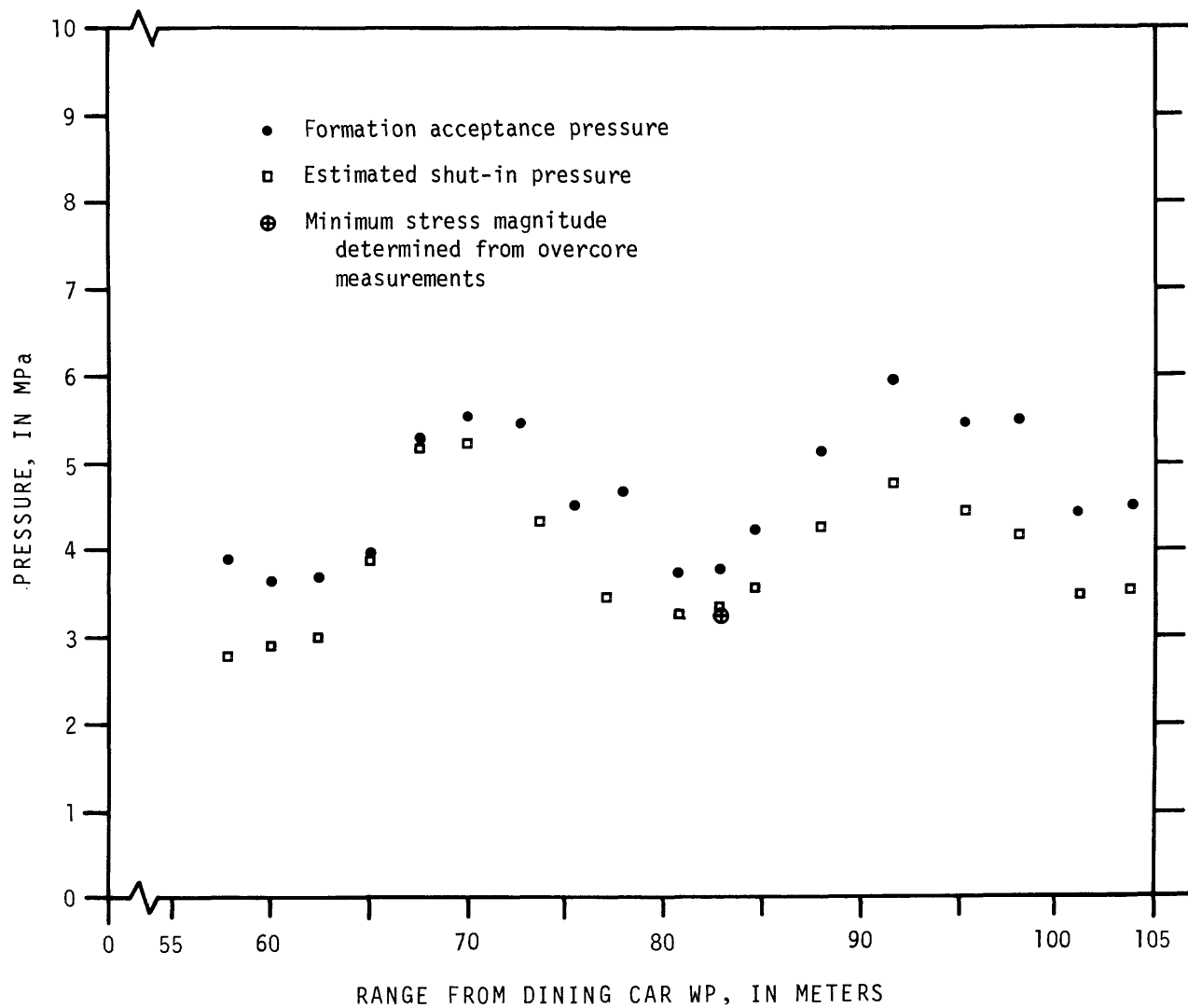
Figure 39.--Hydrofracture results from UG-3 and HF-5 drill holes versus range from Dining Car WP using three-term moving average filtering technique.

101

As discussed above, conditions of the rock mass beyond about 55-m (180.4-ft) range from the Dining Car WP may have been responsible for the variability observed in the hydrofracture data. Similarly, properties of the composite rock mass may have had an influence on the average minimum stress profile of figures 38 and 39. Figure 40 is a histogram of dynamic Young's and bulk moduli of core samples from the UG-3 and HF-5 drill holes averaged over 3-m (9.8-ft) intervals and plotted as a function of range from the Dining Car WP. It can be seen from the plot that there is a subtle correspondence of zones of relatively high moduli values with the zones of relatively high minimum stress magnitude shown on figure 39. This suggests that the higher strength zones in the rock mass, as indicated by the higher moduli, are supporting greater stress than the weaker adjacent rock. The variation in the average moduli values on figure 40 is not dramatic, and under normal in situ conditions would probably not influence stress distribution to the extent indicated by figure 39. Conditions in the vicinity of Dining Car are not normal, however, in that the rock was subjected to large displacements and high magnitude explosion-induced stresses from the event. The subsequent dissipation of these stresses and readjustments within the rock mass apparently resulted in the retention of greater stress in the more competent, or stiffer, zones. The stress lost by the weaker rock could also have been transferred to the higher modulus zones. The minimum stress profile of figures 38 and 39 is possibly the result of an initial explosion-induced stress distribution which, during the process of dissipation, has been modified substantially by creep and relaxation in a rock mass containing zones of differing stress-strain characteristics.
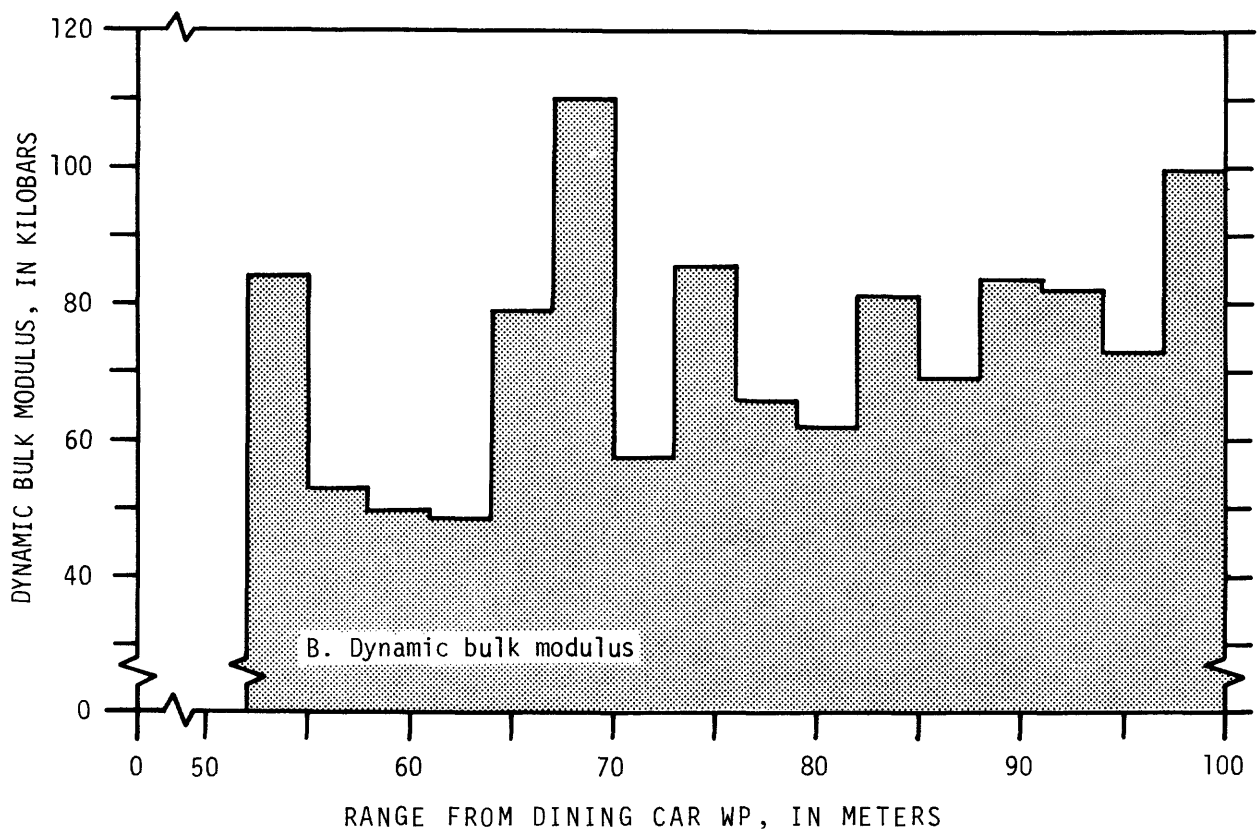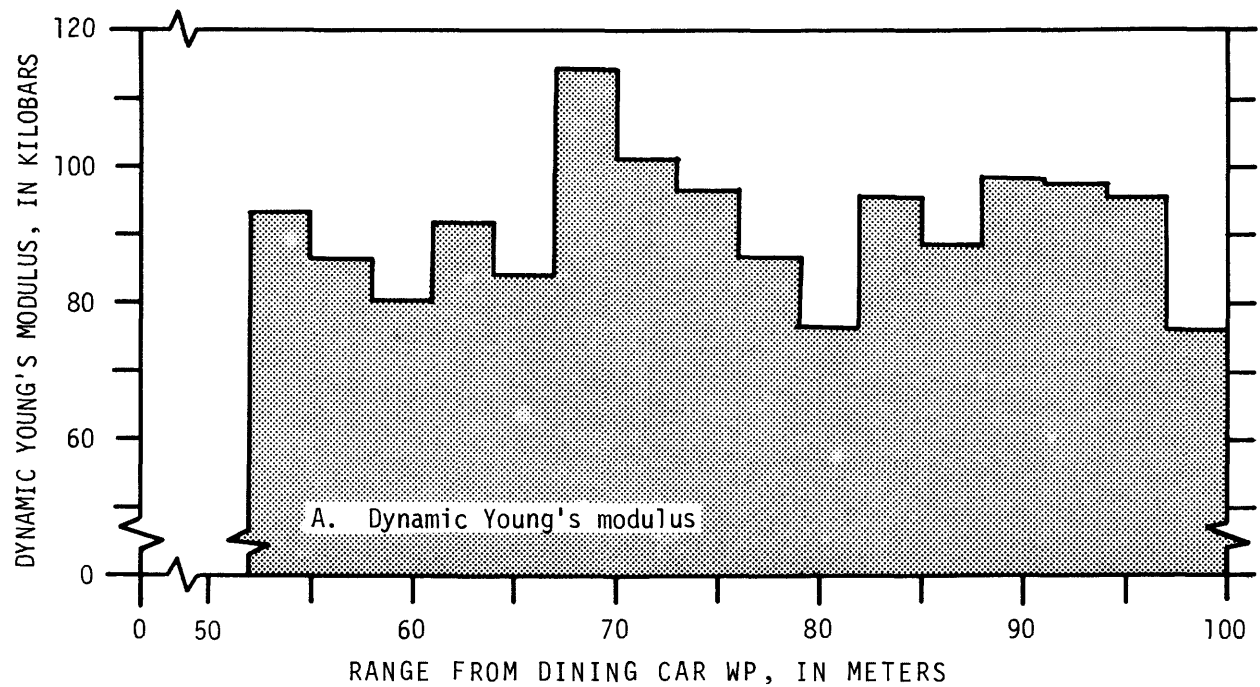
Figure 40.--Histogram of dynamic modulus (A, Young's; B, bulk) average over 3-m intervals and plotted as a function of range from Dining Car WP.

103

DISCUSSION OF RESULTS

Results of both overcore and hydrofracture measurements within 100 m
(328 ft) of the Dining Car event indicate that alterations in the pre-Dining
Car in situ stress field have occurred as a result of the event.
Hydrofracture data indicate low minimum stress magnitudes near the Dining Car
chimney with a general trend of increasing minimum stress magnitude with
increased range from the chimney. An interesting feature of the hydrofracture
results is the two zones of relatively high minimum stress magnitude at ranges
of about 69 and 90 m (226.4 and 295.3 ft) from the Dining Car WP. These zones
of relatively high stress may be attributable in part to variations in average
mechanical properties of the rock mass. Results of the overcore stress
determination at the Hybla Gold WP indicated stress magnitudes comparable to
pre-Dining Car values, but that the orientation of the principal stress
components was different than pre-Dining Car. Horizontal stress components
determined at the ISS-7A and ISS-9 drill-hole locations also indicated
directional variations from the pre-Dining Car horizontal stress state.

In order to examine these changes further, in light of Dining Car effects,
it is beneficial to briefly review aspects of the present theory of nuclear
containment and explosion-induced stress effects.

An underground nuclear detonation is believed to result in the formation
of a greatly enhanced compressive stress field around the explosion-produced
cavity. This induced stress field, often referred to as the "residual" stress
cage[9], is beneficial to containment in that it decreases the potential for

[9]"Residual" stress, as used in this context, refers to the quasi-permanent
stresses induced in the medium surrounding an underground nuclear explosion
as a result of the detonation and dynamics of cavity formation.

high pressure cavity gases to escape from the cavity by hydrofracturing the surrounding rock. Computer calculations and modeling routines indicate that the stress cage has a general distribution as shown on figure 41 (Rimer, 1977), where σ_r and σ_θ are respectively the radial and tangential components of stress relative to the explosion cavity. Peak stresses and lateral dimensions of the distribution vary depending primarily on the strength properties of the surrounding media. The stress distribution of figure 41 was calculated for the Dido Queen event in E tunnel. This event was similar in the relevant aspects to the Dining Car event, and as such, the Dining Car event would have had a very similar calculated stress cage. It is noted that on figure 41 the in situ state of stress, which was modeled as hydrostatic and equal to 6.0 MPa, is included in the stress distribution. The σ_r and σ_θ curves must therefore be referenced to the 6.0 MPa value to arrive at the magnitude of the explosion-induced stress changes.

Recently, evidence has emerged which suggests that the duration of the stress cage may be short, perhaps on the order of months (Rimer and Lie, 1980). Results of the measurements in the vicinity of Dining Car certainly do not indicate the presence of any unusually high compressive stress magnitudes. If a stress cage such as that predicted by modeling was formed by the Dining Car event, it had apparently dissipated almost completely in the 2 years subsequent to the event. Variations observed in the orientation of stresses in the Dining Car area, however, indicate the presence of remnant stress changes. Although the amount and nature of time-dependent dissipation and alteration of the explosion-induced stress state is unknown, these remnant stress changes provide some inferences regarding the original character of the explosion-induced stress state.
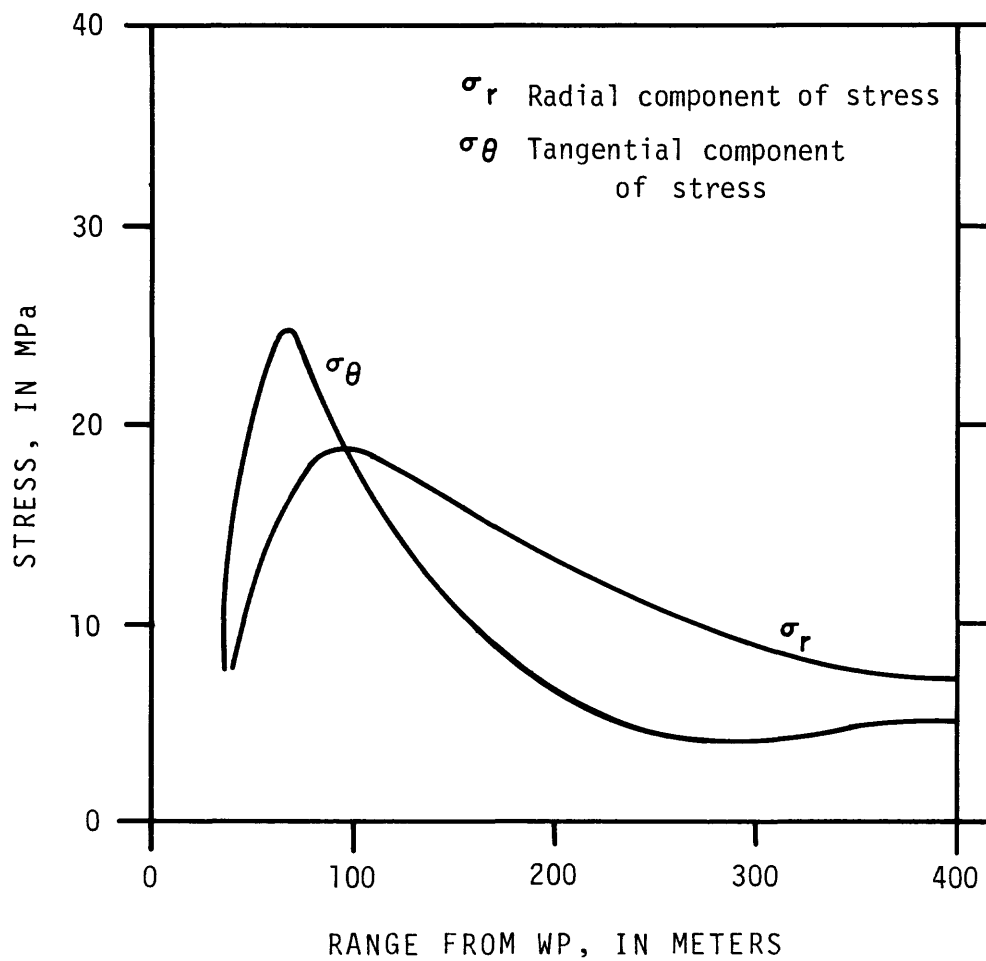
105

Figure 41.--Typical nuclear explosion-induced "residual" stress cage as predicted by computer modeling for Dido Queen event (after Rimer, 1977).

If it is assumed the pre-Dining Car stress field was uniform, then the remnant stress changes can be determined by subtraction of pre-Dining Car normal and shear stress components from the normal and shear stress components determined in the Hybla Gold workings. These resultant stress change components can then be used to calculate the principal stress changes at the Hybla Gold WP and the horizontal principal stress change components at the ISS-7A and ISS-9 locations. Because the pre-Dining Car stresses are subtracted out, the resultant principal stress changes are the result of permanent changes induced by Dining Car, including the unknown time-dependent alteration and any effects from the presence of the rubble-filled chimney.

It is important to emphasize that these calculated remnant stress changes are subject to uncertainties in the Hybla Gold and pre-Dining Car measurements. The most potentially significant uncertainties occur in the elastic moduli values used in the Hybla Gold stress calculations. For isotropic conditions, however, the modulus uncertainty at each measurement site effects the calculated stress magnitude at that site equally (i.e., calculated stress magnitudes are directly proportional to the elastic modulus). Therefore, regardless of the modulus related uncertainty in the Hybla Gold stress magnitudes, the relative sense of change between the stress component at each location is algebraically the same. In other words, unless the stress change components happen to be equal in magnitude and sign, the same component at each location will always be algebraically greater than the other, even if the Hybla Gold stress components are increased or decreased by any common factor. This allows for at least a qualitative evaluation of the pattern of stress change versus range from the Dining Car WP. Because the pre-Dining Car stress state has been subtracted, the stress changes should theoretically be independent of direction from the WP.

The complete state of stress determined at the Dining Car WP prior to that event (Miller and others, 1975) is shown in table 12. The remnant stress changes at the Hybla Gold WP, determined by subtracting the pre-Dining Car stress state from that determined at the Hybla Gold WP (table 9) is shown on figure 42. These remnant stress changes, although relatively small in magnitude, indicate a compressive stress increase in the N. 58° W. direction and a compressive stress decrease in the N. 36° E. direction. Both of these stress change components are within a few degrees of horizontal and their alinement is within about 22° of being radial and tangential, respectively, to the Dining Car WP. The third, more nearly vertical, stress change component is negligible. Similarly, the horizontal remnant stress changes can be estimated for the ISS-7A and ISS-9 locations. These components of stress change are shown on figure 43, along with the horizontal stress change components resolved from the Hybla Gold WP data of figure 42.

The remnant horizontal principal stress changes of figure 43 suggest two possible interpretations regarding Dining Car induced stress effects. The most obvious is that a compressive stress decrease is indicated in the north-northeast south-southwest direction, accompanied by a compressive stress increase in the west-northwest east-southeast direction. The orientation of these horizontal stress changes is very similar to the orientation of the pre-Dining Car horizontal principal stresses, suggesting that a simple reduction in the deviatoric part of the pre-Dining Car stress state has occurred. This interpretation has physical significance in that mechanical properties tests on core samples from the Hybla Gold workings indicate a general decrease in shear strength compared to samples tested prior to the Dining Car event (Gardiner and Butters, 1977). A reduction in shear strength of the rock medium would logically result in a decrease in the deviatoric stresses present

Table 12.--State of stress determined at Dining Car WP prior to detonation

[---, not applicable]

	Stress magnitude MPa	Standard deviation MPa	Bearing	Inclination (+ degrees above horizontal; - degrees below horizontal)
Principal stresses	(+, compression)			
S_1 (minimum)	+2.8	±0.4	N. 75° W.	+12°
S_2 (maximum)	+6.9	±0.4	N. 4° E.	-40°
S_3 (intermediate)	+6.0	±0.4	N. 28° E.	+48°
Normal stress components in X, Y, Z (east, north, vertical) coordinate system	(+, compression)			
σ_x	+3.1	±0.4	East	Horizontal
σ_y	+6.3	±0.4	North	Horizontal
σ_z	+6.2	±0.3	---	Vertical
Shear stress components in X, Y, Z coordinate system [1]				
τ_{xy}	+0.8	±0.3	---	---
τ_{yz}	-0.6	±0.3	---	---
τ_{zx}	+0.6	±0.3	---	---

[1]Positive or negative sign on shear stress magnitude indicates direction of shear stress with respect to X, Y, Z coordinate system.

$S_1 = + 1.8$ MPa N.58°W. +27° inclination

$S_2 = - 2.0$ MPa N.36°E. +9° inclination

$S_3 = $ No significant change

+, increased compression

−, decreased compression

DINING CAR WP N. 78° W.
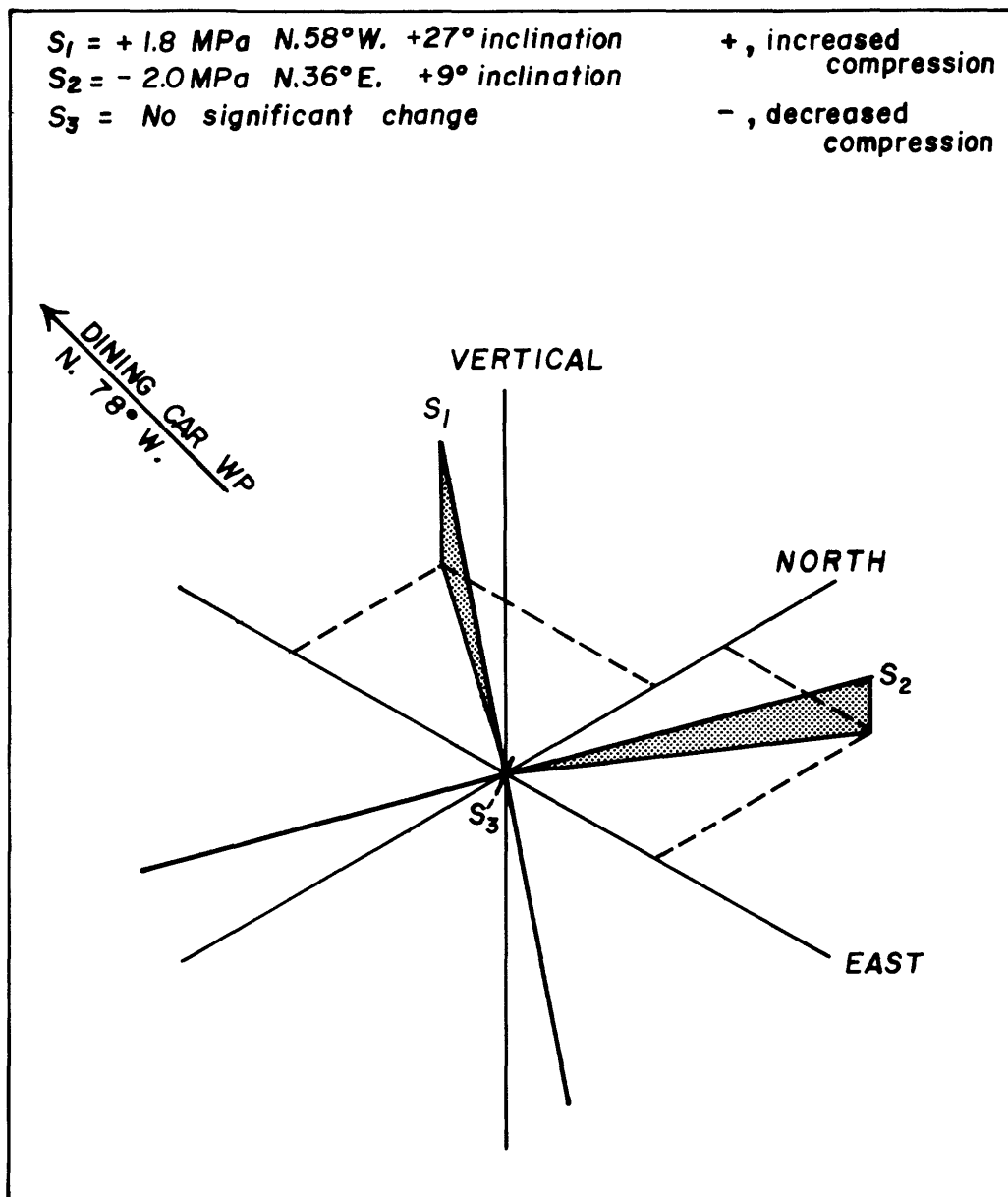
VERTICAL

S_1

NORTH

S_2

S_3'

EAST

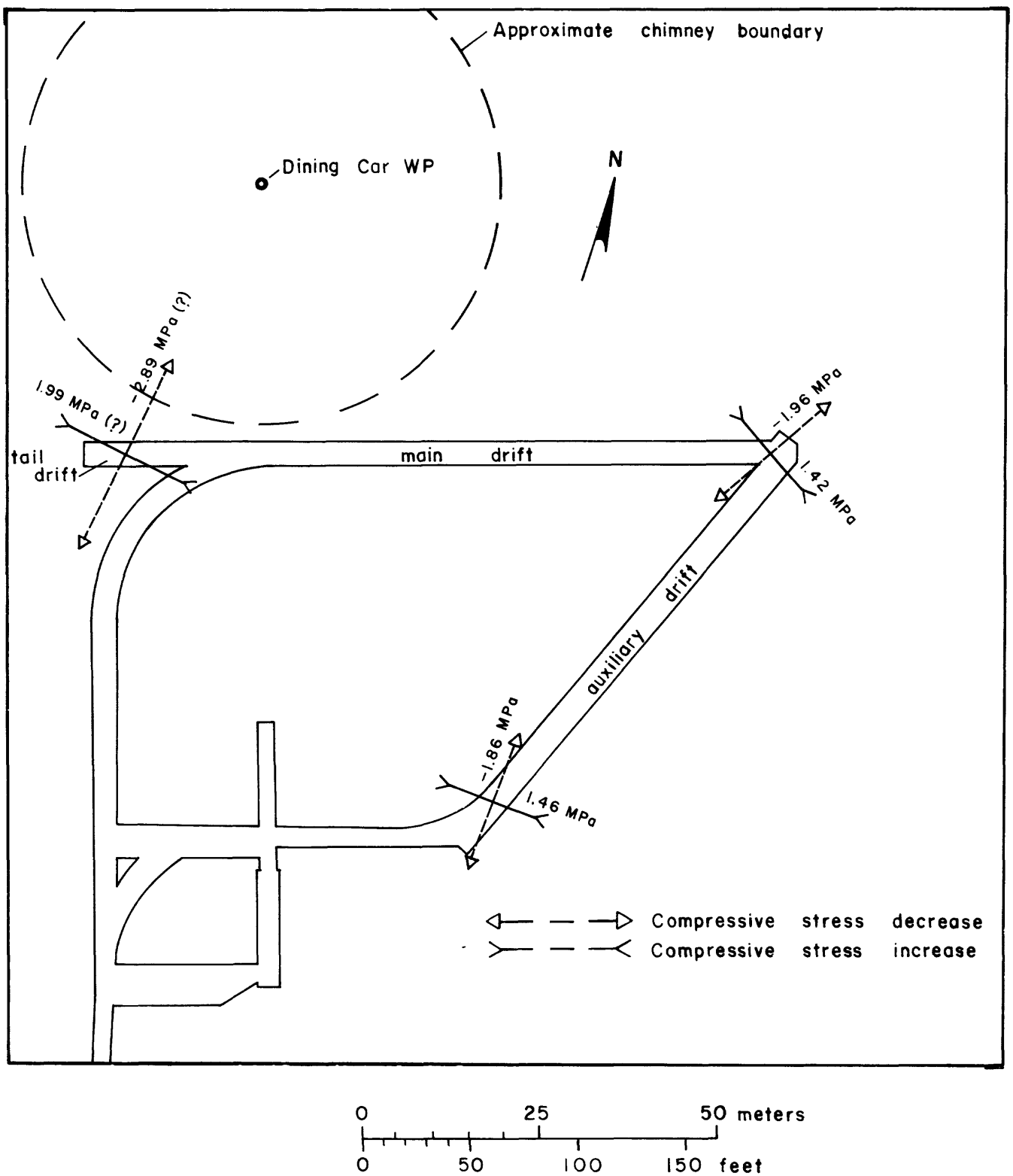Figure 42.--Remnant principal stress changes at Hybla Gold WP.

Figure 43.--Remnant horizontal principal stress changes in U12e.20 drifts.

prior to the event. The major difficulty with this interpretation, however, is that it implies no geometric or directional relationship of the remnant stress changes to the Dining Car explosion source. Considering the magnitude of nuclear explosion-induced stresses and displacements, it seems reasonable to expect that, even after 2 years, there should be some directional relationship between the stress changes and the Dining Car WP.

A directional relationship of the horizontal stress changes to the Dining Car WP is suggested at two of the three locations on figure 43. At the ISS-9 location, which is nearest the Dining Car chimney, the stress change components are radial and tangential to the chimney, and at the Hybla Gold WP they are within 25° of radial and tangential. At the ISS-7A location, however, the stress change components aline at about 45° to the Dining Car radial, thus showing no tendency for radial and tangential alinement. This lack of alinement could possibly be the result of geologic inhomogeneities affecting the initial distribution of explosion-induced stresses and (or), more likely, subsequent readjustments and modifications to the stresses during the 2 years after the event. It is also possible that the pre-Dining Car stress field was not uniform as assumed.

The overcore data are therefore not definitive with regard to the mechanism that resulted in the remnant stress changes observed around the Dining Car event. The authors suspect, however, that the stress changes result primarily from a geometric relationship to the explosion source, rather than a simple readjustment in deviatoric stresses owing to a shear strength reduction in the rock medium. Likely, the reduction in shear strength played a secondary role in subsequent modification of the induced stress distribution. The fact that all of the observed remnant horizontal stress changes do not exhibit a perfect or consistent trend of radial and tangential

112

alinement to the Dining Car WP is not especially disturbing considering the potential for measurement uncertainties owing to rock conditions, the unknown effect of time-dependent stress redistribution, and the fact that the geologic medium is not perfectly homogeneous.

Even though the principal horizontal stress changes did not all aline radial and tangential to the Dining Car WP, the pattern of radial and tangential stress change can still be examined. The radial and tangential components of horizontal stress change, determined by rotation of the horizontal principal stress changes, are shown on figure 44. Figure 45 is a plot of these radial and tangential stress change components versus range from the Dining Car WP. It is again emphasized that the magnitudes of these stress changes are subject to uncertainties in the magnitudes of the Hybla Gold measured stresses, especially at the ISS-9 location. The most significant feature of figure 45, however, is the pattern of stress change; that is, at each location the pattern indicates which component of stress change, σ_r or σ_θ, is relatively more compressive than the other.

Ignoring the stress change magnitudes on figure 45, the following can be said about the pattern of stress change. Near the Dining Car chimney at the ISS-9 location (44-m (144.4-ft) range from Dining Car WP), the tangential component of stress change is relatively more compressive, while at the Hybla Gold WP site (83-m (272.3-ft) range from Dining Car) the radial component of stress change is relatively more compressive. At the ISS-7A location (93-m (305.1-ft) range from Dining Car) the change in both radial and tangential components is approximately equal and insignificant. The pattern of stress change therefore indicates a "crossover" of the radial and tangential components of stress change somewhere between 44- and 83-m (144.4- and 272.3-ft) range from the Dining Car WP, most probably between about 60- and
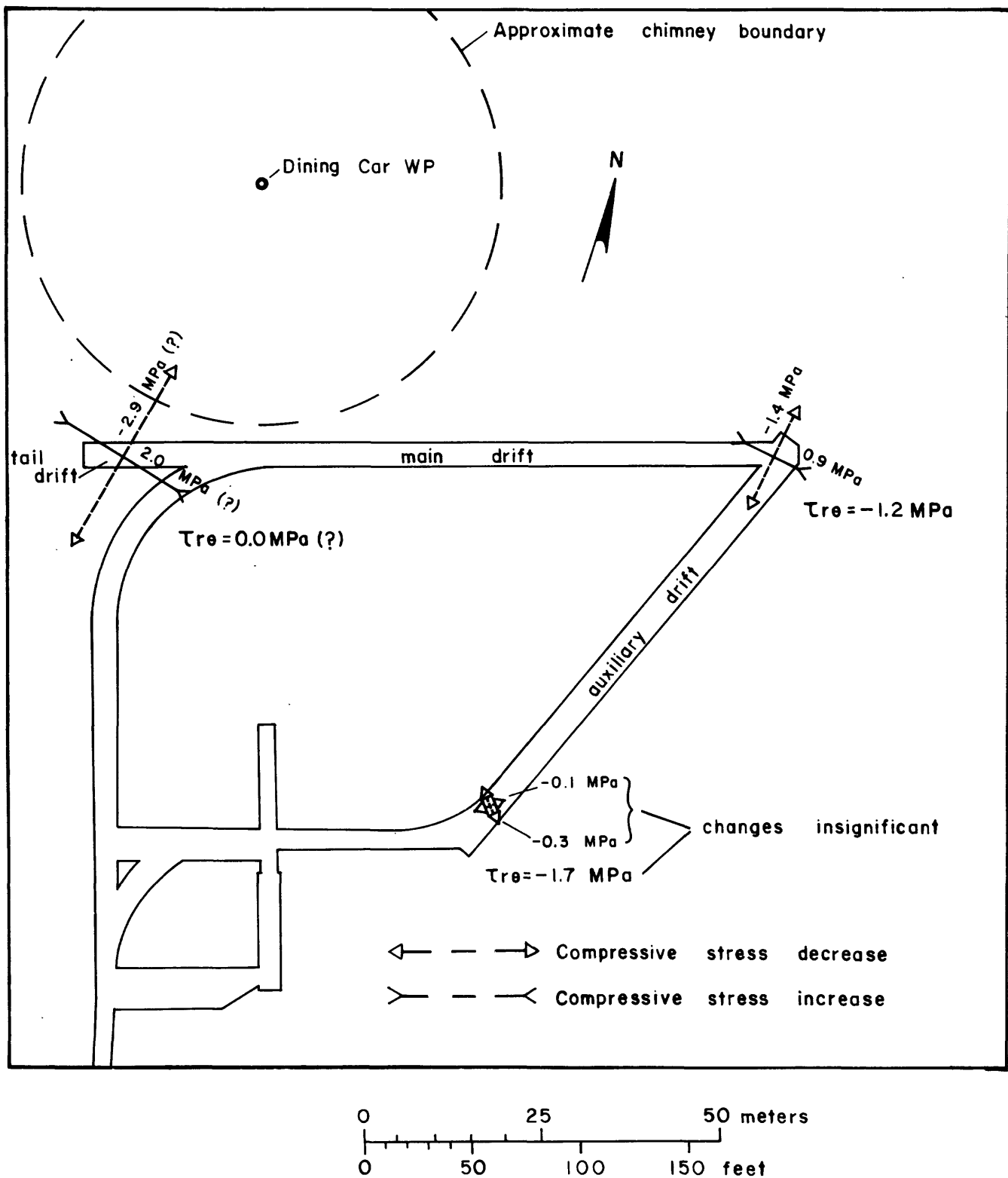
Figure 44.--Components of remnant horizontal stress change radial and
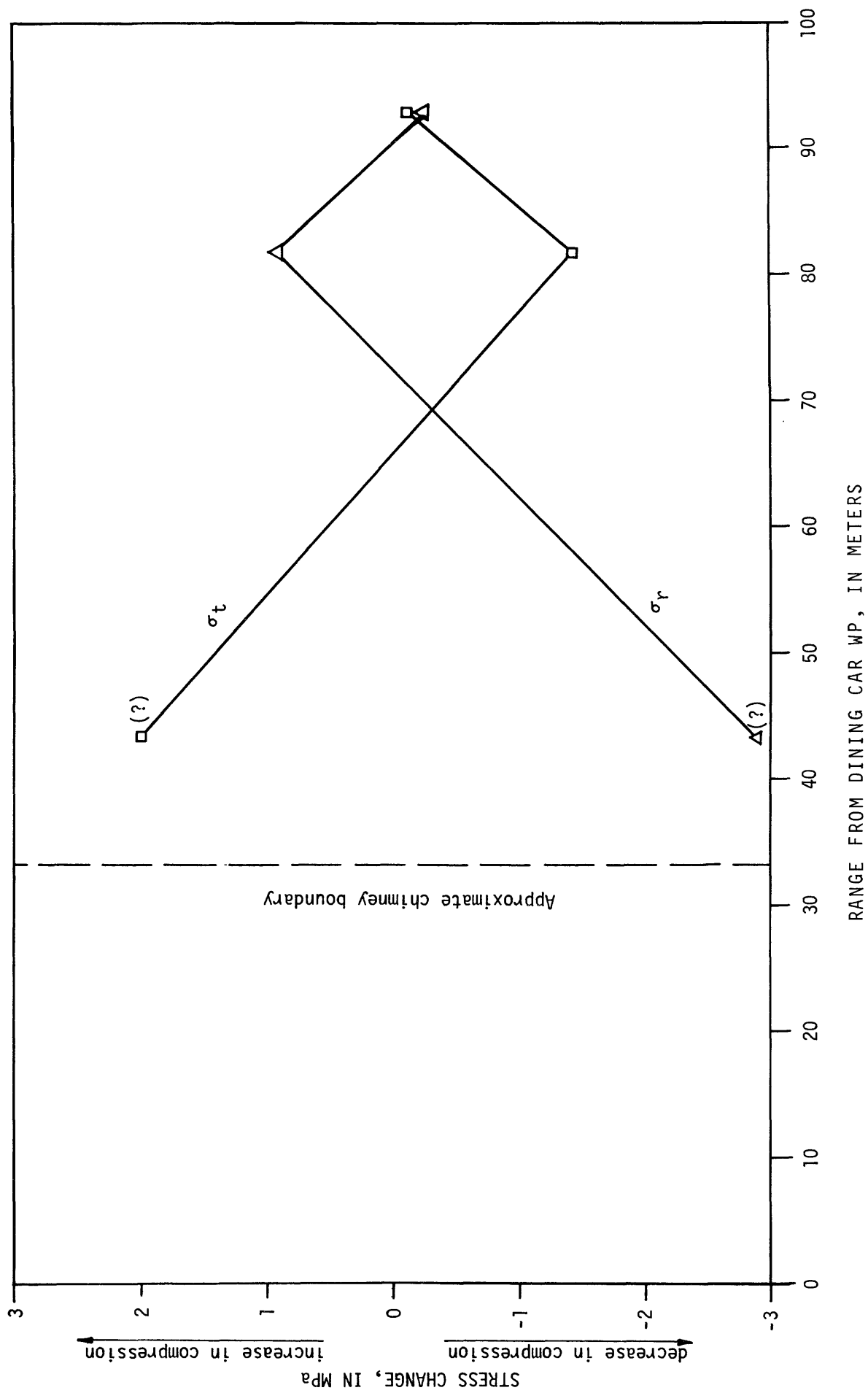tangential to the Dining Car chimney.

Figure 45.--Radial (σ_r) and tangential (σ_t) components of remnant horizontal stress change versus range from Dining Car WP.

70-m (196.9- and 229.7-ft) range. In order to provide a visual comparison of the measured radial and tangential remnant stress changes to the induced stresses predicted by the Dido Queen model, figures 41 and 45 are combined in figure 46. The zero stress-change line of figure 46 is equivalent to the 6 MPa value of figure 41 such that only stress-change magnitudes are presented.

It is obvious from figure 46 that the magnitude of the measured components of remnant stress change do not approximate the stress increase predicted by the calculational model. This does not imply that the results of the model are invalid, because the effects of creep and other time-dependent phenomena on the explosion-induced stress distribution are largely unknown. It is apparent from this comparison, however, that if the calculational models provide a reasonable estimate of explosion-induced "residual" stresses, then these stresses do not persist for long periods of time in the low modulus rocks of Rainier Mesa. If it is accepted that the orientation and relative magnitudes of the measured horizontal stress changes are an artifact of the original induced stresses, then it is noteworthy that the pattern of change is qualitatively similar to that predicted by the model. That is, near the chimney the tangential component of stress change is most compressive, but at greater range the radial component of stress change becomes most compressive. It is therefore suggested that the pattern of remnant stress change in the vicinity of Dining Car provides a qualitative indication based on field measurements that a "stress cage" once existed around the Dining Car cavity, and that the geometric characteristics of this "stress cage" were similar to those predicted by numerical modeling. Unfortunately, the data provides no indication as to what the probable magnitudes or lateral dimensions of the induced stresses were shortly after execution of the Dining Car event.
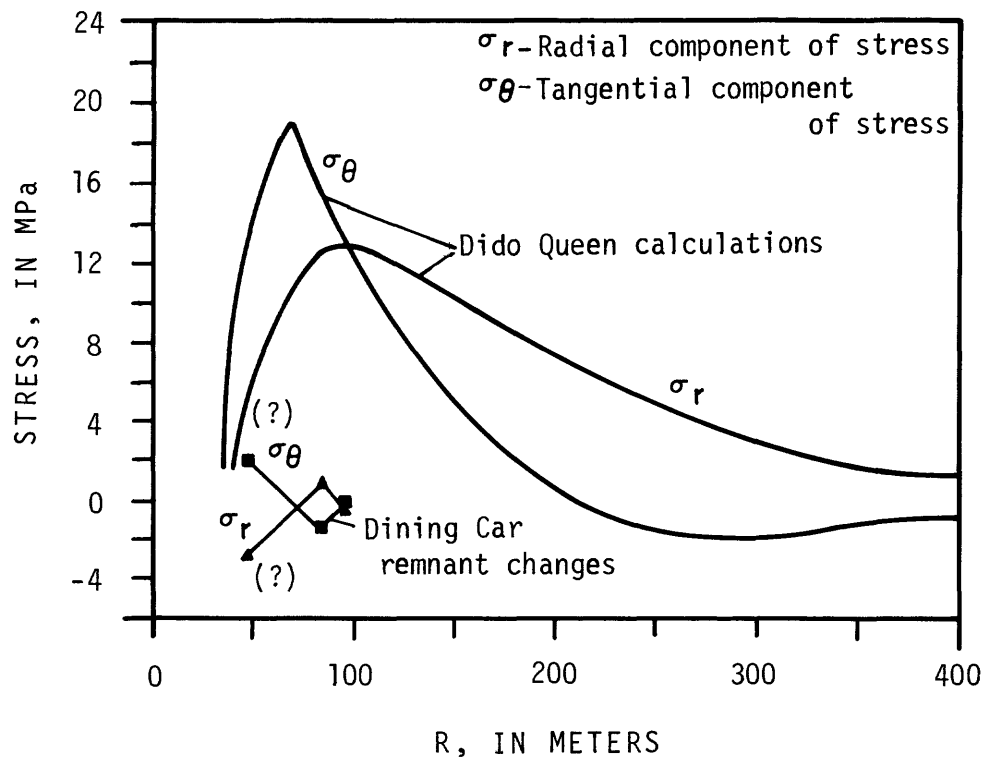
Figure 46.--Comparison of calculated "residual" stress cage for Dido Queen event to remnant stress changes determined in vicinity of Dining Car event.

117

SUMMARY

Overcore and hydrofracture measurements obtained in the proximity of the expended Dining Car event indicate perturbations in the stress field attributable to that event. It is evident that the observed stress variations are a result not only of the original explosion-induced stresses, but also of secondary processes such as creep and stress relaxation, possible readjustments along discontinuities, reductions in rock matrix strength properties near the chimney, and apparent variations in rock-mass strength, or stiffness, in the area of investigation. These secondary processes no doubt greatly altered the stress conditions present shortly after detonation of the Dining Car event. Additionally, the rock conditions encountered during the Hybla Gold measurements adversely affected the quantitative quality of data, especially nearer the Dining Car chimney. The results do, however, provide the following qualitative observations and inferences relevant to nuclear explosion-induced stress effects in Rainier Mesa. These observations are significant, if not entirely conclusive, in that they are derived from field measurements.

1. Field measurements did not indicate the presence of any unusually high compressive stress magnitudes within 93-m (305.1-ft) range from the Dining Car WP. This would seem to indicate that explosion-induced "residual" stresses, as predicted from numerical modeling, do not persist for long periods of times after execution of an event.

2. Hydrofracture data indicated an increase in minimum stress magnitude (compressive) with increased range from the Dining Car WP, probably reflecting an increase in rock strength with range from the WP. The weakened and apparently highly microfractured rock nearer the chimney, and the rubble-

filled chimney, probably served as a "stress sink" for the time-dependent dissipation of high-magnitude explosion-induced stresses.

3. Hydrofracture data also indicated two narrow zones of relatively higher minimum stress magnitude at about 69- and 90-m (226.4- and 295.3-ft) range from the Dining Car WP. These zones generally correlate with zones of average increased mechanical properties of the rock mass as determined by sonic-velocity tests on core samples, suggesting that the higher stress zones occur within zones of apparent increased strength, or stiffness, of the rock mass.

4. Horizontal principal stress components determined from overcoring measurements suggest two possible interpretations regarding the observed remnant stress changes. One interpretation is that there has simply been a general relative decrease in compressive stress in the northeast-southwest direction and a relative general increase in stress in the northwest-southeast direction, with no directional relationship to the Dining Car WP. The second interpretation, guided by present nuclear containment theory, is that the observed remnant stress changes reflect a pattern of radial and tangential alinement to the WP.

5. The radial and tangential components of remnant stress change versus range from Dining Car indicate a pattern of relative change qualitatively similar to predictions based on numerical modeling. Even though the induced stress magnitudes have apparently dissipated with time, the remnant pattern of change would seem to suggest that a "stress cage" similar in concept to that predicted by numerical models once existed around the Dining Car event.

REFERENCES CITED

Aggson, J. R., 1977, Test procedures for non-linearly elastic stress-relief
  overcores: U.S. Bureau of Mines Report of Investigations 8251, 9 p.

Davis, J. C., 1973, Statistics and data analysis in geology: John Wiley and
  Sons, Inc., p. 222-232.

Diment, W. H., and others, 1959, Geologic effects of the Rainier underground
  nuclear explosion: U.S. Geological Survey Open-File Report TEI-355,
  95 p.

Fitzpatrick, John, 1962, Biaxial device for determining the elasticity of
  stress-relief overcores: U.S. Bureau of Mines Report of Investigations
  6128, 13 p.

Gardirer, D. S., and Butters, S. W., 1977, Material properties for the Hybla
  Gold event: Terra Tek, Inc. (Salt Lake City),TR 77-46, 32 p.

Haimson, B. C., 1977, Stress measurements using the hydrofracturing technique,
  in Field Measurements in Rock Mechanics: Proceedings of the
  International Symposium, Zurich, 1977: A. A. Balkema/Rotterdam, v. 1,
  p. 233-247.

Hooker, V. E., and Bickel, D. L., 1974, Overcoring equipment and techniques
  used in rock stress determination: U.S. Bureau of Mines Information
  Circular 8618, 32 p.

Miller, C. H., and others, 1975, Determination of in situ stress at U12e.18
  working point, Rainier Mesa, Nevada Test Site: U.S. Geological Survey
  Report USGS-474-217, 21 p.; available only from U.S. Department of
  Commerce, National Technical Information Service, Springfield, VA 22161.

Panek, L. A., 1966, Calculation of the average ground stress components from
  measurements of the diametral deformation of a drill hole: U.S. Bureau of
  Mines Report of Investigations 6732, 41 p.

Rimer, Norton, 1977, The influence of clay and water in rock on containment of underground nuclear explosions: Systems, Science and Software Report SSS-R-77-3339, 40 p.

Rimer, Norton, and Lie, K., 1980, Spherically symmetric calculations of the SRI grout spheres experiment for four different laboratory configurations: Systems, Science and Software Report DNA 5274T, 47 p.